FACOLTÀ DI AGRARIA, Università degli Studi della Tuscia, Viterbo

DIpartimento di Scienze e Tecnologie Agroalimentari

(AGR/15)

CORSO DI DOTTORATO DI RICERCA

Biotecnologie degli Alimenti - XXIII CICLO

TITOLO TESI DI DOTTORATO DI RICERCA

Assessment of Tarocco Orange Fruit Firmness by Standard and Non-Destructive Tests

TUTOR

***Pr*of. Ing. Mauro Moresi**

DOTTORANDO

Federico Pallottino

COTUTOR

Dr. Paolo Menesatti

COORDINATORE

Prof. Marco Esti

Anno Accademico 2009-10

TITOLO TESI DI DOTTORATO DI RICERCA

Assessment of Tarocco Orange Fruit Firmness by Standard and Non-Destructive Tests

Federico Pallottino

INDEX

Riassunto breve

Nell'ottica di identificare test dinamometrici non-distruttivi (ND) appropriati per caratterizzare il comportamento reometrico e la durezza di cultivar di agrumi, per il sorting online e per lo svolgimento di fini analisi di laboratorio, sono state messe a punto due procedure basate sull'analisi di immagine per misurare la effettiva superficie di contatto (A) delle arance sottoposte a test di compressione al variare della deformazione relativa nell'intervallo 3-21%. I valori sperimentali di A, ricavati tramite dette procedure, differivano in media del 6.5%, nonostante i coefficienti di variazione variassero dal 18 al 30%. Per contro, la loro stima tramite il metodo standard ASABE (2008) od un modello matematico che assume costante il volume dei campioni durante il test meccanico era affetta da errori medi, rispettivamente, del 42 e del 22%.

Conseguentemente questa tesi di dottorato ha affrontato la determinazione delle proprietà reometriche (coefficiente apparente di Poisson, modulo apparente di elasticità, costanti viscoelastiche e spettro dei tempi di rilassamento), chimico-fisiche (solidi totali, acidità, consistenza di Magness-Taylor, coordinate CIE L*a*b* dell'epicarpo e del succo, spessore della buccia) e sensoriali di arance rosse della varietà Tarocco. Attraverso l'analisi dei risultati dei test di compressione non-distruttivi, l'identificazione del range viscoelastico lineare dei frutti e la classificazione di questi in base al miglior modello per una rapida stima della *firmness*, validata da *panel test*, è stato possibile individuare uno strumento operativo per la selezione on-line di arance con resistenza specifica (F/D) compresa fra 220 e 420 N m^{-1}. Altresì, mediante la definizione di procedure ed attrezzature basate sull'analisi d'immagine, non raccomandabili per il sorting online, è stato possibile identificare la struttura di test di laboratorio più fini come strumenti di supporto ai genetisti che lavorano al breeding di cultivar di Tarocco di maggiore consistenza.

Summary

This PhD thesis dealt with the assessment of the rheometrical (apparent Poisson's ratio, apparent modulus of elasticity, viscoelastic constants and relaxation time spectrum), chemico-physical (total solid content, titratable acidity, Magness-Taylor firmness, rind and juice colorimetric analyses and rind thickness), and sensory properties of Tarocco blood oranges, as well as the real contact surface during fruit compression tests by two innovative image analysis techniques. An operating tool to grade on-line orange fruits with a resistance per unit diameter (F/D) ranging from 220 to 420 N m^{-1} was identified.

1. Introduction

In accordance with the PhD thesis project previously described (Pallottino, 2008), this oral communication reports the main results of the following activities directed to:

i) review the state of the art and gather existing models to analyze citrus-fruit uniaxial compression tests;
ii) perform a first series of conventional parallel plate compression tests up to rupture to determine engineering stress (σ_{Rz}) and strain (ε_{zR}) at breakage and design stress-relaxation tests at different cross-head speeds (VT) and initial strains (ε_{z0}) to assess the range of linear viscoelasticity;
iii) determine the contact area (A) of the fruit under squeezing as a function of εz for $\varepsilon_z \ll \varepsilon_{zR}$ by means of two different image analysis-based methods to convert the typical force-deformation curves into stress-strain relationships and thus determine the real orange fruit mechanical properties;
iv) submit a large number of orange fruits to non-destructive compression tests up to ε_{zR} = 0.05 to classify the specimens into three high-, medium- or low-firmness classes before performing the destructive Magness-Taylor test and assessing some chemico-physical and sensory properties;

v) analyze the statistical significance of all the measurements to establish a practical rule to sort on-line citrus fruits.

2. State of the art

Citrus production represents an important share of the Italian fruit market. In the emerging markets of Japan, North America and Australia, Tarocco cultivars are presently preferred to blond oranges because of their higher nutraceutical and organoleptic properties. Unfortunately, their lower firmness results in persistent deformation, especially after long-term shipping, this involving stock rejection once the fruit firmness has been monitored using the so called Magness-Taylor (MT) test (USDA, 2003). In citrus fruits, the relationship between puncture force and firmness is concealed by the differences in the tissue types directly under the puncture probe (Shmulevich et al., 2003). Other techniques based on visible (VIS) or near-infrared (NIRS) spectroscopy, impaction or acoustic impulse resonance frequency have so far exhibited inaccurate results (García-Ramos et al., 2005; Ruiz-Altisent & Ortiz-Canavate, 2005; Valero et al., 2003). Nowadays, just two non-destructive on-line high-speed systems (i.e., Intelligent Firmness Detector, iFD, Greefa, Trich, NL; Sinclair Internal Quality-Firmness Tester, SIQFT, Sinclair Systems International, Fresno, CA, USA) have been developed and commercialized for testing the firmness of individual fruits by resorting to the so called impact methods, coping with the free fall of the fruit over a force (piezoelectric) sensor or vice versa. Despite such systems have been successfully applied to grade several fruits (Howarth et al., 2003; Valero et al., 2003), its application to citrus fruit sorting is still undocumented. There is therefore an urgent need for novel tests to assess the citrus fruit mechanical properties in a rapid, objective and reproducible way (Menesatti et al., 2008).

3. Materials and Methods

3.1 Raw material, mechanical tests and image acquisition

Citrus fruits cv Tarocco Arcimusa were provided by the experimental farm Palazzelli (Lentini, Siracusa, Italy) of the Research Centre for Mediterranean Crop of the Agricultural Research Council (CRA-ACM) at the time of harvest. All mechanical tests were performed using a table-top digital dynamometer, Zwick 1.0 Universal Testing Machine (Zwick/Roell Testing System, Kennesaw, GA, USA) equipped with a transparent graduated Plexiglas® plate, conventional metal compression plate or 1 cm^2 flat probe, so as to perform uniaxial compression tests in conjunction with contact area image analyses, non-destructive compression tests or destructive penetrometric tests, respectively. Based on preliminary trials (Pallottino, 2008) and literature (Ruiz-Altisent et al., 2005), the cross-head speed (VT) was set at 15 mm s^{-1}. All details about these tests were previously reported (Pallottino, 2009a; Pallottino et al., 2010). Fig. 1 shows the combined system used to perform compression testing and image acquisition of fruit shape and contact area during the 2008-2009 harvesting campaign. In the subsequent 2009-2010 campaign, about 150 kg of Tarocco oranges, corresponding to about 400 fruits, were numbered and then compressed by 5% to measure the corresponding fruit resistance (F). After that they had been ordered with respect to the tension per unit diameter (F/D), they were discriminated into three different lots, designated as high (HF), medium (MF) or low (LF) firmness one. Any class consisted of 65 specimens, that were randomly subdivided into two subgroups. Forty specimens were sequentially submitted to rind colorimetric analysis, MT test, and rind thickness measurement along the axes x and y on the equatorial plane. The MT tests were carried out as previously described (Menesatti et al., 2009). All juices expressed were assayed for colorimetric analysis, total soluble solids (TSS) using the Abbey refractometer and titratable acidity (TA) using a NaOH standard solution. Under the supervision of Prof. C. M. Lanza, the remaining 25 fruits were assayed by 12 skilled panelists of the Laboratory for Sensory Analyses of the Department of Orto-Floro-Arboricoltura e Tecnologie Agroalimentari (University of Catania, Catania, Italy), this being certified by UNI ISO 8589 (1990). By referring to an ordinal scale ranging from 1 (absence) to 9 (maximum intensity) (Pagliarini, 2002), each panelist was asked to evaluate 14 different descriptors, namely shape, shape defects, compactness, ease of peeling, ease of segment separation, typical orange odour, off-odour, juiciness, acidity, sweetness, bitterness, typical orange flavour, off-flavour, and overall sensory evaluation. The experimental design was planned to submit two orange fruits randomly selected from any of the three aforementioned lots to any panellist.

3.2 Contact area and fruit size assessment

Three cams [i.e., an AVT Camera Guppy (Allied Vision Technologies, Stadtroda, Germany) and two LifeCams VX-6000 (Microsoft Corporation, Redmond, WA, USA)] were respectively positioned along the axis lines z , x, and y to collect a triplet of the projection images X, Y and Z of the fruit under testing (Fig. 1).

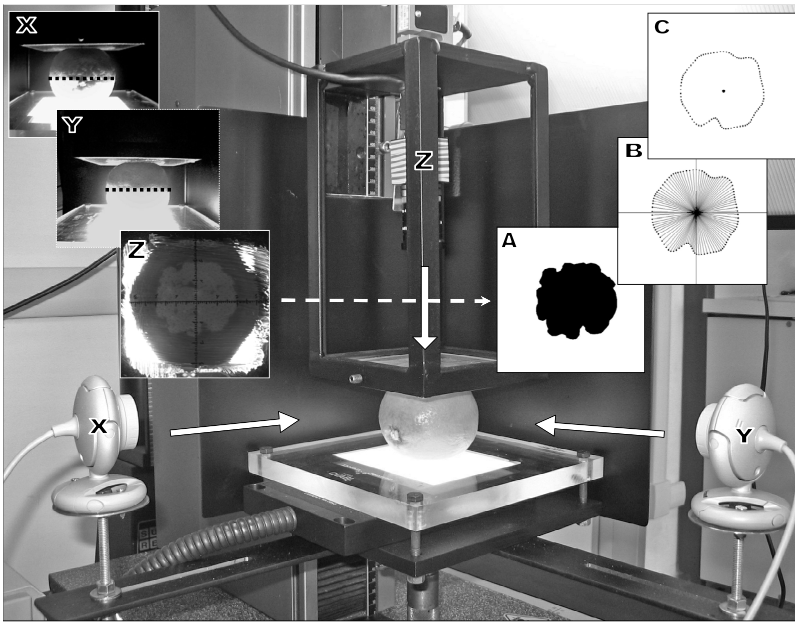

Figure 1 Picture of the experimental apparatus equipped with fixed (lower) and moving (upper) Plexiglas® plates and three web cams, positioned along the axis lines x, y and z to collect the projection images X, Y and Z of the fruit under testing, sequentially binarized (A), digitized (B) and finally submitted to Elliptic Fourier Analysis (C).

The fruit size and deformation relative to x or y axis were detected via the y or x camera, respectively. Any size expressed in pixel was converted into mm by resorting to a pre-calibrated standard metric reference. The effective contact area was acquired by the vertical (z) camera (Fig. 1). As reported previously (Costa et al., 2009), the projection images were binarized (Fig. 1-A) and digitized (Fig. 1-B), before submitting their outline coordinates to Elliptic Fourier Analysis (EFA) to examine the shape changes in the contact surface, as well as its area (A_{EFA}), as a function of the deformation (H) applied along the z-axis (Fig. 1-C). Knowledge of the effective contact area (A) allowed the force F-vs.-H curves to be converted into engineering stress (σ_z) vs. strain (ε_z) ones:

$$\sigma_z = F/A; \qquad \varepsilon_z = [H0 - H]/H0 \qquad (1)$$

where H0 and H are the initial and current heights of each orange fruit under testing.

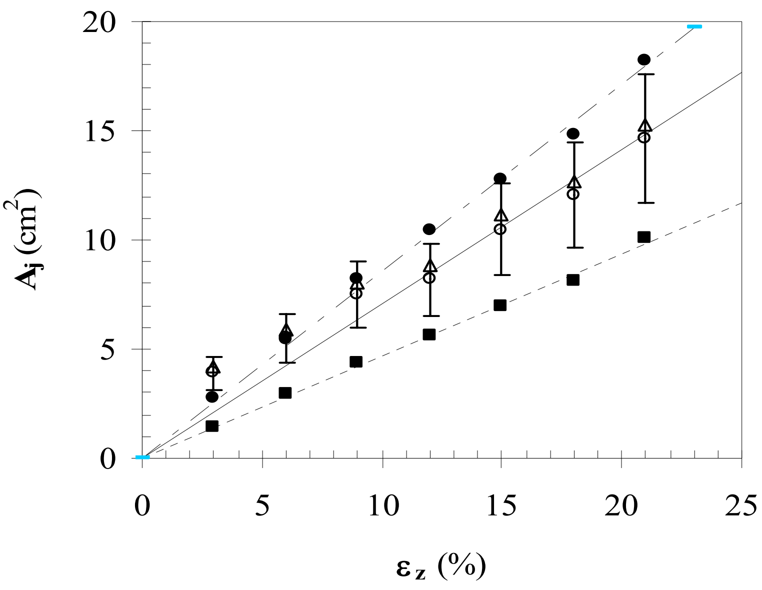

Figure 2 Main results of compression testing on orange fruit samples at VT=15 mm s-1: Effect of ε_z on the contact area (Aj), as acquired by image analyses using EFA (A_{EFA}: ○) or bounding-box method (A_{BB}: △), or calculated using the ASABE standard method (2008) (A_{ASM}: ■) or assuming the fruit volume constant (A_V: ●). The continuous line was plotted using Eq. (2), while the broken and dotted lines coincided with their corresponding regression lines.

3.3 Stress-relaxation tests

Several stress-relaxation tests were performed by setting the initial strain (ε_{z0}) and cross-head speed (VT) to 5, 10, 15 and 20% and 15 mm s^{-1}, respectively.

3.4 Statistical analysis of data

All tests were replicated at least 20 times (ASABE, 2008). Mean values of test results are given together with their corresponding standard deviations. The average responses of the samples tested were compared by One-Way analysis of variance (ANOVA) and discriminated on the basis of their Least Squares Differences (LSD). A Student's t-test was also applied to test whether the experimental mean values of the contact areas found by image analysis and Elliptic Fourier Analysis (A_{EFA}) or bounding box (A_{BB}) were significantly different.

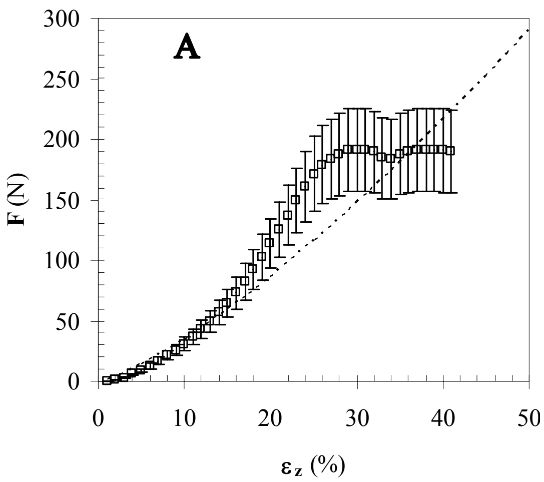

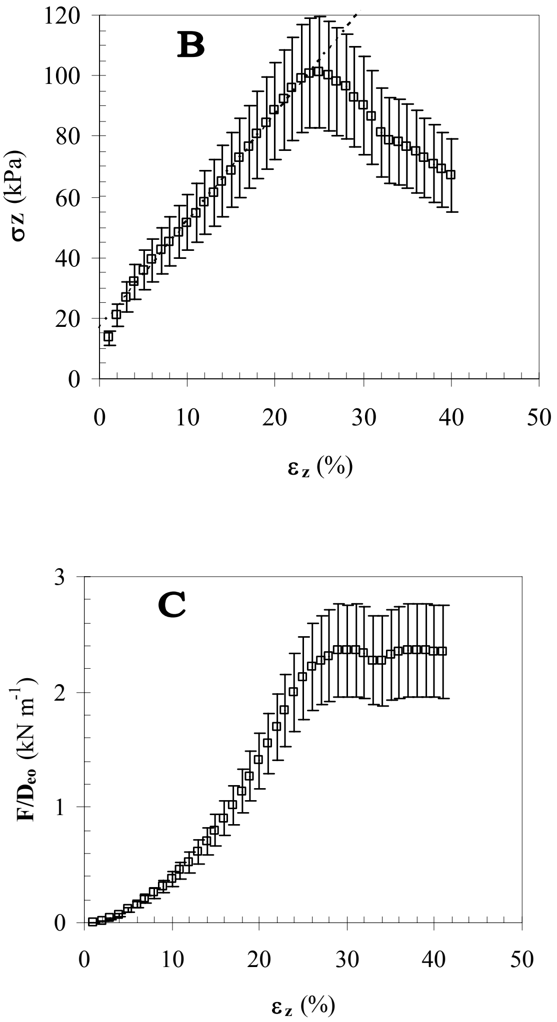

Figure 3 Main results of the parallel plate compression testing up to rupture performed on 20 orange fruit samples at VT=15 mm s^{-1}: a) Average fruit resistance (F) against engineering strain (ε_z); b) Average compressive engineering stress (σ_z) vs. ε_z; c) Average specific compressive load per unit equivalent diameter (F/D_{eo}) vs. ε_z.

4. Results and discussion

4.1 Contact area assessment via image analysis

The effective contact surface area (A_{EFA}) for any single sample, as detected by image EFA (Fig 1-C), was found to be quite irregular, especially at the smaller strains (Costa et al., 2009). Nevertheless, when the average contours of A_{EFA} were calculated, the shape of each contact area was assimilated to quite a perfect ellipse. Despite an average variation of about 20%, the AEFA values appeared to vary linearly with ε_z (Fig. 2):

$$A_{EFA}=(71\pm3)\ \varepsilon_z \qquad (r2 = 0.99) \qquad (2)$$

By inscribing the images acquired by the z camera in a minimum rectangle (the so called bounding box) having sides parallel to the axes of the ellipse- or circle-like shape of the acquired contact area, it was possible to estimate the contact areas (A_{BB}), their average values being shown in Fig. 2.

By resorting to the classic inequality of the hypothesis test for means, it was possible to reject any statistical difference between A_{EFA} and A_{BB} values at a probability level of 0.01.

By using the camera y or x, it was possible to measure the citrus fruit expansion along x or y axis, when compressed along the axis z, and then estimate the apparent Poisson's ratios ν_x and ν_y. Their average values practically coincided (0.16±0.09), this confirming the almost homogeneous behaviour of the fruit samples examined.

All the data collected allowed the contact area to be even predicted in accordance with the ASABE standard method (2009), their mean values (ASABE) being plotted in Fig. 2. Finally, by assuming that the overall volume of the fruit under compression was constant, it was possible to calculate the cross-sectional area (A_V) against ε_z (Fig. 2), as previously reported (Pallottino et al., 2009a). The estimated AASABE and AV values differed from those derived from image analyses (A_{EFA}) by about 45 and 19%, respectively.

4.2 Compression testing up to rupture

Fig. 3a shows the average values and standard deviations of fruit resistance (F) against ε_z up to rupture. By using Eq. (1), it was possible to convert such a curve into the σ_z-vs.-ε_z relationship (Fig. 3b). Despite the uncertainty in the estimation of A, especially for $\varepsilon_z<3\%$, σ_z exhibited an initial trend of the power-law type that practically became of the linear type for ε_z increasing from 4% to 24%. Beyond such a strain, σ_z reached a maximum burst value (109±15 kPa) at $\varepsilon_{zR}=(28\pm3)\%$, then tended to decline. The linear region in the σ_z-vs.-ε_z curve enabled the apparent modulus of elasticity of the whole orange fruit to be estimated (353±3 kPa, r2=0.998).

Since the fruit rind thickness (s) is very small compared to the fruit radius of curvature, the thin shell theory may be applied and bending effects ignored (Carin et al., 2003). Thus, the resulting stresses in the orange rind may be replaced by the forces per unit length of a line element in the median plane. In Fig. 3c the average force per unit equivalent diameter (F/D_{eo}) is plotted against ε_z, this plot being referred to 20 orange fruit specimens with roughly the same equivalent diameter (D_{eo}=81±3 mm), variety and maturity.

4.3 Stress-relaxation testing

To assess the range of linear viscoelasticity, citrus fruits were loaded at V_T=15 mm s^{-1} to generate engineering strains along the z axis in the range of 5-20%. Once the cross-head had been stopped, the stress relaxation was monitored for as long as 900 s, this being much longer than the time required (0.2-1.0 s) to deform the samples.

During all tests the dimensionless relaxation modulus $G^*(t, \varepsilon_z)$, expressed by the ratio between the actual F and initial F_0 reactions provided that the contact area (A) of the sample tested is constant and independent of time, exhibited an asymptotically decaying trend with a residual value different from zero whatever the engineering strain applied. By associating the response of citrus fruit to that of a generalized Maxwell body (a spring in parallel to n Maxwell elements) (Rao, 1992a), G* may be described as follows:

$$G^*(t, \varepsilon_z) = A_0 + \sum_{1}^{n} A_i \, e^{-t/\tau_i} \qquad (3)$$

where A_i represents the generic dimensionless viscoelastic coefficient.

By fitting G*-vs.-t data with an initially arbitrary spectrum of relaxation times (Nussinovitch et al., 1989) via the least squares method, it was possible to reconstruct the time course of G* by accounting for just two statistically significant Maxwell elements in parallel to an elastic spring element, the latter being characterized by the following relaxation times: τ_1 = 2.0 s, and τ_2 = 204 s. It can be noted that the smallest relaxation time (τ_1) was 2 to 20 times greater than the loading times (Rao, 1992b). The corresponding viscoelastic constants (A_i) resulted to be approximately constant:

$A_0 = 0.42 \pm 0.02$; $A_1 = 0.17 \pm 0.02$; $A_2 = 0.41 \pm 0.02$

In particular, the elastic component (A_0), responsible for the equilibrium residual stress, represented about 42% of the initial relaxation modulus, this confirming that any fruit behaved as a linear viscoelastic solid, at least on the time-scale and deformation range examined.

The deformation strain up to 20% affected neither the relaxation time spectrum of the delayed elastic components nor the percentage mass loss (0.04±0.03%) of any fruit tested. On the contrary, the percentage volume loss increased from 2±1 to 6±1% as ε_z was increased from 5 to 20%.

4.4 Chemico-physical and sensory testing

After assessing the resistance at ε_z=0.05 of about 400 orange fruits, these were discriminated into three different classes (i.e., high, HF; medium, MF; low, LF, firmness ones), provided that the force per unit diameter (F/D) ranged from 390 to 420 N m^{-1}, from 300 to 320 N m^{-1} or from 220 to 240 N m^{-1}, respectively.

Within each class, forty specimens were sequentially submitted to rind colorimetric analysis, MT test, and rind thickness measurement along the axes x and y on the equatorial plane. The variation in the orange rind CIELAB coordinates (L_r*=62±2; a_r*=38±2; b_r*=59±3) and thickness (s=1.8±0.5 mm) was found to be statistically insignificant at the confidence level of 99%; while the MT firmness, that ranged from 40 to 123 N, was able to discriminate only the orange fruits in the HF class with MT=73±16 N from those belonging to the MF (MT=59±9 N) and LF (MT=49±6 N) ones.

This finding was also confirmed by the CIELAB coordinates (L_j*=37±3; a_j*=13±2; b_j*=10±4) of the orange juices extracted from HF oranges, that significantly differed from those (L_j*=42±3; a_j*=12±2; b_j*=14±5) of the juices squeezed by MF and LF oranges. On the contrary, whatever the firmness class of the orange fruits the resulting juices did not statistically differ in the total soluble solid content (TSS=11.7±0.5°Brix) and titratable acidity (TA=1.38±0.04 % w/v of citric acid). This was also congruent with the panel assessment of the great majority of the sensory descriptors, namely shape (7±2), shape defects (3±2), typical orange odour (7±2), off-odour (2±1), juiciness (7±2), acidity (4±2), sweetness (5±2), bitterness (2±1), typical orange flavour (6±2), off-flavour (2±2), and overall sensory evaluation (6±2). Moreover, the sensory professionals recognized the greater compactness (7±2) and lower peeling (4±2) and segment separation (4±2) easiness of the HF oranges, while they were unable to discriminate the corresponding sensory descriptors (5±2; 6±2; 5±2) pertaining to the orange fruits grouped in the MF and LF classes.

Therefore, orange fruits differing in a range of MT or (F/D) firmness of 40-86 N or 220-320 N m^{-1}, respectively, were not discriminated by sensory panellists, even if for the oranges assayed the range of MT or (F/D) firmness was by far wider (40-123 N or 220-420 N m^{-1}).

5. Conclusions and future perspectives

Two image analysis-based methods (i.e., EFA and bounding box), set up in this PhD thesis, allowed accurate assessment of the contact area between the plates and specimen during parallel plate compression, this being quite greater than that estimated using the ASABE standard method (2008). However, none of them can be recommended as routine procedures to sort on-line citrus fruit, even if they might be useful to for cultivar characterization.

By resorting to the thin shell theory (Carin et al., 2003), it would be possible to characterise orange fruit firmness by replacing the stress exerted in the orange rind with the fruit resistance per unit diameter (F/D), as shown in Fig. 3c. Since Tarocco orange fruits behaved as linear viscoelastic solids for compression strains up to 20%, non-destructive determination of the fruit resistance at a compression strain of 5% gave rise to negligible fruit mass (0.04±0.03%) and limited volume (2±1%) losses. Thus, such a parameter may be regarded as a sensitive tool to pilot efficiently industrial high-speed orange fruit sorting lines. Since for all the specimens tested there was no statistically significant difference in terms of overall sensory evaluation (6±2), it would be reasonable to grade only the orange fruits with specific resistance (F/D) varying within a deviation band of 220-420 N m^{-1}.

Further work is needed to validate this operating procedure on a continuous pilot-scale sorting line.

6. References

ASABE Standards (2008) Standards Engineering Practices Data. Compression test of food materials of convex shape. America Society of Agricultural and Biological Engineers, 55th edn., pp. 671-678, ASABE, St. Joseph, MI, USA.

Carin M, Barthès-Biesel D, Edwards-Levy F, Postel C, Andrei DC (2003) Compression of biocompatible liquid-filled HAS-Alginate capsules: determination of the membrane mechanical properties. Biotechnol Bioeng 82: 207-212.

Costa C, Menesatti P, Paglia G, Pallottino F, Aguzzi J, Rimatori V, Russo G, Recupero S, Reforgiato Recupero G (2009) Quantitative evaluation of Tarocco sweet orange fruit shape using opto-electronic elliptic Fourier based analysis. Postharvest Biology and Technology 54: 38-47.

García-Ramos FJ, Valero C, Homer I, Ortiz-Cañavate J, Ruiz-Altisent M (2005) Non-destructive fruit firmness sensors: a review. Spanish Journal of Agricultural Research 3(1): 61-73.

Howarth MS, Shmulevich I, Raithatha C, Ioannides Y (2003) Online non-destructive avocado firmness assessment based on low-mass impact technique. In Proceedings V World Avocado Congress (Actas V Congreso Mundial del Aguacate), pp. 679-685.

Menesatti P, Pallottino F, Lanza G, Paglia G (2009) Prediction of blood orange MT firmness by multivariate modelling of low alterative penetrometric data set: A preliminary study. Postharvest Biol Technol 51: 434-436.

Nussinovitch A, Peleg M, Normand MD (1989) A modified Maxwell and a nonexponential model for characterization of the stress relaxation of agar and alginate gels. J Food Sci 54: 1013-6.

Pagliarini E (2002) Valutazione sensoriale: aspetti teorici, pratici e metodologici. Ulrico Hoepli Editore, Milano.

Pallottino, F. (2008) Rheometrical Characterization and Firmness Assessment of Citrus Cultivars by Non-Destructive Tests. In Proceedings of the 13th Workshop on the Developments in the Italian PhD Research on Food Science and Biotechnology, Alba (Italy), 10-12 September, pp. 554-555.

Pallottino F (2009) Use of image analysis to asses the effective surface area of orange fruit submitted to uniaxial compression tests. In Proceedings of the 14th Workshop on the Developments in the Italian PhD Research on Food Science and Biotechnology, Oristano (Italy), 16-18 September, pp. 337-339.

Pallottino F, Costa C, Menesatti P, Moresi M (2009) Compression testing of o-range fruit. In Proceedings of the 9th International Conference on Chemical and Process Engineering, Roma (Italy), 10-13 May, Chemical Engineering Transactions 17, 885-890.

Pallottino F, Moresi M, Giorgi S, Menesatti P (2010) Orange fruit rheometrical characterization using stress-relaxation tests. In Proceedings of the XVIIth Congress of the International Commission of Agricoltural and Biosystem Engineering (CIGR), Quebéc City, Canada, 13-17 June, pp. 256.

Rao MA (1992a) Measurement of viscoelastic properties of fluid and semisolid foods. In Viscoelastic properties of foods, MA Rao and JF Steffe (Eds) pp. 207-231, Elsevier Applied Science, London.

Rao VNM (1992b) Classification, description and measurement of viscoelastic properties of solid foods. In Ibidem, pp. 3-47.

Ruiz-Altisent M, Ortiz-Canavate J (2005) Instrumentation and procedures for commercial non-destructive determination of firmness of various fruit. ASAE Paper n°056176.

Shmulevich, I., Galili, N., & Howarth, M.S. (2003) Non destructive dynamic testing of apple for firmness evaluation. Postharvest Biology and Technology 29: 287-299.

UNI 8589 (1990) Analisi sensoriale – Criteri generali per la progettazione di locali destinati all'analisi. Ente Nazionale Italiano di Unificazione, Milano.

USDA (2003). Agricultural Marketing Service. Available at: www.ams.usda.gov/AMSv1.0/getfile?dDocName=STELPRDC5050384. Accessed Febr., 15th, 2010.

Valero C, Bowerman E, Crisosto CH, Garner D, Slaughter D (2003) Introducing Nondestructive Flesh Color and Firmness Sensors to the Tree Fruit Industry. Acta Horticolturae 604: 597-600.

Introduction

The orange *Citrus sinensis* [(L.) Osbeck], is the most cultivated citrus fruit in Italy. Seventy percent of the citrus fruit is pigmented while the remaining is blond. Citrus fruits and juices generally serve as primary sources of human daily requirement of vitamin C, their demand for and acceptance depending mainly on their nutritional value, flavour, aroma and then on colour, texture and cloudiness (Tressler & Joslyn, 1961).

Among citrus fruits there is currently a growing interest for blood orange fruit, a natural variety of *Citrus sinensis*, with crimson, blood-coloured flesh owing to the presence of anthocyanins (Rapisarda et al., 2000), highly recommended to reduce the risk of heart disease, some types of cancer, and low-density lipoprotein (LDL) cholesterol accumulation (Wrolstad, 2001; Hou, 2003).

In the pigmented group, the tree most common types are "Tarocco" cultivar (native to Italy), "Sanguinello" (native to Spain) and "Moro" (native to Italy) (Hodgson, 1967). Among the pigmented varieties, "Tarocco" has registered an almost constant increase. These varieties show, in comparison with the blond oranges, higher biological properties due to the content of anthocyanins (Bonina et al., 1998; Maccarone et al., 1998; Rapisarda et al., 2001). Another peculiar characteristic of pigmented oranges is the better taste and high concentration of vitamin C (Rapisarda & Russo, 2000). New markets (Japan, North America, Australia), owing to the health-benefiting properties of pigmented oranges, have shown interest in their importation.

In details, the Tarocco is a seedless medium-sized fruit that is perhaps the sweetest and most flavorful of the three types. In fact, owing to its °Brix-to-acid ratio generally above 12.0, juiciness and ease of peeling, the Tarocco is the most popular table orange fruit in Italy and is presently preferred to blond ones in the above mentioned markets.

Unfortunately this variety normally shows lower firmness with respect to the blonde orange. This is the main cause for the fruit persistent deformation, especially after long-term shipping to the abroad markets (Menesatti et al., 2009) thus causing the rejection of the entire fruit stock (Rivero et al., 1979; Menesatti et al., 2009).

Furthermore fruit quality attributes, such as size, absence of defects, colour and “firmness”, can be measured by several different methods, all these attempting to grasp the way the general consumer perceives and interprets the fruit quality. Actually, when picking a fruit piece a consumer tends to squeeze it gently by hand to assess instantaneously its ripeness.

The presence in Italy of *Ceratitis capitata* (Wiedemann), or Mediterranean fruit fly, restricts access for Italian citrus fruit to some world markets because of plant quarantine regulations. Citrus intended for export to some overseas markets requires postharvest treatments to eliminate the presence of insect pests that are of quarantine significance. Several importing countries allow fresh citrus from competing regions if it has undergone cold treatment. Cold treatment is an approved method to control medfly and replaces fumigation with methyl bromide that has been banned in many countries. It involves storage of fruit at low temperature for specified periods to ensure their freedom from insects (Lanza et. al., 2005). The period of time and temperature required are defined in protocols established by phytosanitary authorities of the importing countries. At the arrival the product is normally evaluated for the presence of defects, appearance and texture (Oranfrizer, 2008).

Fruit lacking firmness loses its fresh look and becomes less readily marketable (Sarig & Nahir, 1973) and, as mentioned before, is associated to increased deformation, that is the major problem for long distance shipped fruit (Rivero et al., 1979). The reference test today still taken into consideration when evaluating fruit firmness can be identified with the Magness-Taylor test (MT) (Kader, 2002). Such a test uses a hand-held penetrometer, also known as *fruit pressure tester* (Magness & Taylor, 1925), and gives a direct measure of the peak force at rupture. Such a force has been used as an index of maturity and firmness for several different crops, especially apples (Reid, 1985; DeLong et al., 2000), where the time course of fruit firmness can be detected by measuring the force required to puncture the fruit surface. Even if in citrus fruit, the relationship between puncture pressure and firmness is obfuscated by differences in tissues types directly under the puncture probe, the test has been used as index of firmness (Turrell et al., 1964; Oberbacher, 1965; Ferguson et al., 1982; Coggins & Henning 1988).

In many countries, generally for oranges, firmness is not measured with standard methods, but it is considered an important parameter to evaluate of quality according to the standards for grades used in many importing countries (USDA, 2003).

The MT hand-held test do not ensure homogeneous readings likely the electronic ones available nowadays which provide more standardized methods (Bourne, 1974; Harker et al., 1996; Lehman-Salada, 1996; DeLong et al., 2000).

Different non-destructive (ND) systems for firmness prediction, in relation to MT or other textural parameters (e.g. elasticity), have been studied for over 40 years.

These systems are mainly based on three approaches: spectroscopic techniques in the visible near infrared or near infrared spectral range (VIS-NIR or NIRS), acoustic and impactive response; contact devices.

Ruiz-Altisent & Ortiz-Canavate (2005) indicate that it is very difficult to get direct measurement of fruit firmness using VIS and NIR systems. Also Peano et al. (2006) found that firmness prediction by NIRS in nectarines appeared to be cultivar dependent and not sufficiently accurate. Gómez et al. (2006) found instead a good correlation between destructive compression and VIS-NIR values in citrus texture (mandarin). Also personal communication with Italian producer of optical selectors underlines that prediction of the MT firmness results difficult through NIR and VIS-NIR techniques, because these cannot achieve a standard error of prevision (SEP) namely equal or lower then 8-10 N.

Wang et al. (2006) found that acoustic impulse response gives a good indication of firmness change for mandarin during storage, although the test refers to compression force.

Valero et al. (2003) show good correlations between MT firmness and ND index obtained by commercial contact device on different fruit, not including citrus fruit.

Therefore, the assessment of the rheometrical and textural characteristics of citrus cultivars appears to be crucial for their selection and commercialization, since they affect the consumer choice (Steenkamp, 1997).

Among the fruit testers used in practice but not commercialized at industrial level, it is worthy citing the Durofel instrument (Agro-Technologie, Tarascon, France), equipped with 10-, 25- or 50-cm^2 flat probes to measure the force at a prefixed deformation, or the Analogue/Digital Firmness Meter (DFM) (Commonwealth Scientific & Industrial Research Organisation, CSIRO, Clayton South, Australia), that measures the fruit deformation under a 40-mm flat probe charged with 500 g for 30 s (Barreiro et al., 2004).

Similarly, other techniques based on VIS or NIRS spectroscopy, impaction or acoustic impulse resonance frequency (AIF) have so far exhibited inaccurate results (García-Ramos et al., 2005; Ruiz-Altisent & Ortiz-Canavate, 2005), unless they are operated in a destructively manner or two or more systems are used together to improve flesh firmness prediction. In particular, it is worth citing their use in combination with non-destructive flesh colour readings (Valero et al., 2003), as successfully tested to determine the optimum harvest date and quality characteristics of apple (Zude et al., 2006) or mandarin fruit (Gómez et al., 2006), respectively, or with artificial neural network software to predict kiwifruit firmness (Ragni et al., 2010).

Nowadays, just two non-destructive on-line high-speed systems have been developed and commercialised for testing the firmness of individual fruits by resorting to the so called *impact methods* coping with the free fall of the fruit over a force (piezoelectric) sensor or vice versa. In particular, the *Intelligent Firmness Detector* (iFD, Greefa, Trich, NL) consists of a wheel equipped with piezoelectric sensors with a maximum capability of 12 fruit pieces per second per lane (www.greefa.nl). Alternatively, the *Sinclair Internal Quality-Firmness Tester* (SIQFT, Sinclair Systems International, Fresno, CA, USA) uses several heads, each one capable of injecting compressed air over a piezoelectric element placed on the tip of a bellow (Harrison, 2003; Howarth et al., 2003). Any of this bellow impacts on moving fruits and this generates a voltage that is converted into a firmness index ranging from 1 to 100, the lower value representing the softer fruit, this allowing up to 10 fruits/s per lane to be tested (Sinclair In., 2008). Despite such a system has been successfully applied to grade apples, avocados, mangoes, peaches, plums, and kiwifruits (Howarth et al., 2003; Valero et al., 2003), its application to citrus fruit sorting is still undocumented.

The only standard practice to assess the firmness of fruit presenting convex shape is reported by the American Society of Agricultural and Biological Engineers (ASABE). Even their standard methodology (ASABE, 2008) applied in this research resulted inaccurate, despite it is recommended to determine the resistance to mechanical injury of food materials of convex shape. It relies upon the determination of the radii of curvature of the convex surfaces of any sample at the points of contact with the upper and lower plates of the dynamometer as well as the *a priori* knowledge of Poisson's ratio (ν) of the food material under testing, so as to estimate the contact area of the fruit undergoing compression.

In food materials, linear viscoelasticity is often observed at strains smaller than 1%, although for fresh fruits and processed foods, such as frankfurters, it was found to be as great as 1.5-3.0% (Mohsenin & Mittal, 1977) or 3.8% (Skinner & Rao, 1986), respectively.

Knowledge of the viscoelastic properties of food and agricultural products is useful to predict internal stress and cracking during harvesting, handling, transportation, processing, and storage. Since in viscoelastic material stress relaxation and strength properties are time dependant, it is necessary to identify its relaxation time spectrum in order to estimate how fast the material dissipates stress after receiving a sudden deformation.

The basic of stress relaxation testing is reported in several technical books, such as Bourne (2002), Rao & Steffe (1992), Steffe (1996), etc. Recently, stress relaxation data were used to supply information about fruit ripening (Hassan et al., 2005), fruit firmness (Blahovec, 1996), staling of cereal products (Limanond et al., 2002), phenomenon of checking, that is delayed fracturing in cracker structure (Kim & Okos, 1999), cooking behaviour of various spaghetti types (Sozer & Dalgic, 2007), response of reconstituted cassava dough to different processing conditions (Rodríguez-Sandoval et al., 2009), as well as several solid-like foods of the bulky or spongy type, such as agar gel, meat, ripened cheese, mozzarella cheese and white pan bread (Del Nobile et al., 2007). No data on the rheological behaviour of citrus fruits are currently available.

Actually, in the aforementioned sorting systems pre-graded fruits of about the same size are continuously tested by measuring their resistance (F_z) at a prefixed small strain (ε_z) in order to select just those with a resistance falling within a pre-defined acceptable standard deviation band.

To apply efficiently such a grading system, it is essential to know which is the critical fruit resistance, as well as the difference in orange fruit firmness, that the average consumer is able to detect. For instance, apples differing in firmness by 5 to 15 N were barely discriminated by sensory panellists, as a consequence of memory visual and auditory interference effects (Harker & Hallett, 2004). Nevertheless, the firmness for the apples sold in the marketplace was found to range from 50 to 100 N. Thus, a discrimination threshold of 5-15 N was regarded as too much sensitive to pilot efficiently an industrial high-speed apple sorting line (Harker & Hallett, 2004).

The limited knowledge about the non-destructive evaluation of citrus fruit firmness in relation to an industrial application suggest an urgent need for novel tests capable of assessing the mechanical properties of citrus fruit in a more objective and reproducible way (Menesatti et al., 2009).

The primary goal of this PhD thesis was to develop the sorting rule to assess mechanically citrus fruit firmness in a fast, reproducible, no-destructive way so as to be applied in a continuous sorting belt to select on-line more consistent blood oranges to export;

To achieve such a goal it was necessary to investigate finely the rheo-metrical properties of Tarocco orange fruit via compression and stress-relaxation tests with simultaneous assessment of the real fruit-plate contact area. This knowledge is expected to help genetists in breeding firmer varieties.

In details, this was accomplished by resorting to stress-relaxation tests in order to assess the range of linear viscoelastic engineering strains and determine the maximum strain applicable with no permanent fruit deformation. This information was expected to be useful to fill the gap concerning basic rheometrical properties and to develop methods to measure on-line citrus fruit firmness without any irreversible structural changes resulting from orange fruit cell rind rupture and/or albedo air release.

Moreover, to fulfil the gap between instrumental selection and consumer perception of the firmness it was attempted to extract a sorting rule for Tarocco orange fruit from a series of chemical-physical and sensory tests performed on a marketable lot manually pre-graded at the farm gate.

Chapter 1: State of the Art on Fruit Quality and Firmness Measurement

1.1 Introduction

Consumers are more and more demanding high quality citrus fruits, especially in terms of fruit taste, appearance, shape, and consistency, as well as purity and freshness of citrus juices. Furthermore they ask for being informed about the food they are consuming through appropriate labelling, tracking and traceability schemes.

The attributes important to producers, Large Organized Distribution (LOD) and consumers declared in the Codex Alimentarius (Stan 245, 2004) are referring to commercial varieties of oranges grown from *Citrus sinensis* to be supplied fresh to the consumer, after preparation and packaging. Oranges for industrial processing are excluded. Normally the parameters to respect are set by the standard as follows.

1.1.1 Provision Concerning Quality

1.1.1.1 Minimum Requirements

In all classes the oranges must be: -whole with no rotting or deterioration; -clean, practically free of any visible foreign matter; free of pests affecting the general appearance of the produce; free of damage caused by pests; free of abnormal external moisture; free of any foreign smell and/or taste; free of damage caused by low and/or high temperatures; free of damage caused by frost; free of signs of internal shrivelling; practically free of bruising and/or extensive healed-over cuts.

The oranges must have been carefully picked and have reached an appropriate degree of development and ripeness.

The development and condition of the oranges must be such as to enable them to withstand transport and handling and to arrive in satisfactory condition at the place of destination.

1.1.1.2 Maturity Criteria

The maturity of oranges is defined by the different parameters such as colouring, and the minimum juice content calculated in relation to the total weight of the fruit, and after extraction of the juice by means of a hand press.

The degree of colouring should respect the normal development; the oranges reach their normal variety colour at their destination point, taking into consideration the time of picking, the growing area and the duration of transport.

Colouring must be typical of the variety. Fruits with a light green colour are allowed, provided it does not exceed one-fifth of the total surface area of the fruit.

Oranges produced in areas with high air temperatures and high relative humidity conditions during the developing period can be of a green colour exceeding one fifth of the total surface area, provided they satisfy the minimum juice content requirement. This last in the case of blood oranges is equal to the 30%, for navels group equal to the 33% and the remaining varieties the 35%.

1.1.1.3 Classification

Oranges are normally classified in three classes defined as:

i) EXTRA Class - Oranges in this class must be of superior quality. In shape, external appearance, development and colouring, they must be characteristic of the variety and/or commercial type. They must be free of defects, with the exception of very slight superficial defects, provided these do not affect the general appearance of the produce, the quality, the keeping quality and presentation in the package.

ii) Class I - Oranges in this class must be of good quality. They must be characteristic of the variety and/or commercial type. The following slight defects, however, may be allowed, provided these do not affect the general appearance of the produce, the quality, the keeping quality and presentation in the package: -slight defect in shape; slight defect in colouring; slight skin defects occurring during the formation of the fruit, such as silver scurfs, russets, etc.; slight healed defects due to a mechanical cause such as hail damage, rubbing, damage from handling, etc. The defects must not, in any case, affect the pulp of the fruit.

iii) Class II - This class includes oranges which do not qualify for inclusion in the higher classes, but satisfy the minimum requirements of maturity. The aforementioned defects, however, may be allowed, provided the oranges retain their essential characteristics as regards the quality, the keeping quality and presentation.

1.1.2 Fruit Size

Size is determined by the maximum diameter of the equatorial section of the fruit and indicated by 13 classes of which the 1st shows diameters in the range 92-110 mm and the 13th in the range 53-60 mm. Oranges of a diameter below 53 mm are excluded. Oranges may be packed by count. In this case, provided the size uniformity required by the Standard is retained, the size range in the package may fall outside a single size code, but within two adjacent codes.

1.1.3 Tolerances

Tolerances in respect of quality and size of the fruit shall be allowed in each package for product that do not satisfy the requirements of the class indicated. About the tolerances in terms of the quality for the EXTRA Class are of the 5% by number or weight of oranges, the 10% for the Class I and the Class II.

In terms of size tolerances for all classes is of the 10% by number or weight of oranges corresponding to the size immediately above and/or below that indicated on the package.

1.1.4 Fruit Presentation

The contents of each package must be uniform and contain only oranges of the same origin, variety and/or commercial type, quality and size, and appreciably of the same degree of ripeness and development. The visible part of the contents of the package must be representative of the entire contents. In addition, uniformity of colouring is required for Extra Class. Furthermore oranges must be packed in such a way as to be protected. The materials used for the package must be new, clean and of a quality such as to avoid causing any external or internal damage to the product. Oranges shall be packed in each container in compliance with the Recommended International Code of Practice for Packaging and Transport of Fresh Fruits and Vegetables (CAC/RCP 44, 1995).

The containers shall meet the quality, hygiene, ventilation and resistance characteristics to ensure suitable handling, shipping and preserving of the oranges. Packages must be free of all foreign matter and smell. The oranges may be presented arranged in regular layers in the package. This form of presentation is mandatory for Extra Class and optional for Classes I and II. Class I and II shouldn't be arranged in packages. In individual packages for direct consumer sale of a weight less than 5 kg, either made up by number or by weight of fruit.

1.1.5 Fruit Labelling

The requirements for the Labelling of Prepackaged Foods are dictated by the Codex General Standard (CODEX STAN 1, 1985) as follows. This indicates the information that have to be reported and those optional in both cases consumer packages and non retail ones. The info that often must be included while packing are inherent the origin of the products (country of origin and, optionally, district where grown or national, regional or local place name), the commercial identification (class, size code for fruit presented in accordance with the size scale or the upper and the lower limiting size code in the case of three consecutive sizes of the size scale, size code or when fruit packed by count fall under two adjacent codes, size codes or minimum and maximum diameter in mm), number of fruit, in the case a statement indicating the use of preservatives and the net weight (optional). Official inspection mark may be present.

1.1.6 Fruit Contaminants

All products should comply with the maximum levels of the Codex General Standard for Contaminants and Toxins in Food and Feed (CODEX STAN 193, 1995). The product following this standard need to respect the maximum residue limits for pesticides established by the Codex Alimentarius Commission.

1.1.7 Hygiene

The recommended International Codes of Practice to which orange fruit should regard to is the general Code of Hygienic Practice for Fresh Fruits and Vegetables (CAC/RCP 53, 2003). Moreover the product should comply with any microbiological criteria established in accordance with the Principles for the Establishment and Application of Microbiological Criteria for Foods (CAC/GL 21, 1997).

1.2 Citrus Production and Market

Citrus fruits are the first fruit crop in international trade in terms of value. In the citrus sector it is possible to enucleate the fresh citrus fruits market, with a predominance of oranges, from processed citrus products market, mainly orange juice. Over the last two decades, owing to the different consumer preferences, there has been the growth in the trade of small citrus fruits, such as tangerines, clementines, mandarins and satsumas, at the expense of fresh oranges.

World production of citrus fruit has experienced continuous growth in the above last decades. Total annual citrus production was estimated at over 105 million tons in the period 2000-2004, orange fruits accounting for more than half of global citrus production. The rise in citrus production is mainly due to the increase in cultivation areas and the change in consumer preferences towards more health and convenience food consumption and the rising incomes.

Fig. 1.1 shows the evolution of world production for total citrus fruits and the different types of citrus.

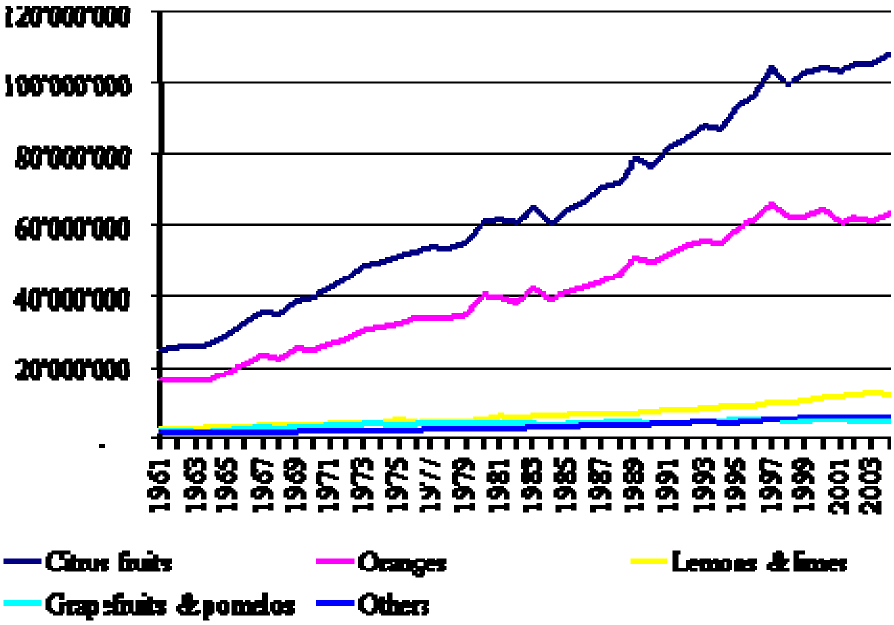

Figure 1.1 World citrus fruit production 1961-2004 (in metric tons), as extracted from FAO data.

Citrus fruits are produced all around the world. According to FAO data, in 2004, 140 countries produced citrus fruits. Most citrus fruits are grown in the Northern Hemisphere, accounting for around 70% of total citrus production. More than two thirds of global citrus fruit production is located in Brazil, the Mediterranean countries, the United States (especially California, Arizona, Texas, and Florida) and China (Fig. 1.2).

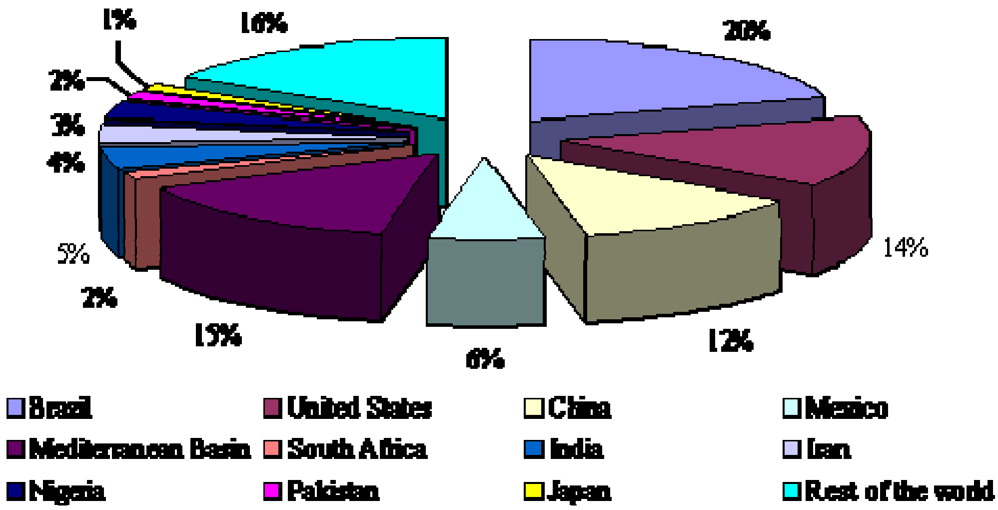

Figure 1.2 Geographical distribution of fresh citrus production for 2000-2004, as extracted from FAO data.

For the different types of citrus fruits, major producing countries are the following, ranked as for 2004 FAO data:

- Oranges — Brazil, United States, Mexico, India, Spain, China, Iran, Italy, Egypt, Indonesia.
- Small citrus — Nigeria, China, Syria, Guinea, Japan, Saudi Arabia, India, Sierra Leone, Angola, Tunisia.
- Lemons and limes — Mexico, India, Iran, Spain, Argentina, Brazil, United States, China, Italy, Turkey.
- Grapefruit — United States, China, South Africa, Mexico, Israel, Cuba, Argentina, India, Turkey, Tunisia.

In the Mediterranean countries, citrus fruits are produced mainly for fresh fruit consumption. Spain is the leading producing country in the area. USA and Brazil are the leading producing countries of processed citrus fruits. In United States most of the production is consumed domestically, as in Asian countries.

As shown in Fig. 1.3, citrus fruits are mainly consumed in developed countries, although consumption per capita is increasing in developing countries, such as Mexico, India, Argentina, Brazil and China, as levels of income increase.

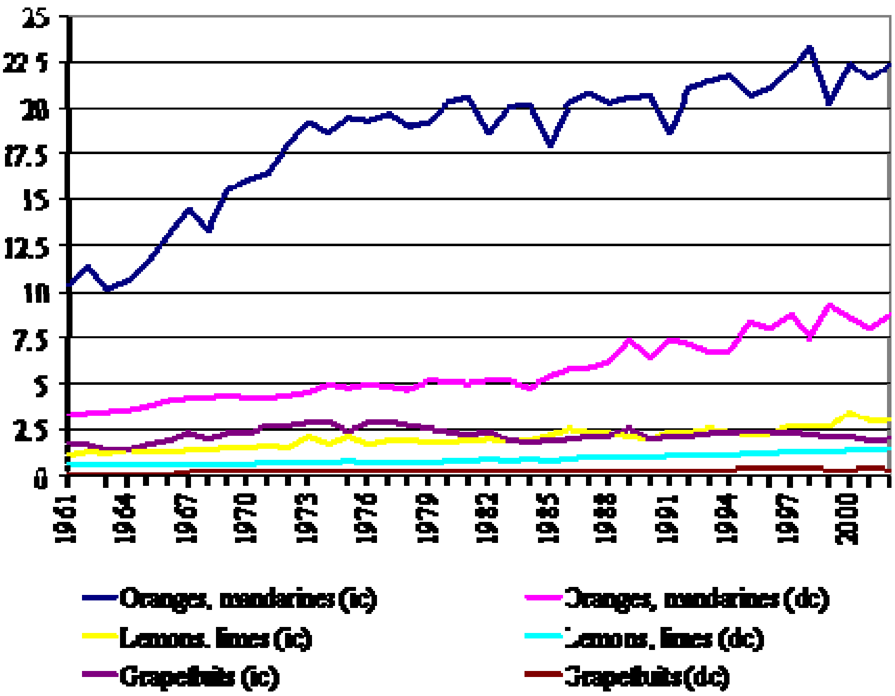

Figure 1.3 Citrus fruit per capita consumption (kg/Cap/yr) in 1961-2002, as extracted from FAO data: ic - industrialized countries, dc - developing countries.

According to FAO, fresh orange consumption is declining in developed countries mainly because it has been replaced by orange juice consumption, as well as improvements in transportation and storage have improved longer availability of substitute fruits.

Exports of fresh citrus fruits represent roughly 10% of total citrus fruit production. Fig. 1.4 shows the time course of citrus fruit exports in 1961-2003.

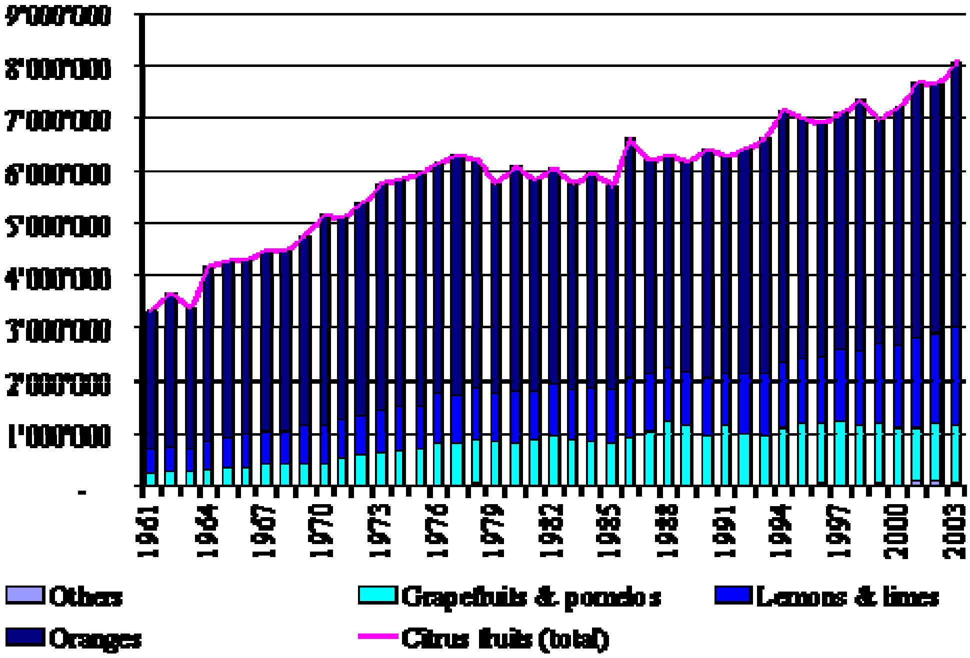

Figure 1.4 World citrus fruit exports 1961-2003 (in metric tons), as extracted from FAO data.

The bulk of exports of fresh citrus fruits is situated in the Northern Hemisphere, accounting for around 62% of world fresh citrus fruit exports in 2003. The Mediterranean region plays a prominent role as fresh citrus exporter, providing nearly 60% of global fresh citrus fruits exports.

Southern Hemisphere countries, such as Argentina, Australia and South Africa are increasing their presence in international trade by providing off-season citrus fruits to the North. This has been favoured by the improvements in storage and transportation technologies.

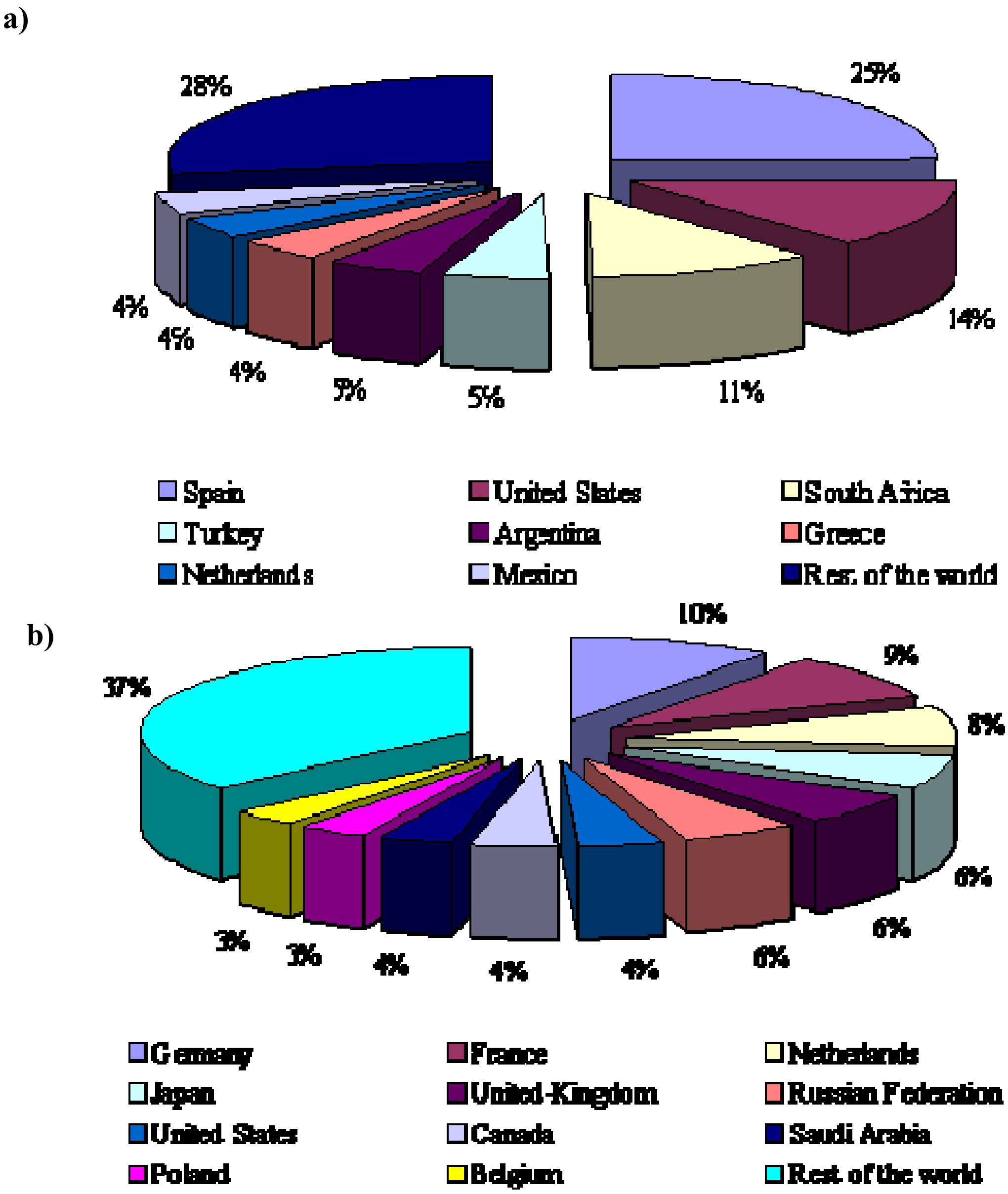

Figure 1.4 Geographical distribution of fresh citrus exports (**a**) and imports (**b**), as averaged for 1999-2003 (FAO data).

The production of citrus fruits is an important part of the Italian fruit and vegetable market. Italy, in fact, turns out to be among the largest producers of blood oranges recognized and identified with the EU label PGI (*Protected Geographical Identification*). The cultivar Tarocco, Moro and Sanguinello, produced in Sicily on a large scale, recently did generate a considerable interest, especially in the emerging markets of Japan, North America and Australia. This interest is due to their organoleptic properties and nutraceutical values that are significantly greater with respect to blond oranges (Bonina et al., 1998; Maccarone et al., 1998; Rapisarda & Russo, 2000), most commonly sold in international markets. Another feature of blood oranges appear to be the best tasting and highest concentration of vitamin C (Rapisarda & Russo, 2000).

1.3 Assessment of Citrus Quality

Fruit quality is quite a complex characteristic, being related to qualitative aspects regarding internal (sugar content, firmness, acidity, etc.) and external (external defects, shape, size, colour, etc.) attributes. Nowadays there is an increasing demand for high quality products which is leading to the development of sensors suitable for an objective and fast online determination of the fruit properties. The companies involved in citrus products logistics and packaging need to measure the diverse quality parameters in a non-destructive way.

Therefore, several research groups and manufacturers are currently attempting to develop novel sensors and evaluation protocols. On the other hand, the assessment of the physical and mechanical properties of fruits is useful to direct genetic and plant breeding studies towards new varieties and clones with specific characteristics to satisfy specific market and consumers.

The hardness, or firmness, is one of the most important quality index representing an indirect measure of maturity that, if carefully evaluated, allows the definition of the appropriate storage times and conditions of carriage (García-Ramos et al., 2005). More generally, the texture of a food product is defined by the British Standards Institution as *the attribute of a substance resulting from the combination of physical properties perceived by the senses of touch (including kinesthetic and palatability) vision and hearing* (Anonymous, 1975). The texture is also defined as an attribute that can be defined only in a sensorial way (Brennan, 1984). The firmness is a qualitative concept that represents only a small part of the sensations of texture in the mouth. Even if the texture is described in sensorial terms, such as juiciness and crispness, instrumental measures may define the mechanical properties of the tissues of fruits in terms of strength and compression energy (García-Ramos et al., 2005).

Each of the different mechanical properties measured instrumentally describes the firmness or texture in a particular way. Conventionally available instruments for measuring firmness are sensitive to a particular mechanical property, as the force required to produce a deformation or the answer/ propagation of an impulse of light, sound, etc.

1.4 Citrus fruit: Firmness Characterization and Evaluation

Rheometrical properties and texture characteristics are crucial for the selection of new cultivars being highly influential on the consumers' choice.

Indeed, the stocks for export are usually evaluated for the presence of defects, appearance and texture. Among the controlled parameters special attention is given to the hardness or firmness (USDA, 2003). The lack of consistency is generally associated to a loss of product freshness (Sarig & Nahir, 1973). A decrease in the hardness of the fruit also compromises the possibility for the fruit to recover its initial spherical shape, this yielding persistent deformations, especially after being boxed for long-term shipments, (Rivero et al., 1979), and resulting in the rejection of the entire stock (Oranfrizer, 2008). Another example of the importance of the rheometrical characteristics of citrus fruits is proved by several researches aimed at assessing the effectiveness of gibberellins to extend or increase elasticity and hardness of citrus fruits (Porat et al., 2001; Di Martino Aleppo et al., 2002; Fidelibus et al., 2002; Tumminelli et al., 2005; D'Aquino et al., 2006).

At the moment the reference test for assessing the firmness is the MT test, generally used on various fruits, especially apples (Reid, 1985; Kader, 2002; Shmulevich et al., 2003). The test makes use of a manual penetrometer, also known as "fruit pressure tester", which records the maximum force (in N) necessary for penetrating a probe into the fruit flesh. For instance, by monitoring the loss of such a force over time it was possible to account for apple maturity (DeLong et al., 2000).

In citrus fruits, the relationship between penetration force and firmness is obfuscated by the types of tissue immediately beneath the probe that is the fruit pericarp. Moreover, this test, being manually operated, does not ensure consistent and reproducible readings with respect to alternative tests using electronic devices

(Bourne, 1974; Harker et al., 1996; Lehman-Salada, 1996; DeLong et al., 2000; Shmulevich et al. 2003). Nevertheless, the penetration test is still used as an index of firmness for citrus fruit although several authors demonstrated its inappropriateness for such purpose and characterization (Turrell et al. 1964; Oberbacher 1965; Ferguson et al. 1982; Coggins & Henning 1988), being applicable just on a stock sample.

For several years several non-destructive testing systems have been studied to predict firmness by referring to the MT index or other parameters related to texture, such as elasticity, with normally poor results. These systems are generally based on three different approaches:

- spectroscopic analysis of the reflectance in the VIS-NIR or NIR;
- techniques analyzing the responses to acoustic or impactive stimulus;
- mechanical techniques operating by contact.

Ruiz-Altisent & Ortiz-Canavate (2005) assessed the poor performance of firmness prediction using spectroscopy in both VIS and NIR ranges.

Gómez et al. (2006) found a good correlation between destructive compression tests and VIS-NIR spectral analysis in the case of mandarin cultivars.

In a recent paper by Menesatti et al. (2009), it was attempted to correlate the response, i.e. the force-deformation curve, collected during non-destructive penetrometric tests and the MT index for citrus fruits, as reported by the work, with a predictive value of r=0.76 and a SEP of about 3 N, accounting approximately for the 8.4% of the average force appreciated while compression at 3% of H_0 of the fruit, as a results of the Partial Least Squares (PLS) applied. In such a work the MT values were used as Y to be predicted ($Y^{'}$) using as X variables all the force values interpolated composing the whole curve up to the 3% of deformation.

Wang et al. (2006) observed that the response to a noise impulse may be used as a good indicator of firmness for mandarins during storage when referring to a compression, not the classic MT, penetrometer test. Another positive experience is represented by the industrial instrument iQ Firmness Tester designed and marketed by Sinclair International (Fresno, CA, United States), apparently based on inertial systems, even if no details have been disclosed for a proper evaluation on this sorting system for citrus fruits.

1.5 Systems for Citrus Fruit Firmness Determination

These tests involve the measurement of several variables, extracted from non-destructive force-deformation curves or deformation under a given impact force, acoustic responses to vibrational or impactive stimuli, measurement of the optical properties and nuclear magnetic resonance (NMR). Such techniques have been used to assess the firmness of different fruits, but they have rarely or never been applied to citrus fruits. The NMR technique has been waived for the high equipment cost when referring to the application of concern.

1.5.1 Sensors Based on Force-Deformation Curves Determination

These sensors were developed by accounting for the Hertz theory that is valid for an elastic body. In the circumstances, when one of the body is a fruit and the other is a flat plate or a rounded or spherical probe, the compressive stress between these bodies is directly proportional to their elasticity moduli and inversely proportional to their radii.

By applying a small force of deformation, so as to avoid any damage, use of a piezoelectric sensor or a spring positioned opposite to the probe tip allows the non-destructive force-vs.-deformation curve to be recorded.

Such a curve is generally produced in two ways, that is by applying a small load for a certain period of time (Macnish et al., 1997) or by determining the force required to achieve a deformation default (Fekete & Felfoldi, 2000). These techniques producing micro-deformation allowed several instruments to be developed, such as:

1) the device developed by CEMAGREF (*Centre National du Machinisme Agricole, du Génie Rural, des Eaux et Forêts*), where a sensor detects the force exerted by the fruit when a probe ball applies a deformation of about 2

mm (Steinmetz et al., 1996), thus showing an index of firmness on a special scale.

2) The DUROFEL, developed by COPA Technology in collaboration with CTIFL (*Centre Interprofessionnel des Fruits et Techniques Légumes*), is an instrument equipped with three interchangeable tips having metallic flat heads with areas of 10, 25 or 50 cm^2, built on the base of the former Durometer Shore A (nowadays produced by a number of companies) which measures the depth of an indentation in the material created by a given force on a standardized presser foot where this depth is dependent on the hardness of the material, its viscoelastic properties, the shape of the presser foot and the duration of the test. The hardness values, measured in the case of the DUROFEL in a destructive manner, are obtained by penetrating one of the three probes into the pulp of the fruit and expressed by an index ranging from 0 to 100. Analogical versions of this instrument, equipped with arms or spring, electronic sensors and digital display interfaced with a PC, have been widely used to assess the firmness of apricots (Jay et al., 2000), tomatoes (Planton, 1991), cherries (Clayton et al., 1998), etc… .

3) the *Analogue Firmness Meter* (AFM) and the *Digital Firmness Meter* (DFM), developed by CSIRO (Commonwealth Scientific and Industrial Research Organisation) were tested on tomatoes and mangoes, respectively (Macnish et al., 1997). In the first case, the fruits are placed in a V-shaped structure and a load of 500 g is applied using a disk with of a diameter of 40 mm connected to a gauge that measures the displacement after the load has been applied for 30 s. In the second case, the device was quite similar, but analogical. It is worth noting that the application of a fixed load on fruits with different diameters leads to very different deformations.

4) the instrument, known as *Laser-Air Puff*", was developed by HortResearch. It operates on the same principle by applying the force using an air jet at 69 kPa for 100 ms (Hung et al., 1998). McGlone et al. (1999) successfully tested this system on kiwifruits, thus suggesting its usage for soft fruits only.

1.5.2 Inertial and Impact Devices

Even these devices using inertial methods are based on the theory of elastic bodies (Timoshenko & Goodier, 1951).

Chen & Ruiz-Altisent (1996) simulated the impact of a fruit on a hard surface, or vice versa the impact of a sphere on a fruit, as that between two elastic bodies, by assuming that the intensity and duration of the impact were directly related to firmness of the fruit. Traditionally, this methodology was adopted for assessing the susceptibility to mechanical damage of onions (Jarén, 1994), even if Mohsenin (1970) was the first using such a technique to study the fruit firmness by resorting to a pendulum. For instance, Desmet et al. (2002) applied such a devise to test tomato firmness.

Impact sensors generally operate in two ways:

a) so as to hit the target with a product that includes the sensor element;

b) so as to place the fruit on a load cell and drop a known weight on it.

Chen et al. (1985) developed a tool to measure the impact response of the fruit to a small hemispherical mass, connected to an accelerometer and dropped from a given height on the fruit. Different studies proved that the best results were associated to small masses (Jarén, 1994; Chen & Ruiz-Altisent, 1996). This system was subsequently adopted to estimate non-destructively the firmness of apples and pears (Jaren & García-Pardo, 2002) and that of peaches in combination with spectroscopic techniques in the infrared range (Ortiz, 1999). Such a technique was subsequently combined to IR spectroscopy to assess the firmness of apples (Salvatores et al., 2000) and peaches (Ortiz et al., 2001).

Chen & Ruiz-Altisent (1996) developed a new side impact sensor hitting the fruit via an arm with a ball nose connected to a piezoelectric accelerometer to estimate the firmness on the assumption that the impact was similar to that between two elastic spheres. Chen (2001) described the amplitude of the peak strength in relation to the characteristics of the fruit and ball impact speed, mass, Poisson's ratio, modulus of elasticity and bending radius of their point of contact.

This approach has led to the development of a portable field gun (Chen & Thompson, 2000; Chen et al., 2000).

Another technique previously used by Moltó et al. (1996) was to place the fruit on a load cell and hit it with a mass of 128 g by a known height of 1 cm.

These techniques have been implemented in several production lines for sorting fruits according to their hardness. The properly adjusted side-impact sensors were mounted on a conveyor belt at the University of California (Davis) with a capacity of 6 fruits per second for peaches and apples (Chen & Ruiz-Altisent, 1996). The values obtained were related to the MT index, the coefficient of determination (r^2) being 0.84 for peaches and 0.40 for apples (Tjan, 1997; Chen & Tjan, 1998). Later, Chen & Thompson (2000) added to this system a second sensor. By averaging the responses of both sensors, it was possible to increase the correct classification of the fruits on the base of their average hardness.

This detection system was improved by García-Ramos et al. (2003), who radically changed its structure, delivery system, electronic and software control system in order to use it in commercial packing lines (Fig. 1.5).

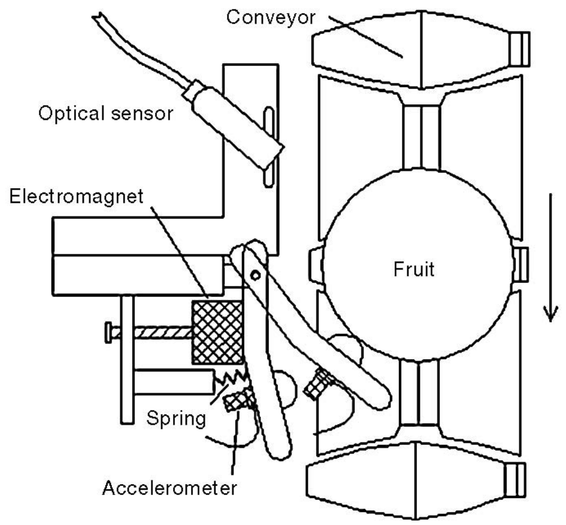

Figure 1.5 Online lateral impact sensor (García-Ramos et al., 2003).

Initial tests showed as this prototype could discriminate in a manner similar to the bench top version, validating an extensive work previously performed. Tests carried out with this sensor by other authors (Homer et al., 2002) on peaches and nectarines showed it to be 88% successful in classifying fruits into three groups of firmness (below and above 10 N) and 82% successful in classifying them into three groups (between 10 and 30 N).

A different system was developed and tested by Moltó et al. (1996), where a load cell was used to record the impact force when a fruit was dropped on it.

Successively, the system used by Moltó was used by Gutiérrez et al. (2003) in combination with NIR sensors with the improving its effectiveness. However, Burgos et al. (2002) reported as the correlation between the sensor responses and MT index was rather poor, with coefficient of determination (R^2) being 0.32 or 0.68 for the two variety of peaches tested, respectively.

All tests mentioned were developed by research groups and are currently in the form of prototypes. Some companies have marketed this kind of devices to estimate on-line of the firmness of various fruits, although little information is available about them. The sensors are typically piezoelectric; thus, they provide an electric voltage proportional to the force of impact:

- The *iFD* (intelligent firmness detector), manufactured by GREEFA, consists of a large wheel provided with multiple heads (sensors) that rotate above the processing line and hit the top surface of the fruit. The system estimates the firmness of the fruit mediating a number of values ranging from 9 to 20 each for a processing speed of 7 fruits s^{-1} (GREEFA, 2008).
- The *Sinclair iQ firmness tester*) uses a measuring head equipped with a group of four sensors that follow each other in each sorting belt. Each piezoelectric sensor is coated with rubber and activated by compressed air. In this way, there is a vertical displacement to hit a processing speed of 10 fruits s^{-1} (Sinclair International, 2008). A table version of the equipment is available for laboratory testing.

1.5.3 Acoustic Sensors: Response to Vibrations

The response of fruit and vegetables to vibrations depends on their modulus of elasticity, their mass and their shape. Different types of vibrations can be used, the most common being acoustic and mechanical (which in some cases are very similar). Using a microphone or a piezoelectric sensor, acoustic methods measure the signal (in the audible range 0-20,000 Hz) issued by the fruit after making it vibrate by means of a small impact. The acoustic signal captured is Fourier transformed and the main frequency calculated. The range varies from 5 MPa for green fruit to 0.5 MPa for overripe fruit (Studman, 1999).

Studman (1999 and 2001) reported the following relationship to estimate the modulus of elasticity (E):

$$E = C\ f^2\ m^{2/3}\ \rho^{1/3} \tag{1.1}$$

where E is the coefficient of elasticity (Pa), C is a constant, f is the frequency for the highest amplitude (Hz), m the mass (kg) and ρ the density (kg m^{-3}).

The acoustic answer is then used to estimate the overall texture of the fruit (Studman, 1999). The theory of vibration analysis assumes that the object is approximately spherical for small elastic deformations. In fact, Abbot & Massie (1998) reported that most of the fruits, in spite of the fact that are viscoelastic body, are treated as elastic bodies when subjected to strains of low magnitude (Diezma et al., 2002).

Other studies have opted for the use of a piezoelectric film instead of a microphone to gather information on the impact (Shmulevich et al., 1996).

A system still different than that experienced by Muramatsu et al. (1997), in which the acoustic impulse is given by a small and powerful speaker while the response is collected through a small microphone on the other side of the fruit.

Different equations based on the modulus of elasticity have been developed in order to obtain a firmness or stiffness index (S) as a function of f (Hz) and m (kg). Abbott et al. (1998) and Fekete & Felföldi (2000) proposed the following equation to estimate the firmness index:

$$S = f^2 m \tag{1.2}$$

where f and m are the frequency and mass, respectively.

This equation was used by De Belie et al. (2000) to measure the firmness of pears in the field, once the fruit was hit near the stem and the frequency recorded by an accelerometer on the opposite side. In a manual prototype, it was developed another correlation between the firmness of apples (S) and their mass, roughly estimated from the average diameter (Landhal et al., 2002):

$$S = f^2\ m^{2/3} \tag{1.3}$$

Different companies have developed tools to assess the firmness based on these principles.

An example is represented by the Acoustic Firmness Sensor (AFS), manufactured by AWETA G&P (HG Nootdorp, Netherlands). This is a laboratory instrument, where the initial impulse is generated mechanically, that was applied to assess the firmness of apples and tomatoes (De Belie et al., 2000).

A second example is the Firmalon Eshet Eilon Ltd. (Kibbutz Eilon, Israele), equipped with three hammers, three piezoelectric sensors and an electro-mechanical system measuring the sonic response to impact (Shmulevich et al., 1996). A force transducer measures the mass compensating the signal. Firmness is estimated by using the average of the two closest first resonant frequencies supplied by the sensors.

1.5.4 Firmness optical measure

Interaction of light with fruit tissue can be used to estimate the internal quality of fruit. Optical systems to assess fruit firmness consists of a light source and a receiver capable of recording different frequencies. Depending on the light path of the signal coming from the sample, two kind of techniques can be identified, namely the *reflectance* (i.e., the fraction of incident light at a specified wavelength that a given surface is able to reflect) and *transmittance* (i.e., fraction of incident light that passes through a sample). Based on the wavelength used by the sensor there are different kinds of spectral analysis in the firmness assessment, but the one that over the years has produced the most satisfactory results operates in the NIR range.

NIR reflectance spectroscopy measures the reflection spectrum of a sample illuminated with a halogen lamp preferably thermally stable.

Lu (2001) attempted to classify different cultivars of cherries by comparing the spectral values with the MT index ranging as follows: <3.5; 3.5-6; and >6 N. The correlation coefficient (r) between spectral values at 800 or 1700 nm and the MT values were 0.8 or 0.65, with a standard error of prediction of 0.55 or 0.44 N, respectively.

Choi et al. (1997) attempted to evaluate the sugar content and hardness of different apple cultivars by using both VIS and NIR spectra. The PLS analysis produced satisfactory results in the case of the estimation of the sugar content (r=0.94), but failed to predict the MT index.

On the contrary, Lammertyn et al. (1998) were able to predict the soluble solids content, acidity, and firmness of Jonagold apples cv using a multisensory approach among which NIR spectroscopy. The authors compared the light spectra with the stiffness factor (acoustic response) and the force/deformation ratio (MT test): the correlation with the former was found to be better (r=0.9 compared to r=0.75).

Using the NIR spectroscopic analysis McGlone et al. (1997) obtained quite a good correlation (r^2=0.70) with the classic penetrometric test in the case of kiwifruits.

Chapter 2: Food Rheometry

2.1 Introduction

Rheology is the branch of science that deals with the flow and deformation of materials. The materials under investigation can range from low-viscosity fluids (i.e., water, wine, beer, and fruit juices) to semisolids and gels (i.e., tomato paste, alginate or κ-carrageen gels) to hard, solid-like (i.e., cheese, meat) food products. A knowledge of the rheological and mechanical properties of various food systems is of paramount importance to design flow processes, control food quality, predict storage and stability measurements, and understand texture.

Most of the pertinent mechanical theories used to describe the rheological behaviour of foods and biological materials were originally developed for non food engineering materials, especially polymers. Since food materials may be highly anisotropic, non uniform, and chemically or physically unstable, this results in strong time-dependent mechanical properties. Moreover, the classical definition of rheology is applied to measure the deformation of most solid-like materials or the flow of predominantly fluid-like ones. Thus, it is difficult to assess clearly the mechanical properties of all foods that simultaneously possess the properties of both solids and liquids.

This chapter will only survey the basic mechanical terminology, as extracted from a few technical books, such as Bourne (2002), Moskowitz (1987), Rao & Steffe (1992), and Steffe (1996), and describe the rheological methods used in this PhD thesis to characterize orange fruit.

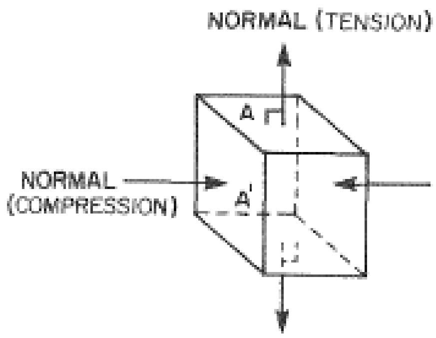

Figure 2.1 Normal and shear forces and stresses.

2.2 Stresses, Strains and Rates

Normal forces (F) are perpendicular to the surface on which they act. They can be either tensile or compressive (Fig. 2.l).

Normal compressive or tensile stress is the compressive or tensile force applied per unit area. If it is calculated by dividing the magnitude of the applied force by the initial area of the specimen (A_o), it is presented as *the apparent or engineering stress*:

$$\sigma_E = \frac{F(t)}{A_o} \tag{2.1}$$

If the force is divided by the momentary cross-sectional area (A(t)) of the deformed specimen, the resulting stress can be defined as a *true stress*:

$$\sigma_T = \frac{F(t)}{A(t)} \tag{2.2}$$

Normal deformation (ΔH) is the absolute elongation (or length decrease) in the direction of the applied force (Figure 2.2). The *apparent* or *engineering* or *Cauchy strain* (ε_E) is the ratio between the deformation and the initial length of the specimen (H_o):

$$\varepsilon_E = \frac{\Delta H}{H_o} \tag{2.3}$$

For large, absolute deformations, it is necessary to subdivide the overall compressive strain into a series of momentary differential strains ($d\varepsilon$), during which the length (H) of the specimen can be assumed to be practically unchanged, thus leading to the so called *natural* or *true strain* as defined by Hencky (Steffe, 1996):

$$\varepsilon_T = \int_{H_o}^{H} -\frac{dH}{H} = \ln\left(\frac{H_o}{H_o - \Delta H}\right) \tag{2.4}$$

When one of these strains is known, the other can be calculated via the following conversion equation:

$$\varepsilon_T = -\ln(1 - \varepsilon_E) \tag{2.5}$$

It can be noted that the engineering strain has a range between 0 and 1.0 (or 100%), while the true strain has a range between zero and infinity. For small deformations, the engineering strain can also be considered as a true strain; for increasing displacements their values more and more diverge.

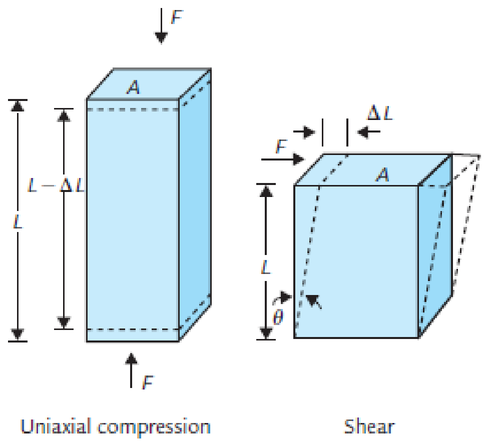

Figura 2.2 Uniaxial compression and shear of an elastic solid. In shear the angle θ equals the shear strain γ.

Shear occurs when a force is applied laterally to a solid body, the lower face of which is stationary (Fig. 2.2). For small deformations, the shear strain (γ) is given by:

$$\gamma = \tan(\theta) = \frac{\Delta L}{L} \qquad (2.6)$$

where ΔL is the deformation, and L is the specimen height. For small deformations the angle θ, expressed in radians, tends to the shear strain, that is

$$\gamma = \tan(\theta) \rightarrow \theta \qquad (2.7)$$

The relationship between the shear stress (τ), that is the applied force parallel to the solid per unit area, and shear strain (γ) is

$$\tau = G\,\gamma \qquad (2.7)$$

where G is the *shear modulus* or *modulus of rigidity*.

Linear elasticity describes those materials in which the strain is directly proportional to the stress, and the strain returns to zero when the stress is removed.

In food materials, linear viscoelasticity is often observed at strains smaller than 1%, although for fresh fruits and processed foods, such as frankfurters, or alginate gels, it was found to be as great as 1.5-3.0% (Mohsenin &

Mittal, 1977), 3.8% (Skinner & Rao, 1986) or 5-8% (Mancini et al., 1999a), respectively. Unfortunately, most mechanical tests on solid foods use large strains that are well beyond the linear elastic range.

Because most solid food materials are viscoelastic in nature (see below), the rate at which they are loaded or deformed may significantly affect their mechanical response.

Most Universal testing machines operate under constant cross-head speed (V_T). In the circumstances, for any given lapse of time (t) the distance travelled by the cross-head is ΔH ($=V_T\, t$). Thus, if the deformation is small and the changes in the specimen length are negligible ($H \approx H_o$), the true strain (ε_T) coincides with the Cauchy strain (ε_E) and its rate ($\dot{\varepsilon}$) can be approximated to a constant:

$$\dot{\varepsilon} = \frac{V_T}{H_o} \tag{2.9}$$

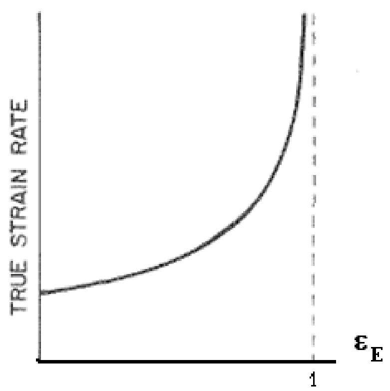

Figure 2.3 Relationship between the true strain rate and the engineering strain (ε_E) in a uniaxial compression test performed at a constant cross-head speed (V_T).

In compression, when the deformation becomes large, the true strain rate actually experienced by the specimen progressively increases with the advance of the deformation (Fig. 2.3) and tends to an infinite value as the specimen length is reduced to zero:

$$\dot{\varepsilon}_T = \frac{V_T}{H_o - V_T\, t} \tag{2.10}$$

In tension testing, the true strain rate progressively decreases since the specimen length increases.

2.3 Rheological Behaviour of Solid Foods

2.3.1 Uniaxial Deformation and Stress-Strain Relationships

In most uniaxial compressive tests, a food specimen, usually shaped as a cylinder or cube, is deformed at a constant deformation rate. By recording continuously the reaction force, it is possible to obtain a typical relationship between force and time (or absolute deformation, $\Delta H = V_T\ t$), as that plotted in Fig. 2.4a. The generally observed concave upward trend is in part due to the increasing cross-sectional area and the nonlinearity of the strain. Thus, such a *row curve* does not express the real rheological behaviour of the food material under testing. Once such a curve is converted into the *true* stress-strain relationships (using for instance Eq.s 2.2 and 2.4), it is possible to extract more appropriate rheological information, as shown schematically in Fig. 2.4b.

The concave upward curve (a) in the plane (ε_T, σ_T) is typical of a mostly compressible material (i.e., bread, sponges), while the concave downward curve (c) is characteristic of a mainly yielding material that undergoes significant structural collapse as its deformation increases. The linear or about linear relationship (b) may be not only distinctive of an essentially elastic or rubber-like material, but also of the antithetic effects of structural destruction and yielding compaction, and structure collapse. In some case, the above effects may prevail at different strains, thus resulting in a relationship with alternating concave and convex regions.

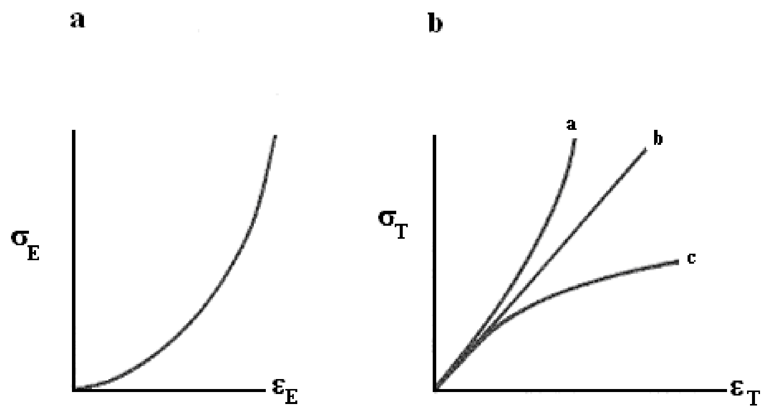

Figure 2.4 Engineering (**a**) and true (**b**) stress-strain relationships.

In tension, the trend of the true stress-strain curve reverses, mainly because the cross-sectional area decreases with increasing deformation.

If the sample is uniform in shape and composition and the deformation is small, it is generally assumed that the stress is regularly distributed throughout the sample. When the sample does not present a flat surface to receive the force (e.g., a sphere such as an orange fruit), the sample is not uniform in structure or composition (e.g., a bread roll) or the cross-head applying the force has an uneven surface (e.g., the cusp of a molar), the stress is irregularly distributed throughout the sample. Also, if the deformation is large, or if the material splits, crumbles or breaks the stress is unevenly distributed. In these cases, which are frequent in foods, it becomes very difficult, and often impossible to map the distribution of stress throughout the sample.

A convenient parameter to quantify the stiffness of a material is the slope of the true stress-strain relationship.

When an elastic material is submitted to low strains, both the true and apparent curves are practical straight lines. In this case, the slope of the stress-strain relationship represents the Young's modulus (E) and its meaning is unequivocal. Since most foods are viscoelastic in nature, and many are of heterogeneous shape, size and structure, the stress-strain relationship is frequently non-linear with a shape depending on the specimen size and deformation rate

(Peleg, 1987), the incremental stress-to-strain ratio is expressed as a *modulus of deformability* or *apparent Young's modulus*, and its magnitude is not treated as an absolute material property, but as a relative one, its usefulness being limited to the particular conditions tested. Mohsenin & Mittal (1977) pointed out the importance of maintaining the purity of rheological terms, using them only when measurements and definitions are in accordance with accepted rheological definitions.

If an ideal elastic body is subjected to a compression-decompression cycle (Fig. 2.5a), it will continuously return to its original shape, and all the deformation energy will be recovered.

In most non-ideal elastic materials (i.e., rubber), some energy is lost owing to internal friction. Nevertheless, the specimen will return to its original shape and will exhibit the same or almost the same properties if submitted to a subsequent deformation cycle. The energy that dissipates in the process, usually in the form of heat, is represented by the area of the hysteresis loop of the force-deformation curve (Fig. 2.5b).

In most solid food materials, part of the deformation (H_p) will remain permanent after decompression (plastic deformation). Also a portion of the energy used to deform the specimen is irrecoverable due to both internal friction and irreversible structural modifications (Fig. 2.5c).

The ratio between the recoverable and total deformations ($(\Delta H - H_p)/\Delta H$) was expressed as a *degree of elasticity*, while the ratio between recoverable and irrecoverable works was regarded as a characteristic of the material (Peleg, 1987). The magnitude of these parameters are highly dependent on the final strain level, as well as the specimen dimensions and deformation rate, and may be interpreted in terms such as continuous structural disintegration, build-up of hydrostatic pressure, etc.

Since the mechanical behaviour of most of solid foods is neither purely elastic nor purely viscous, their characteristics, being intermediate between both of them, are labelled as viscoelastic and are not only dependent on the strain applied, but also on the rate at which it is applied.

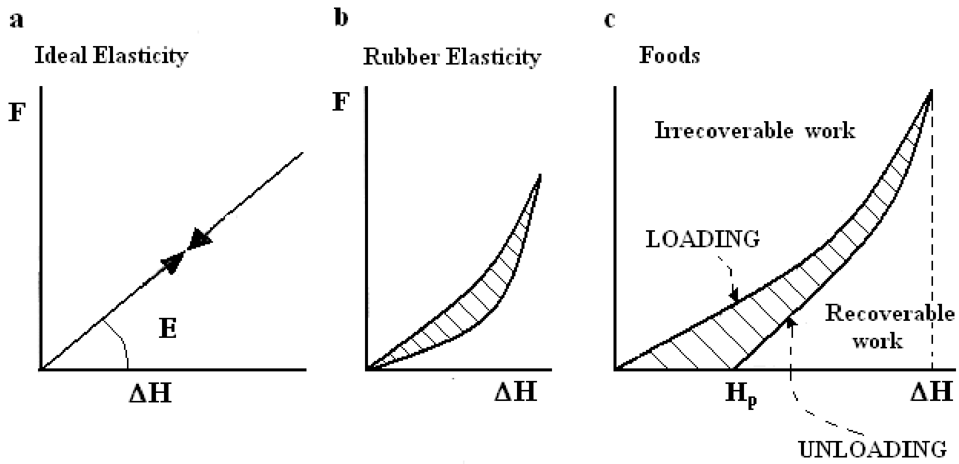

Figure 2.5 Different types of compression-decompression force-deformation curves.

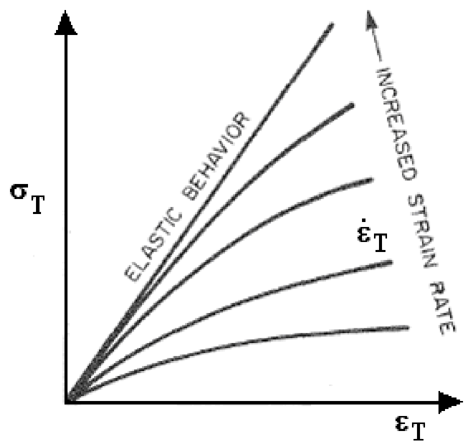

Figure 2.6 Theoretical effect of the strain rate ($\dot{\varepsilon}_T$) on the true stress(σ_T)-vs.-strain (ε_T) relationship of a linear viscoelastic material.

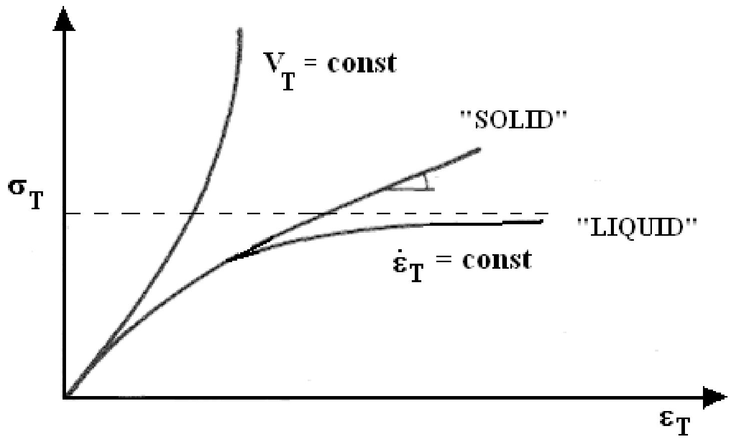

Figure 2.7 Typical difference in the true compressive stress(σ_T)-vs.-strain (ε_T) of a specimen deformed at constant strain rate ($\dot{\varepsilon}_T$) or deformation rate (V_T).

Generally, the faster the rate, the higher the stress will be (Fig. 2.6). At high rates, the response of a viscoelastic body tends to that of an elastic body. Generally, rigid food materials, such as unripe fruits and vegetables, are less rate-sensitive than soft foods like some cheeses. Thus, the distinction between true solid and liquid on the basis of the shape of the stress-strain relationship is not as straight-forward as in the case of a constant strain rate deformation history (Fig. 2.7).

From a theoretical point of view, the uniaxial compressive stress-strain relationship for an ideal elastic material has to be independent of the specimen size. In the compressive tests of specimens with an height-to-width or height-to-diameter ratio of about unity or less, such a relationship may vary depending on (i) the *frictional forces* along the contact surfaces and/or (ii) the *hydrostatic pressure build-up* in those tissues of plant or animal origin, that are fluid containing structures. Both these causes apparently improve the specimen strength.

Nevertheless, how hydrostatic pressure dissipates depends on the total resistance to the fluid outflow toward and through the specimen walls, that is on the density, porosity, and microstructure of the compressed solid matrix and total length of the fluid path. This may also result in liquid or oil leakage too.

In the case of oriented structures or structural elements with a size comparable with that of the specimen itself (i.e., fibrous and flaky materials), the specimen size affects the effects of the deformation rate and may lead to conflicting reports about the mechanical properties of the given food material.

2.3.2 Poisson's Ratio

When compressed in one direction, any material undergoes a transverse expansion, that is governed by a material property known as *Poisson's ratio* (ν), this being defined as minus the transverse strain (ε_x) divided by the axial strain (ε_z) in the direction of compression force:

$$\nu_{xz} = -\frac{\varepsilon_x}{\varepsilon_z} \tag{2.11}$$

Its numerical value can, theoretically, range from zero (totally compressible material) to 0.5 (incompressible material).

For food materials such a ratio varies with specimen size and strain applied and it is generally named as the *apparent Poisson's ratio* (Bourne, 2002). The isotropic upper limit of 0.5 is also typical of rubbers and soft biological tissues (Steffe, 1996). Foods with a high level of cellular gas, such as apple flesh, would have values near to 0.2; whereas foods with high water content, such as fresh fruits and vegetables, would have a Poisson's ratio close to 0.5, such as potato or peach flesh (ASABE, 2008). Highly compressible products such as fresh bread crumb have a very low apparent Poisson's ratio. Individual cereal grains usually have a Poisson's ratio between 0.25 and 0.4. Researchers often assume a ratio of 0.3 for cereal grains if the actual Poisson's ratio is unknown (Bourne, 2002).

2.3.3 Compression Test of Food Materials of Convex Shape

The ASABE standard method (ASABE, 2008) is regarded as an objective method for determining the mechanical attributes of food texture, resistance to mechanical injury as a result of static loading, and quasi-static force-deformation behaviour of food materials of convex shape, such as fruits and vegetables, seeds and grains, and manufactured food materials.

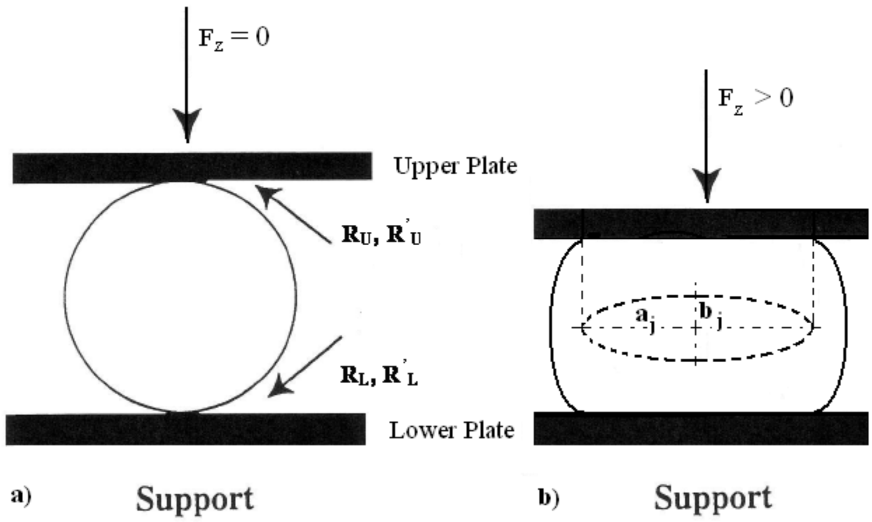

Figure 2.8 Sketch of the loading geometry used to compress a convex body using flat contact plates (ASABE, 2008): **a**) initial sample setting; **b**) compressed sample and projected ellipsoidal-like contact area on the upper or lower plate with corresponding semi-major (a_j) and semi-minor (b_j) axes.

The ASABE standard method relies upon the determination of the radii of curvature of the convex surfaces of any sample at the points of contact with the upper and lower plates of the dynamometer (Fig. 2.8), as well as the *a priori* knowledge of Poisson's ratio (ν) of the food material under testing, so as to estimate the contact area of the fruit undergoing compression.

By referring to the loading geometry shown in Fig. 2.8, Table 2.1 lists the basic equations of this method, that were adapted from the theory of contact between convex surfaces of elastic materials, since most of food and biological materials exhibit linear behaviour at small deformation (ASABE, 2008).

Table 2.1 Synopsis of the basic equations necessary to evaluate the semi-major (a_{ASM}) and semi-minor (b_{ASM}) axes of the *a priori* assumed elliptical contact area (A_{ASM}), the maximum stress ($\sigma_{,max}$), and the apparent modulus of elasticity (E) of food materials of convex shape, as derived from ASABE (2008) and referred to Fig. 2.8

Parameter	Equation	Unit
$\cos\theta$	$= \dfrac{\frac{1}{R_U} - \frac{1}{R'_U}}{\frac{1}{R_U} + \frac{1}{R'_U} + \frac{1}{R_{CD}} + \frac{1}{R'_{CD}}}$	-
c_1	$= 1.0382 (\cos\theta)^2 + 0.4807 (\cos\theta) + 1.0$	-
c_2	$= 1.0 - 0.5672 (\cos\theta)$	-
K_j	$= 1.351 + 0.035 (\cos\theta) - 0.4173 (\cos\theta)^2$	-
E	$= \dfrac{0.338\, F\, (1-\nu^2)}{\Delta H^{3/2}} [K_U (\frac{1}{R_U} + \frac{1}{R'_U})^{1/3} + K_L (\frac{1}{R_L} + \frac{1}{R'_L})^{1/3}]^{3/2}$	Pa
E_{CD}	= 3.3	GPa
ν	to be experimentally determined	-
ν_{CD}	= 0.37 for Plexiglas® ≈ 0.30 for Stainless steel	-
κ_S	$= \dfrac{1-\nu^2}{E_S}$	Pa^{-1}
κ_{CD}	$= \dfrac{1-\nu_{CD}^2}{E_{CD}}$	Pa^{-1}
a_{ASM}	$= c_1 \left[\dfrac{3\, F\, (\kappa_S + \kappa_{CD})}{2} (\frac{1}{R_U} + \frac{1}{R'_U} + \frac{1}{R_{CD}} + \frac{1}{R'_{CD}})^{-1} \right]^{1/3}$	M
b_{ASM}	$= c_2 \left[\dfrac{3\, F\, (\kappa_S + \kappa_{CD})}{2} (\frac{1}{R_U} + \frac{1}{R'_U} + \frac{1}{R_{CD}} + \frac{1}{R'_{CD}})^{-1} \right]^{1/3}$	m
A_{ASM}	$= \pi\, a\, b$	m^2
σ_{max}	$= \dfrac{1.5\, F}{A_{ASM}}$	Pa

The Hertz-derived equations, listed in Table 2.1, allow the evaluation of the semi-major (a_{ASM}) and semi-minor (b_{ASM}) axes of the *a priori* assumed elliptical contact area (A_{ASM}), the maximum stress ($\sigma_{,max}$) that occurs at its centre, and the apparent modulus of elasticity (E) of the sample tested.

These equations can be worked out once a few specific data have been measured or estimated. In particular, the maximum (R) and minimum (R') radii of curvature of the compression device (CD) and the sample (S) at their point of contact are to be measured using a radius-of-curvature meter; whereas the constants c_1, c_2, and K_U or K_L, may be approximated by the empirical regressions listed in Table 2.1 and derived from the data by Kozma & Cunningham (1962).

When submitting an almost spherical body to compression under parallel plates (Fig. 2.8) the relationship between applied F and corresponding deformation (ΔH) may be expressed as follows (Fridley et al., 1968):

$$\Delta H = \left[\frac{9}{16} F^2 \frac{(1-\nu^2)^2}{R\,E^2} \right]^{1/3} \tag{2.12}$$

where E is the apparent modulus of elasticity, ΔH the deformation applied, ν the apparent Poisson's ratio; F the force, and R the equivalent radius of the spherical body under testing.

By expressing the strain via Eq. (2.3) with H_o=2 R and introducing such equation into Eq. (2.12), the following can be yield:

$$\varepsilon_E = \left[\frac{9}{2^7} F^2 \frac{(1-\nu^2)^2}{R^4\,E^2} \right]^{1/3} \tag{2.13}$$

By solving Eq. (2.13) with respect to F, it follows:

$$\log(F) = -\log\left[\frac{9}{2^7} \frac{(1-\nu^2)^2}{R^4\,E^2} \right] + \frac{3}{2}\log(\varepsilon_E) \tag{2.14}$$

According to ASABE standard (2008), the applicability of Eq. (2.14) can be validated by plotting the log of applied force as a function of the log of strain. If the equation is valid, the slope of the line should be 1.5 (Fridley et al., 1968; Arnold & Mohsenin, 1971).

By referring to the loading geometry shown in Fig. 2.8, in almost spherical bodies undergoing testing via a contact device (CD) with smooth, polished and flat surface (R_{CD}=∞), such as that used to test Red Delicious apple fruits (ASABE 2008), the differences in the radii of curvature of the convex surface of the sample at the point of contact with the upper (R_U, R'_U) and lower (R_L, R'_L) plates can be neglected by resorting to a unique radius of curvature coinciding with the radius of the equivalent sphere having the same volume of the ellipsoid with different diameters along the three orthogonal axes x, y, and z. In the circumstances, the contact angle (θ) between the specimen and the contact device tends to 90°, this resulting in $c_1=c_2=1.0$, and $K_U=K_L\sim1.35$.

The main limit to the application of this standard method to determine the mechanical properties of a convex body is that it approximates its mechanical response to that of an elastic one. Thus, it is necessary to assess the range of linear viscoelasticity for the body undergoing compression.

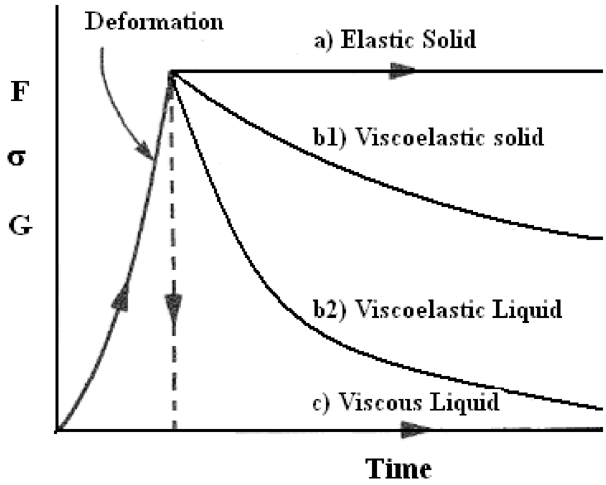

Figure 2.9 The relaxation test used to distinguish the mechanical response of an ideal solid or liquid, and viscoelastic solid- or liquid.

2.3.4 Stress Relaxation

Ideally, a stress relaxation test is performed by a step tensile or compressive deformation of the specimen, after that the force decay against time is recorded while the deformation is kept constant. Since some time has to elapse before the specimen is deformed up to ε_E (Fig. 2.9), the *raw* relaxation curve may be simply plotted in the form of force-*vs*-time relationship (Pallottino et al., 2009b). However, it is generally presented in the normalized form of stress (σ_E) or modulus decay curve (Fig. 2.9).

During all stress-relaxation tests the instantaneous engineering stress (σ_E) is generally a function of time (t) and strain applied (ε_E) and can be converted into the relaxation modulus $G(t,\varepsilon_E)$ defined by:

$$G(t,\varepsilon_E) = \sigma_E(t, \varepsilon_E)/\varepsilon_E \quad (2.15)$$

This material function is defined similarly to the shear modulus of an elastic solid and, as for such a function, it ceases to be a function of strain for small values of ε_E (Steffe, 1996). By referring the instantaneous relaxation modulus to the initial one, it is possible to estimate the dimensionless relaxation modulus, $G^*(t, \varepsilon_E)$, which is equal to the ratio between the actual F and initial F_o reactions, provided that, the cross-sectional area (A) of the sample corresponding to the imposed strain (ε_E) is constant and independent of time:

$$G^*(t, \varepsilon_E) = \frac{\sigma_E(t, \varepsilon_E)}{\sigma_E(0, \varepsilon_E)} = \frac{F(t, \varepsilon_E)}{F_o} \quad (2.16)$$

To assess the rheological behaviour of the food material under study, it is necessary to repeat the test by varying the strain level, and by changing the deformation rate at which the preset deformation is reached.

Because maintaining a fixed deformation is the essence of the analysis, Universal testing machines are typically suitable for such tests.

Once an ideal elastic body has been deformed, it does not relax at all (Fig. 2.9a) and all the deformation energy consumed to deform it will be released on the return of the body to its initial unchanged state. This behaviour can be exemplified by a spring as follows:

$$\sigma_E = E\ \varepsilon_E \quad (2.17)$$

On the contrary, an ideal viscous fluid cannot maintain any stress in the absence of motion, and it will relax instantaneously (Fig. 2.9c). This behaviour can be exemplified by a dashpot (that is made of a piston moving back and forward in a cylinder filled with a Newtonian fluid), where the shear stress (τ) is proportional to shear rate ($d\gamma/dt$) via the so called *coefficient of viscosity* (η):

$$\tau = \eta\ (d\gamma/dt) \quad (2.18)$$

If a hand-operated tire pump is pushed down, it is impossible for the handle to move instantly to the bottom position unless the shear rate is infinitive or η is zero.

In viscoelastic materials, their behaviour is intermediate, that is the force relaxes with a finite rate. This phenomenon is due to molecular and structural reorientation. In certain compressed gels (i.e., alginate gels), it appears that progressive rupture can also be a mechanism through which internal pressure is relieved (Mancini et al., 1999b).

Generally, at any given strain the stress may be assumed as a combination of an elastic stress, that is proportional to the strain only, and of a viscous stress, that is rate-dependent. After a sufficiently long time, the latter will dissipate, while the former will be the residual one.

Thus, the residual stress may be used to measure the *degree of solidity* of the body under testing. In an idea1 elastic solid, 100% of the stress remains unrelaxed, while in liquids all the stress relaxes. (Fig. 2.9).

The main problem in establishing quantitatively the degree of solidity of most foods by resorting to stress relaxation tests is due to its sufficiently long duration, since any food material may undergo to microbial and/or enzymatic decay or to significant moisture exchange with the environment. In these cases, any force measurement after long time may be unrelated to the original rheological properties of the food examined.

To describe the time effects on the mechanical properties of a material, the simplest model is the two-element Maxwell body, proposed by James Clerk Maxwell (Rao, 1992b). As shown in Fig. 2.10, such a body consists of a Hookean solid element (spring, s) connected in series to a Newtonian fluid element (dashpot, d).

During a stress relaxation test using a universal testing dynamometer, a single Maxwell body may be deformed up to a given deformation; then, the cross-head is stopped and the sample held in its extended/compressed position to keep the strain (ε_o) constant throughout the duration of the test.

As soon as the strain is applied to the Maxwell body, only its spring stretches, while the piston in the dashpot does not move. After that, the piston begins to flow and relieve the stress imposed on the spring, this resulting in a stress decreasing with time.

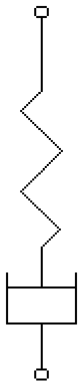

Figure 2.10 Schematic of a two-element Maxwell body: s, spring; d) dashpot.

In the circumstances, the stress on the spring (σ_s) is equal to the stress on the dashpot (σ_d) and both quantities equals the stress (σ) imposed on the entire body:

$$\sigma = \sigma_s = \sigma_d \qquad (2.19)$$

while the strains are additive, being the two elements in series:

$$\varepsilon_o = \varepsilon_s + \varepsilon_d = \text{const} \qquad (2.20)$$

This will give rise to a zero deformation rate:

$$\frac{d\varepsilon_o}{dt} = \frac{d\varepsilon_s}{dt} + \frac{d\varepsilon_d}{dt} = 0 \qquad (2.21)$$

By differentiating Eq. (2.17) and introducing it with Eq. (2.18) into Eq. (2.21), it is possible to obtain the following first-order differential equation:

$$\frac{d\sigma}{E} + \frac{\sigma}{\eta} = 0 \qquad (2.22)$$

Eq. (2.22) can be rearranged as

$$\frac{d\sigma}{\sigma} = -\frac{E}{\eta}dt \qquad (2.23)$$

and integrated as follows:

$$\sigma = \sigma_o e^{-\frac{t}{\tau}} \qquad (2.24)$$

with

$$\tau = \frac{\eta}{E} \qquad (2.25)$$

where σ_o is the initial stress and τ the relaxation time, that is the time required for the stress imposed to decay to (1/e)-th or about 37% of the initial level.

By dividing both sides of Eq. (2.24) by the constant strain (ε_o), it is possible to obtain an equation for the relaxation modulus:

$$G(t,\varepsilon_o) = \frac{\sigma}{\varepsilon_o} = \frac{\sigma_o}{\varepsilon_o} e^{-t/\tau} = E_o\, e^{-t/\tau} \qquad (2.26)$$

where E_o is the modulus of elasticity of the Maxwell body at t=0 or the modulus of elasticity of the spring.

By plotting the natural logarithm of the stress ratio (σ/σ_o) or dimensionless relaxation modulus G* - Eq. 2.16 - against time (t) for a food material, the relationship may be non linear. Therefore, a single relaxation time, as defined by Eq. (2.25), may not be the best representative of the decay pattern. To this end, differently shaped stress-relaxation curves can be reconstructed by arranging more than one Maxwell elements in parallel, either with or without a residual spring, the latter element being necessary to yield the residual stress (Fig. 2.11).

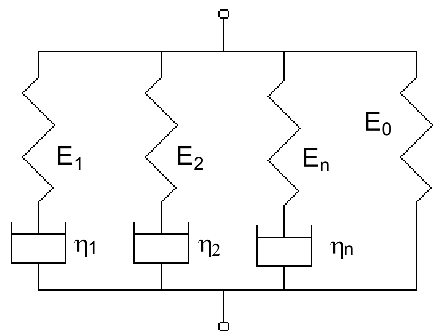

Figure 2.11 Schematic of a generalised Maxwell body with a residual spring element.

The generalised Maxwell model is represented by the following equation:

$$G(t,\varepsilon_o) = E_o + \sum_{1}^{n} E_i\, e^{-t/\tau_i} \qquad (2.27)$$

where E_i is the modulus of elasticity of the spring and τ_i the relaxation time of the dashpot of the i-th Maxwell element.

In this way, it is possible to achieve a more accurate description of the relaxation curve in terms of the so called *relaxation time spectrum*, which may be either discrete (τ_i) or continuous. Despite the higher the number of Maxwell elements, the better the reconstruction accuracy of the material response, for food materials five elements (that is two Maxwell bodies and a residual spring) are generally enough to represent adequately their mechanical behaviour (Rao, 1992b).

By using Eq. (2.16), it is possible to describe the time course of the dimensionless relaxation modulus G* for a generalized Maxwell body (Rao, 1992b) as follows:

$$G^*(t, \varepsilon_o) = A_o + \sum_1^n A_i \exp(-t/\tau_i) \qquad (2.28)$$

with

$$A_o = 1 - \sum_1^n A_i \quad \text{(to fulfill the initial condition: } G^*(0, \varepsilon_o)=1) \qquad (2.29)$$

$$E_i = A_i\, G(0, \varepsilon_o) \qquad \text{for } i=0, 1, ..., n \qquad (2.30)$$

$$\eta_i = E_i\, \tau_i \qquad \text{for } i=1, 2, ..., n \qquad (2.31)$$

where A_i represents the generic dimensionless viscoelastic coefficient; $G(0, \varepsilon_o)$ the initial dimensionless relaxation modulus and E_o the modulus of elasticity of the spring; while E_i, η_i and τ_i refer to the i-th Maxwell element and are the modulus of elasticity of the spring, the viscosity of the dashpot and the relaxation time, respectively.

By applying a non-linear regression method, it is impossible to fit all the experimental G*-t data by the same relaxation time spectrum. This was also observed by other authors (Bertola et al., 1991; Hassan et al., 2005; Masi, 1989). To circumvent such unfeasibility, Nussinovitch et al. (1989) suggested to reconstruct the time course of the experimentally observed dimensionless relaxation modulus by assigning initially an arbitrary steady spectrum of relaxation times as follows:

$$\tau_i = a \times 10^{4-i} \quad \text{for } i=1, ..., 5 \qquad (2.32)$$

where a is a real number a priori assumed as equal to 1 (Nussinovitch et al.., 1989) or ranging from 1 to 9 (Mancini et al., 1999ab). By discarding all the Maxwell elements whose contribution to the reconstruction of G*-t relationship was statistically insignificant at the confidence level of 95%, it is possible to determine the optimal a value by maximizing the coefficient of determinations (r^2) of the following linearized form of eq. (6):

$$Y = 1 - G^*(t, \varepsilon_z) = \sum_{1}^{\nu_M} A_i \,(1 - e^{-t/\tau_i}) \qquad (2.33)$$

where ν_M is the overall number of statistically significant Maxwell elements (Mancini et al.., 1999ab).

If the deformation of the specimen is carried out at a low rate, the recorded relaxation curve, at least initially, will be lower than that expected theoretically for step deformation. How much lower will be determined by both the material rheological properties and deformation rate. For this reason, the initial part of the relaxation curve (that is, the portion reconstructed by the shorter relaxation times of the spectrum) may be an inaccurate account of the true behaviour of the material under study. To deal with this problem, the smallest relaxation time (τ_1) has to be from 5 to 10 times greater than the loading period (Rao, 1992a).

Another aspect of stress relaxation is that most food materials, especially under large deformation, exhibit non-linear viscoelasticity. Thus, any rheological constants (A_i) or parameters (E_i, τ_i) derived from relaxation data may have little significance unless they are presented as a function of the strain and deformation rate. To this end, more extended information is reported in paper by Mancini et al. (1999), where it was firstly by assessed that the compressive stress-deformation curves for alginate gels were independent of the crosshead speed for $V_T \geq 2$ mm s^{-1}, and then that such gels exhibited an apparent linear viscoelastic solid behaviour for $\varepsilon_E \leq 8\%$ and a non-linear one for larger deformations, even if for $\varepsilon_E > 32\%$ their solid viscoelastic behaviour tended to a liquid one.

2.4 Strength and Failure

Strength of materials, in the terminology used in mechanics, is the resistance to break. This usually expressed in stress units, and its magnitude is determined by the compressive, tensile or shear stress at the point of failure. The absolute and relative magnitude of each type of strength depends on the structural and compositional features of the material. It is not uncommon to find materials that offer high resistance to one kind of stress but not to another.

An illustrative example is concrete: it can withstand large compressive stresses, but fails rather readily in tension and, therefore, needs reinforcement.

In actual testing or deformation of a specimen, stresses of different kinds can be developed along planes with different directions. An outstanding example is the development of shear stresses as a result of uniaxial deformation. If these stresses exceed the shear strength, the material can fail in shear, despite the fact that it is only compressed. Generally, the shear stresses that are of relevance to failure are those developed in the compressed specimen that underwent considerable deformation. This behaviour was typical of relatively homogeneous food materials, such as unripe fruit flesh, tubers, and meat emulsion products (i.e., frankfurters, bologna, sausage).

In uniaxial compression, especially if there is appreciable friction at the areas in contact with the moving plate, the specimen tends to bulge or assume a barrel shape. In such cases (e.g., in certain cheeses), failure may be caused, at least in part, as a result of excessive tensile stresses at the specimen bulge region.

Although not clearly identified in foods, one cannot exclude the possibility that failure is caused when a critical level of strain rather than stress is exceeded. This kind of criterion may be associated with the failure of brittle and/or glassy foods.

As previously mentioned, stresses are not evenly distributed within the specimen.

Consequently, in some regions or sites of the specimen stress concentration can lead to local yielding and initiate motion. Typical sites are a structural fault, an existing crack or hole, a dislocation within a crystal or a weak boundary region between crystals or other structural components.

If the material contains distinctly visible structural components (such as flakes or fibres), the specimen will usually disintegrate, at least initially, in a manner that will leave such components intact. Emblematic examples are meats, fish flesh, and fibrous fruits such as pineapple. Where a material is very brittle and hard (e.g., dry bread, biscuit), particles and aggregate can be “shot” out of the specimen at considerable velocities and the specimen remnants and aggregates will be of various sizes.

In many plant and animal tissue materials, failure is also accompanied by a considerable amount of liquid release. There are also foods that deform or flow continuously without exhibiting any clearly identifiable state of an abrupt failure in a large range of defamation level; (e.g., process cheeses, marshmallow).

The failure pattern of food materials may also be totally different under a different type of test. For instance, process cheeses can sustain considerable deformation in compression, but fail after fairly small deformation in tension. Similarly, even the geometry of the test may affect the failure pattern of the material under study.

Chapter 3: Materials and Methods

3.1 Raw Materials

Two lots of blood orange fruits of the same Tarocco variety (*cv.* Arcimusa) were selected and provided by the experimental farm Palazzelli (Lentini, Siracusa, Italy) of the Research Centre for Mediterranean Crop of the Agricultural Research Council (CRA-ACM) during the 2009 and 2010 harvesting campaigns.

The first lot was, represented by around 240 fruits, was used to carry out several mechanical tests, namely the uniaxial compression to a given deformation or up to rupture and stress-relaxation tests. The average characteristics of the specimens tested were assessed by determining the total soluble solid content (TSS=11.75±0.14°Brix), using the Abbey refractometer, and titratable acidity (TA=1.52±0.16% w/v citric acid equivalent), using 0.1 M NaOH standard solution, on the juices expressed from 5 fruits randomly selected from the experimental lot, these data being replicated four times. This allowed their maturity index (MI=TTS/TA) to be estimated as 7.8±0.8 °Brix/(% w/v) (Ladaniya, 2008).

The second lot, made of four hundred fruits, was used to establish a sorting rule on the basis of combined physico-chemical and sensory tests, as reported below.

3.2 Instruments

All mechanical tests were performed using a column table-top digital dynamometer (Fig. 3.1) Zwick 1.0 Universal Testing Machine (Zwick/Roell Testing System, Kennesaw, GA, USA) having the following characteristics: deformation resolution of 0.2265 μm; position repetition accuracy of ±2 μm; speed range of 0.1-30 mm s^{-1}; speed accuracy of 2.08×10^{-4} mm s^{-1}; force range of 0.2-1000 N; force accuracy of 2 N. The software (testXpert®) was used to acquire whole force-deformation curves.

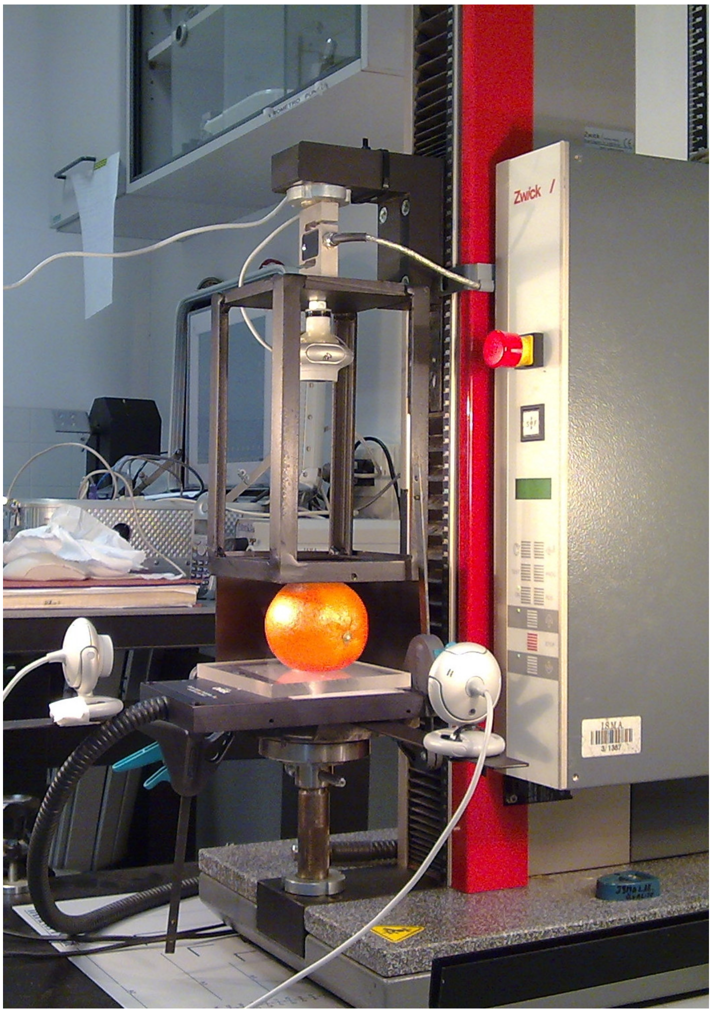

Figure 3.1 Digital dynamometer Zwick 1.0 and relative structure built on purpose to make possible the image acquisition of the real contact surface of the fruit under compression.

For the non-destructive compression, compression up to rupture and stress-relaxation tests the UTM was equipped with transparent graduated Plexiglas® GS 233 (Röhm GmbH, Darmstadt, Germany) upper and lower plates to determine precisely the contact area of each fruit under testing (Fig. 3.2). The software testxpert® was used to acquire whole force-deformation curves. Three cams were positioned along the axis lines x, y (LifeCams VX-6000, Microsoft Corporation, Redmond, WA, USA), and z (AVT Camera Guppy, Allied Vision Technologies, Stadtroda, Germany), so as to perform uniaxial compression tests in conjunction with contact area image analyses (Fig. 3.2).

The modulus of elasticity (E_{CD}=3.3 GPa) and Poisson's ratio (ν_{CD}=0.37) of such a material were extracted from the manufacture product description (Ref. No. 211-April, 1st, 2004).

To perform the penetrometric standard Magness-Taylor (MT) test, the UTM was equipped with a cylindrical probe having a diameter of 11.3 mm (1 cm^2).

The thicknesses of any fruit flavedo was measured using an electronic digital caliper CDJ 15 (Broletti LTF Spa, Cremona, Italy).

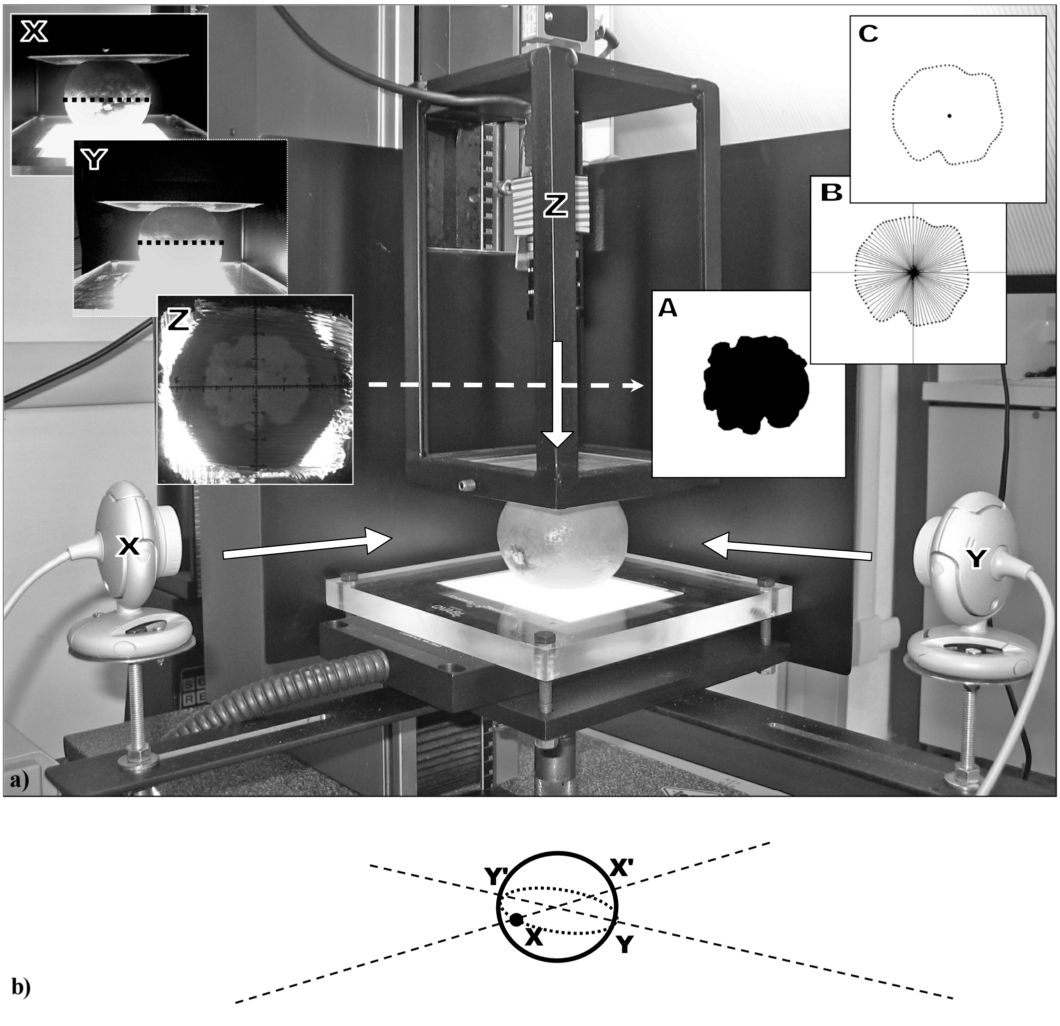

Figure 3.2 **a)** Picture of the experimental apparatus equipped with fixed (lower) and moving (upper) Plexiglass® plates and three web cams, positioned along the axis lines x, y and z so as to collect the projection images X, Y and Z of the fruit under testing, sequentially binarized (A), digitized (B) and finally submitted to Elliptic Fourier Analysis (C). **b)** Schematic drawing of the

fruit equatorial region used to measure the rind thickness in 4 positions labelled x, x', y and y', the former being located near the fruit attachment to stalk.

The colour of the whole fruit as such (p) or halved (ho) was assessed using a portable sphere spectrophotometer X-Rite SP64 (Grand Rapids, MI, USA) with an illuminant D65, a standard observer 10°, a tungsten light, and a 8-mm diameter of specimen aperture, so as to record the corresponding CIELAB co-ordinates (L_k^*, a_k^*, b_k^*).

3.3 Procedures

3.3.1 Parallel Plate Compression

3.3.1.1 Mechanical Tests and Image Acquisition

Three cams, one of which being an AVT Camera Guppy (Allied Vision Technologies, Stadtroda, Germany) and the other two LifeCams VX-6000 (Microsoft Corporation, Redmond, WA, USA), were positioned along the axis lines x, y and z so as to collect a triplet of the projection images X, Y and Z of the fruit under testing (Fig. 3.2).

The fruit size and deformation relative to x or y axis were detected via the y or x camera, respectively. All the measures of length were obtained by converting the size expressed in pixel into mm by resorting to a pre-calibrated standard metric reference. The average error for the x or y camera was equal to 0.4 mm, while that for the z camera was negligible, since each sample under testing was always placed on the same focus plane, that was perpendicular to the objective axis as shown in Fig. 3.2. To allow a proper acquisition of the images by the z camera, the upper Plexiglas® plate was coated with a transparent gel to reveal easily the contact between plate and fruit (Fig. 3.3) while the fruit was illuminated under the lower plate via an optical fibre pad to increase the contrast and thus facilitate the task.

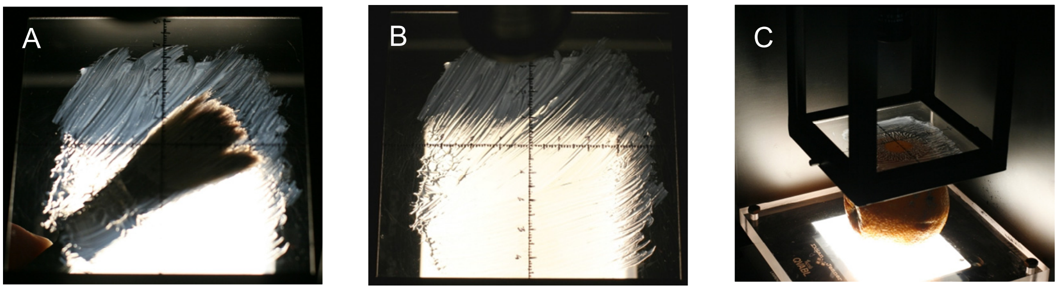

Figure 3.3 Preliminary phases of the real parallel plate-fruit contact area acquisition: A) coating of the plate with a gel using a brush; B) plate rightly coated with the gel film; C) plate under compression with the optical fibre pad light on.

By using a constant cross-head speed (V_T) of 15 mm s^{-1}, any orange fruit was compressed along the z-axis (Fig. 3.2) by varying the engineering strain (ε_z), as defined by Eq. (2.3).

The simultaneous use of cams x and y allowed the determination of the initial (D_{yo}, D_{xo}) and current (D_y, D_x) fruit diameters along the y and x axes, respectively.

Such determinations were performed by varying ε_z in the range of 3 to 21% (step 3%), the latter being quite smaller than the strain at rupture (33±4)% preliminarily established (Pallottino et al., 2009a). At the end of any test, the sample was halved and the rind thickness was measured in the equatorial region (see positions x, x', y and y' in Fig. 3.2).

To account for the variations due to orange fruit shape, size, age and cellular structure as suggested by ASABE Standards (2008), any of these tests was replicated 20 times, thus estimating the mean values together with the corresponding standard deviations.

Finally, under constant V_T (=15 mm s^{-1}), another group of 20 citrus fruits was submitted to compression testing up to rupture. Even in this case, test results were expressed as mean values with the related standard deviations.

To convert the resulting force-deformation curves into stress-strain relationships and estimate the basic orange fruit mechanical properties, the effective contact area between fruit and compression plates was assessed or predicted as reported below.

3.3.1.2 Contact Area Assessment via Image Analysis and Elliptic Fourier Analysis

The effective contact surface area was acquired by the vertical (z) camera. The projection images were primarily binarized with an histogram based threshold (Fig. 3.2-A); then, digitized by accounting for a total number of 100 points (x, y), each one being spaced at equal angular increments relative to the centroid of the object (Fig. 3.2-B), using the software TPSdig2 (Rohlf, 2006). The coordinates were aligned using the Generalised Procrustes Analysis, as modified by Rohlf & Slice (1990) so as to involve the following three steps: i) translate the coordinates of each point to a common centroid located at the origin (0,0) of a reference system of coordinates; ii) scale each outline to the unitary centroid size; and iii) rotate the coordinates to minimize the sum of square distances between the corresponding landmarks. The 100 aligned coordinates were treated as outline data (Costa et al., 2009). By approximating the outline for any contact area to a polygon of x,y-coordinates, Elliptic Fourier Analysis (EFA; Crampton, 1995; Kuhl & Giardina, 1982) was used to reduce the dimensionality of the data set and eliminate redundant information (as determined by high correlation between adjacent coordinates in the raw data set). EFA is based on the separate Fourier decompositions of the incremental changes of the x- and y-coordinates as functions of the cumulative chordal length of the outline polygon. EFA yields the spectrum of the closed contour of the contact area shape in terms of harmonically related trigonometric curves. For each harmonic equation, two Fourier coefficients were computed for both the x- and y-projections; thus the total number of coefficients was 4 x n, where n was the number of harmonics fitted to the outline (Crampton, 1995). In this case, the number of required harmonics was set to 9, as estimated by using the method described by Crampton (1995) and applied previously (Costa et al., 2009; 2010). More specifically, in this study, EFA shape descriptors were used to observe the shape changes in the contact surface as a function of the different compression deformations applied along the z-axis.

3.3.1.3 Contact Area Assessment via Image Analysis and Bounding Box

Any of the images acquired by the vertical (z) camera was also automatically circumscribed by a minimum rectangle (the so called *bounding box*) having sides parallel to the axes of the ellipse- or circle-like shape of the acquired contact area.

In accordance with ASABE (2008), the contact surface area (A_{BB}) was estimated as equal to:

$$A_{BB} = \pi a_{BB}\, b_{BB} \quad (3.1)$$

where a_{BB} and b_{BB} are the semi-major and semi-minor axes of the ellipse-like shape inscribed in the above bounding box.

3.3.1.4 Contact Area Prediction Using the ASABE Standard Method

In this case, the contact area was calculated on the base of the ASABE standard method (ASABE, 2008) (§2.3.3). To this end, the Hertz-derived equations listed in Table 2.1 were used on the assumption that most of food and biological materials exhibit linear behaviour at small (e.g., 3-5% strain) deformation (Mohsenin & Mittal, 1977; Rao, 1992a; Skinner & Rao, 1986).

3.3.1.5 Contact Area Prediction Assuming Constant Fruit Volume

As shown in Fig. 3.4, when the orange fruit is positioned between two horizontal rigid plates, one of which being stationary and the other one moving at a constant speed V_T, and then submitted to compression testing, its original almost spherical shape with an average initial height (H_o) is supposed to be axisymmetrically squeezed in the upper and lower polar regions. Thus, the compressed sphere may be approximately assimilated to two symmetrical spherical segments of two circular bases of radii R_V and a_V, respectively.

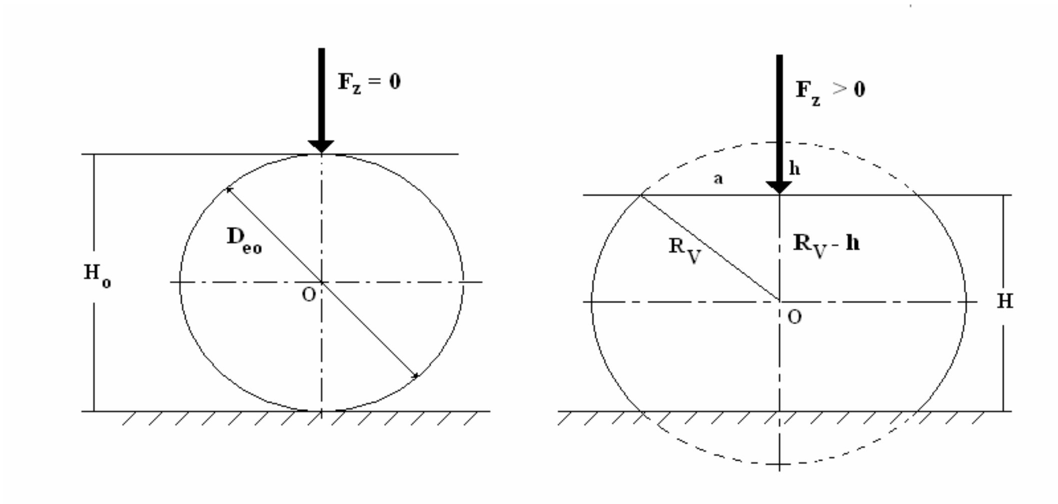

Figura 1.4 Schematic drawing of the changes in the volumetric shape of a spherical orange fruit with an average equivalent diameter (D_{eo}) at the beginning (a) and during (b) compression under a progressively increasing force (F_z).

By assuming that the overall volume of the fruit as such (having an initial equivalent diameter $D_{eo}=H_o$) or deformed to an instantaneous height H ($=D_{eo}$ -2 h, where h is the vertical semi-deformation imposed) is about constant and equal to the initial one ($V_o=\pi/6\ D_{eo}^3$):

$$\frac{\pi}{6} D_{eo}^3 = \frac{1}{3}\pi\ (R_V - h)[3 R_V^2 + 3 a_V^2 + (R_V - h)^2] \quad (3.2)$$

it is possible to estimate the instantaneous radii R_V and a_V of the two circular bases of the equivalent spherical segments as follows:

$$R_V = z_V - p_V/ (3\ z) \quad (3.3)$$

$$a_V^2 = h\ (2\ R_V - h) \quad (3.4)$$

with

$$z_V = \sqrt[3]{\frac{-q \pm \Delta}{2}} \quad (3.5)$$

$$p_V = -\ (3/2)\ h^2 \quad (3.6)$$

$$q = \frac{1}{2} h^3 - D_{eo}^3/8 \quad (3.7)$$

$$\Delta^2 = q^2 + 4\ p_V^3/27 \quad (3.8)$$

Thus, for any compressive engineering strain imposed (ε_z) the instantaneous cross-sectional area (A_V) of the deformed sample under constant volume becomes:

$$A_V = \pi\,(a_V) \qquad (3.9)$$

3.3.1.6 Statistical Analysis of Data

A one-way analysis of variance (One-Way ANOVA) was used to compare the mean values of the parameters (D_{xo}, D_{yo}, D_{zo}, D_{eo}, F_z, μ_x, μ_y, E_S, t_x, $t_{x'}$, t_y, $t_{y'}$, A_{EFA}, A_{BB}) used to characterise all the samples tested under different engineering strains (ε_z). One-Way ANOVA tests the null hypothesis that samples in any number of treatments are drawn from the same population using the F distribution.

ANOVA produces an F statistics, by accounting for the ratio between the variance calculated among the means and the variance within the samples. If the group means are drawn from the same population, the variance between the group means should be lower than the variance of the samples, following central limit theorem. To observe paired differences between any two means i and j a Least Squares Difference (LSD) was computed as suggested by Barcaccia and Falcinelli (2007):

$$LSD = t_{\alpha,df}\sqrt{\frac{s_i^2}{n_i}+\frac{s_j^2}{n_j}} \qquad (3.10)$$

where $t_{\alpha,f}$ is the one-sided Student *t*-test for a confidence level α and f (=n_i+n_j-2) degrees of freedom, s_i and s_j and n_i and n_j are the standard deviation and overall number of the group samples i and j to be compared.

Finally, a Student's t-test was used to assess whether the experimental mean values of the contact areas found by Elliptic Fourier Analysis (A_{EFA}) and image analysis and bounding box (A_{BB}) were significantly different.

3.3.2 Stress-Relaxation Testing

To assess the range of validity of linear viscoelasticity, the Tarocco specimens with an average equivalent diameter of 78±4 mm (as extracted from the average values of V_o in Table 4.4) were loaded at constant deformation rates of 15 mm s^{-1} to generate engineering strains (ε_z) along the z axis of 5, 10, 15 and 20% of the fruit initial height. Once the cross-head had been stopped, the stress relaxation was monitored for as long as 900 s, this being much longer than the time required (0.2-1.0 s) to deform the samples. The deformation rate was identified on the base of preliminary trials (Pallottino et al., 2010) and literature (Ruiz-Altisent & Ortiz-Canavate 2005). The effective contact surface area (A) was acquired by the vertical (z) camera and automatically circumscribed by a minimum rectangle (the so called *bounding box*) having sides parallel to the axes of the ellipse- or circle-like shape of the acquired contact area (§3.3.1.3).

Specimens submitted to stress relaxation testing were weighed and measured with the aforementioned cams before and after each test, thus allowing their percentage variation in mass and dimensions along the axis lines x, y, and z to be respectively estimated.

Since the shape of each contact area was previously assimilated to quite a perfect ellipse (Costa et al., 2009; Pallottino et al., 2009a), the contact surface area (A) was estimated as suggested by ASABE Standards (2008) (2.3.3), so as to convert the instantaneous values of compression force applied F_z and sample height H into engineering stress (σ_z) and engineering (ε_z) strain using Eq.s (2.1) and (2.3), respectively. Use of Eq.s (2.15) and (2.16) allowed the time course of σ_z to be converted into the real ($G(t,\varepsilon_z)$) and dimensionless ($G^*(t, \varepsilon_z)$) relaxation moduli.

By applying the fitting procedure outlined in §2.3.4, it was possible to determine the dimensionless viscoelastic coefficients (A_i) and spectrum of relaxation times (τ_i).

Permanent deformation of the specimens, as well as their relative variation in mass or volume, after stress relaxation tests performed at a constant loading rate of 15 mm s^{-1} was estimated as follows:

$$\delta_x = (D_x - D_{xo})/D_{xo}$$

$$\delta_y = (D_y - D_{yo})/D_{yo} \quad (3.11)$$

$$\delta_z = (D_z - D_{zo})/D_{zo}$$

$$\delta_m = (m - m_o)/m_o \quad (3.12)$$

$$\delta_V = (V - V_o)/V_o \quad (3.13)$$

where D_{xo} and D_x, D_{yo} and D_y, D_{zo} and D_z, or m_o and m are the initial and final values of the diameter along the x, y, and z axes, or masses of each specimen, respectively. Moreover, V_o and V are its initial and final volumes, these being estimated by approximating each fruit to an ellipsoid having its three orthogonal diameters coincident with those of the fruit tested.

One-way analysis of variance (One-Way ANOVA) and Student's t-test were used to assess the statistically differences among the independent (D_{xo}, D_{yo}, D_{zo}, m_o, V_o) and dependent (δ_j, F_z, A) variables under different engineering strains (ε_z).

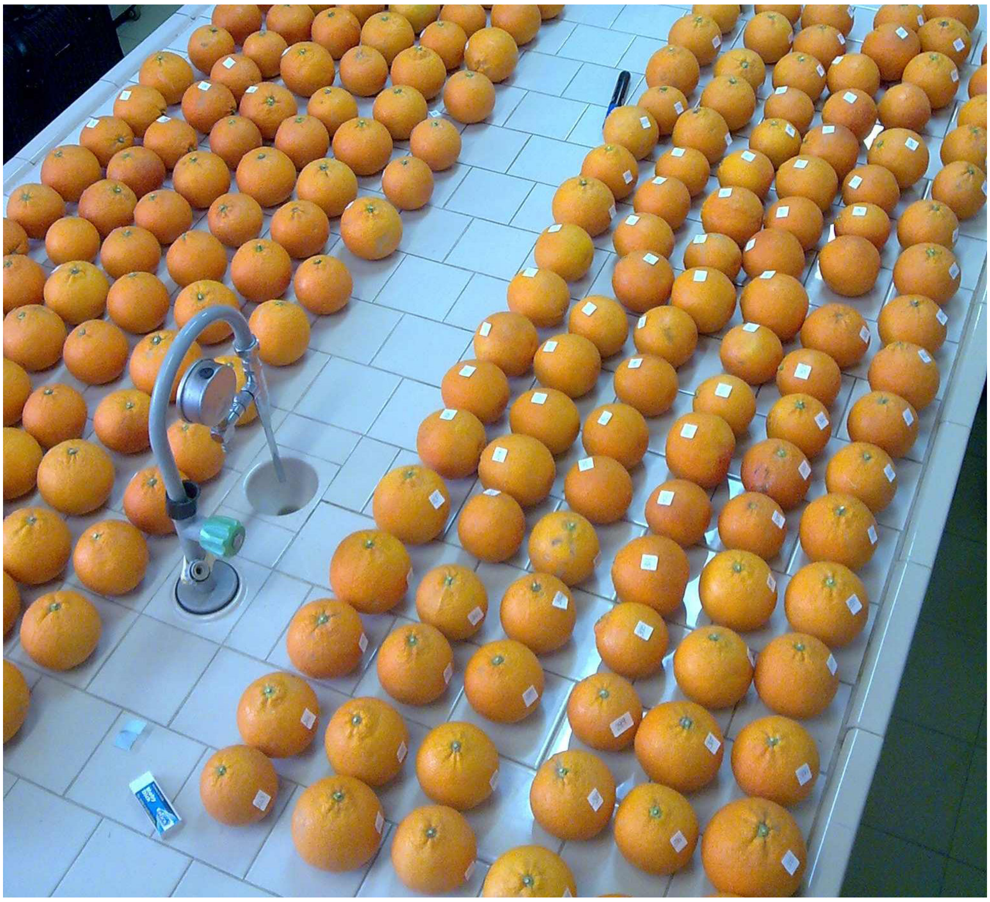

Figure 3.5 Samples numbering as a preliminary step to their classification in different firmness classes via non-destructive testing.

3.3.3 Combined Physico-Chemical and Sensory Testings

3.3.3.1 Procedures

Four hundred samples were numbered (see Fig. 3.5) and then compressed up to 5% while measuring the corresponding resistance (F_z). After that all specimens had been ordered with respect to their tension at ε_z=0.05 per unit diameter ($T_5=F_{z5}/D_{zo}$) as suggested by Carin et al.. (2003), they were discriminated into three different firmness classes, denoted as high (HF), medium (MF) or low (LF) one.

Any of these classes consisted of 64 specimens, that were randomly subdivided into two subgroups.

The first subgroup composed of 40 specimens was sequentially submitted to the rind colorimetric analysis and Magness-Taylor (MT) test (Menesatti et al., 2009). Then, each orange fruit was halved on the equatorial plane to measure firstly its flesh colour and then the flavedo thickness (Fig. 3.6) along two orthogonal axes x and y, the former passing through the fruit-to-stalk attachment, using the electronic digital caliper (CDJ 15, Broletti LTF Spa, Cremona, Italy).

Then, any half was squeezed and the resulting juice was randomly collected in one of four flasks. The resulting juices were assayed for the total soluble solid content (TSS), using an Abbey refractometer and expressed in °Brix, and for titratable acidity (TA), using 0.1 M NaOH standard solution and expressed in % w/v of citric acid equivalent, so as to estimate their corresponding maturity index (MI=TTS/TA) (Ladaniya, 2008).

The second subgroup consisting of the remaining 24 fruit pieces were submitted to sensory analysis, as reported below.

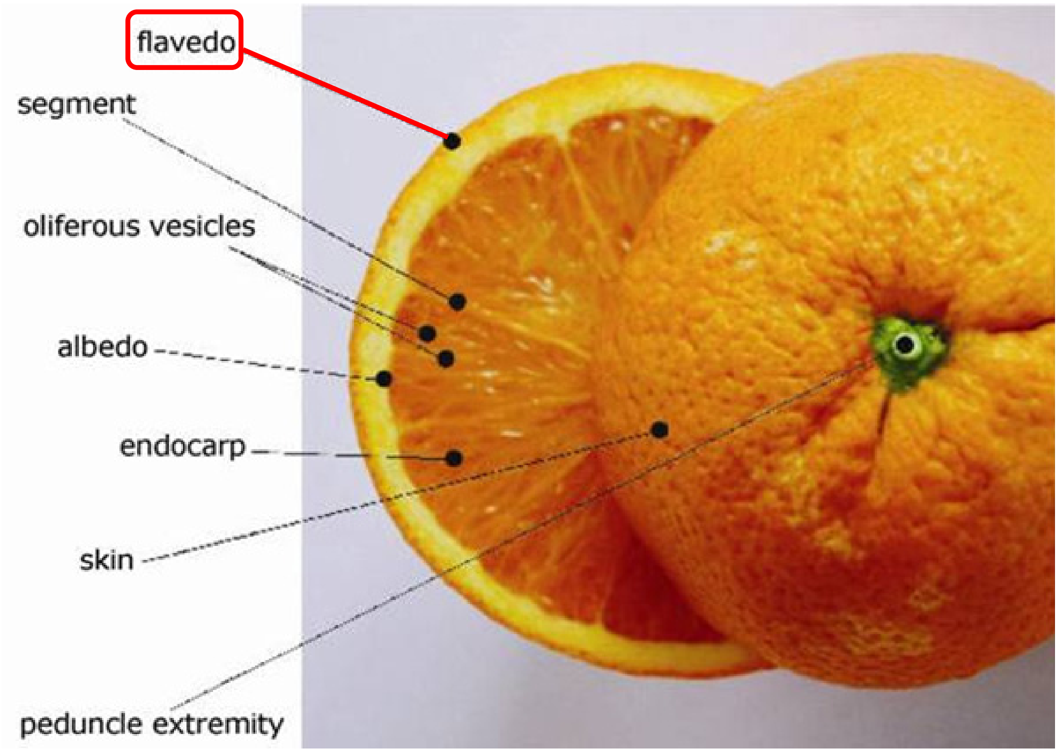

Figure 3.6 Orange fruit internal structure.

3.3.3.2 Colour Measurements

Each measurement on any specimen, either as such or halved, was repeated three times and averaged.

All the 400 Tarocco orange fruits, examined as such or halved, were characterised by the following average CIELAB co-ordinates:

$L_{p,m}^* = 62 \pm 2$; $a_{p,m}^* = 38 \pm 2$; $b_{p,m}^* = 58 \pm 3$

$L_{ho,m}^* = 41 \pm 4$; $a_{ho,m}^* = 12 \pm 2$; $b_{ho,m}^* = 13 \pm 5$

In the colour space (L^*, a^*, b^*), the lightness coefficient (L^*) ranges from 0 (black) to 100 (white). For any generic measured colour lightness (L_k^*), the co-ordinates (a_k^*, b_k^*) locate the colour on a rectangular co-ordinate grid perpendicular to the L^* axis at L_k^*. The colour at the grid origin ($a^*=0$; $b^*=0$) is achromatic (grey). On the horizontal axis, a positive value of a^* indicates a hue of red-purple, while a negative one of bluish-green. On the vertical axis, a positive value of b^* indicates yellow, while a negative one blue (McGuire, 1992).

The characteristic colour points of Tarocco orange peel (p) or flesh (ho) fell in the first quadrant and the shades of yellow were generally predominant ($b_k^* > a_k^*$). Owing to the greater lightness of Tarocco orange peel than that of the orange flesh, the colour of the former was brilliant orange, while that of the latter was definitively reddish.

To better quantify the differences in metric lightness and chromaticity for all the specimens under study, it was calculated the colour difference (ΔE_{ki}) between each i-th specimen and the average one reported above, that is the square root of the squares of the respective differences in L_k^*, a_k^* and b_k^*:

$$\Delta E_{k,i} = \sqrt{(L_{k,i}^* - L_{k,m}^*)^2 + (a_{k,i}^* - a_{k,m}^*)^2 + (b_{k,i}^* - b_{k.m}^*)^2} \quad \text{for k= p, ho} \qquad (3.26)$$

It is worthy noting that the smaller $\Delta E_{k,i}$ between the i-th specimen and the average one, the better their colours match. As $\Delta E_{k,i}$ is smaller than 1, there is an almost invisible colour difference between the specimens of concern, while for $\Delta E_{k,I} \approx 5$ the colour difference is clearly noticeable, but the two colours are still very similar.

3.3.3.3 Sensory Analysis

All samples were evaluated by a trained panel of 12 judges consisting of 10 females and 2 males, selected from the staff members of the laboratory for sensory analyses of the Department of Orto-Floro-Arboricoltura e Tecnologie Agroalimentari (DOFATA, University of Catania, Catania, Italy), this being certified by UNI ISO 8589 (1990) (Fig. 3.7).

Evaluations were performed in individual booths by presenting any fruit sample at about the same temperature of 20°C in 3-digit coded plastic dishes to any panellist. The experimental design was planned so as to submit any panellist two orange fruits randomly selected within the three aforementioned classes (MacFie et al., 1989).

Figure 3.7 Laboratory for Sensory Analyses of the Department of Orto-Floro-Arbori-coltura e Tecnologie Agroalimentari (University of Catania, Catania, Italy), certified by UNI ISO 8589 (1990).

Table 3.1 Definition of the sensory attributes, perceived by skilled panellists in this work and of the minimum and maximum levels assignable to any of them.

Attributes	Definition	Ordinal Scale 1	9
Visually-perceived			
Fruit shape (FS)	Assessment of the fruit shape	Perfectly ovoid	Perfectly spherical
Fruit shape defects (FSD)	Assessment of the presence of shape defects in the fruit.	Absent	Present
Tactilely-perceived in the hand			
Compactness (C)	Assessment of the fruit resistance to compression along the fruit equatorial axis, once the fruit peduncle has been oriented to the panellist right-side.	Very soft	Very hard
Ease of peeling (EP)	Assessment of the peel resistance to a sharp knife.	Very high	Very low
Ease of segment separation (ESS)	Assessment of the resistance of segments to be manually separated.	Very high	Very low
Olfactory-perceived			
Typical orange odour (TOO)	Olfactory perception of the characteristic fresh orange scent	Absent	Very intense
Off-odour (OO)	Olfactory perception of anomalous, unpleasant, or non-characteristic orange smell.	Absent	Very intense
Tactilely-perceived in the mouth			
Juiciness (J)	Assessment of the volume of orange juice expressed while the fruit is squeezed between the teeth.	Juiceless	Very juicy
Tasty-perceived			
Sweetness (SW)	Assessment of sweetness by referring to aqueous solutions containing 4-6 g/dm^3 of sucrose.	Absent	Very intense
Acidity (AC)	Assessment of sourness by referring to aqueous solutions containing 0.2-0.4 g/dm^3 of citric acid.	Absent	Very intense

Bitterness (B)	Assessment of bitterness by referring to aqueous solutions containing 0.2-0.3 g/dm^3 of caffeine.	Absent	Very intense
Flavour			
Typical orange flavour (TOF)	Assessment of the characteristic flavour of a fresh orange fruit as a result of combined taste and olfactory perception during swallowing.	Absent	Very intense
Off-flavour (OF)	Assessment of anomalous, unpleasant, or non-characteristic orange flavour as a result of combined taste and olfactory perception during swallowing.	Absent	Very intense
Overall sensory evaluation (OSE)	Overall hedonistic value based on the intensity of all the attributes assessed.	Very unpleasant	Very pleasant

Each sensory professional was asked to evaluate the intensity of 14 different attributes (i.e., fruit shape, FS; fruit shape defects, FSD; compactness, C; ease of peeling, EP; ease of segment separation, ESS; typical orange odour, TOO; off-odour, OO; juiciness, J; acidity, AC; sweetness, SW; bitterness, B; typical orange flavour, TOF; off-flavour, OF; and overall sensory evaluation, OSE) using a discontinuous ordinal scale ranging from 1 (absence) to 9 (maximum intensity) (Pagliarini, 2002). Table 3.1 lists the definition of all attributes, as well as its minimum and maximum intensities.

The experimental design used for the panel test was a Randomized Complete Block Design (RCBD) (Montgomery, 2005) with three firmness classes (FC), twelve panellists (P) and two replications (R). Each set of responses from the RCBD was analyzed by a three-way ANOVA. The interaction term P-R or P-FC was estimated to assess the panellist behaviour when tasting another sample belonging to the same firmness class or to different classes, respectively; while the interaction FC-R to measure sample homogeneity and correct randomization. The sum of squares (SS) referred to the three-term interaction (FC-P-R) was used as an estimate of the experimental sum of squares of error (SSE).

3.3.3.4 Multivariate Analysis

A Partial Least Squares Discriminant Analysis (PLS-DA) was used to analyse and investigate the relationship between the physical and sensory tests and the three LF, MF, and HF firmness classes.

PLS-DA (Sabatier et al., 2003; Sjöström et al., 1986) is a multivariate regression method establishing a linear relationship between one or more dependent variables (Z) and a group of descriptors (X). X and Z variables are modelled simultaneously to find the latent variables (LVs) in X that will predict the LVs in Z. These LVs (also called PLS components) are similar to the principal components calculated from the principal component analysis (PCA; Massart et al., 1988). These LVs are computed hierarchically, i.e., the first component accounts for the largest percentage of variance explained, followed by the other components that accounts for the residual variance up to the last ones that are mostly responsible for random variations and experimental error. The optimal number of LVs to predict the response Z without any overfitting is determined on the basis of the residual variance in prediction.

In this work, the X-block variables coincided with the 14 sensory attributes, while the dependent categorical variable Z was represented by the three different firmness classes, as discriminated on the basis of the T_5 values (see Section 4.5). The class membership of each fruit belonging to the HF, MF or LF class was expressed in binary form by attributing the value 1 or 0 to the specimen belonging or not to the class of concern. More specifically, three dummy variables (Z_1, Z_2, and Z_3) were used to assign each specimen to the appropriate category. For instance, a specimen of the LF, MF, or HF class was identified in the Z_1, Z_2, Z_3 space by the point (1,0,0), (0,1,0), or (0,0,1), respectively.

The processing was carried out via Matlab (rel. 7.1, PLSToolbox Eigenvector rel. 4.0). The procedure iteratively determines the minimum number (m) of LVs. These variables may be represented in an m-dimensional space and they are used by PLS to calculate the best regression matrix between X and Z. The model includes a calibration phase and a validation phase for which residual errors (*root mean square error*) were calculated as follows:

$$\mathrm{RMSE} = \sqrt{\frac{\sum_{i=1}^{n}(Z_{i,c} - Z_{i,e})^2}{n}} \tag{3.27}$$

where the sum refers to the samples used for calibration (root mean square error in calibration, RMSEC) or for validation (root mean square error in cross-validation, RMSECV), and $Z_{i,c}$ and $Z_{i,e}$ are the calculated and experimental values of the dependent variable at the i-th measurement. In this case, the best model complexity with respect to the number of LVs accounted for was selected by the minimum value of the RMSECV.

The dataset was separated into two subsets, using the Kennard & Stone algorithm (1969). The first subset consisted of 75% of all data (i.e., 54 measurements) and was used as a calibration set to develop the models, while the remaining 25% of the population (i.e., 18 measurements) was used as a validation set.

Chapter 4: Results and Discussion

In this PhD thesis, the experimental work was scheduled as follows:

i) performance of a first series of conventional parallel plate compression tests up to rupture to determine engineering stress (σ_{zR}) and strain (ε_{zR}) at breakage and design stress-relaxation tests at different cross-head speeds (V_T) and strains (ε_z) to assess the range of linear viscoelasticity;

ii) determination of the contact area (A) of the fruit under squeezing as a function of ε_z for $\varepsilon_z \ll \varepsilon_{zR}$ using two different visual methods to convert the typical force-deformation curves into stress-strain relationships and thus determine the real mechanical properties of orange fruit;

iii) classification of a marketable lot of Tarocco orange fruits into three high-, medium- or low-firmness classes using non-destructive compression tests up to ε_z=0.05 as a preliminary step to perform the destructive Magness-Taylor test and assess a few chemico-physical and sensory properties;

iv) analysis of the statistical significance of all the measurements to establish a quality-assured rule to sort on-line Tarocco orange fruits.

4.1 Preliminary Parallel Plate Compression and Stress-Relaxation tests

Orange fruits are quite complex multi-domain systems (Fig 3.6), that consist of a thick rind or peel composed of coloured epicarp, hypoderm and outer mesocarp (*flavedo*) with numerous external oil vesicles, and white spongy inner mesocarp (*albedo*); a variable number (typically 10 to 16) of segments or *carpels*, loosely united with each other, surrounded by a separable rind, and filled with club-shaped juice vesicles and eventually seeds (Tressler & Joslyn, 1961).

Any test, involving fruit compression between two rigid plates while measuring simultaneously the displacement of the plates and the compression force, is hard to interpret in terms of the citrus fruits intrinsic mechanical properties and is often used to measure a bursting force only. To attempt to determine such properties, the area (A) of the fruit exposed to the compression force F(t), as well as its permanent deformation (ε_P), was calculated by assuming constant fruit volume (§3.3.1.5) so as to identify the most appropriate way to construct stress-strain relationships for orange fruits.

To this end, orange fruit of the Tarocco variety were acquired in a local market and those with about a spherical shape were selected (Pallottino et al., 2009a).

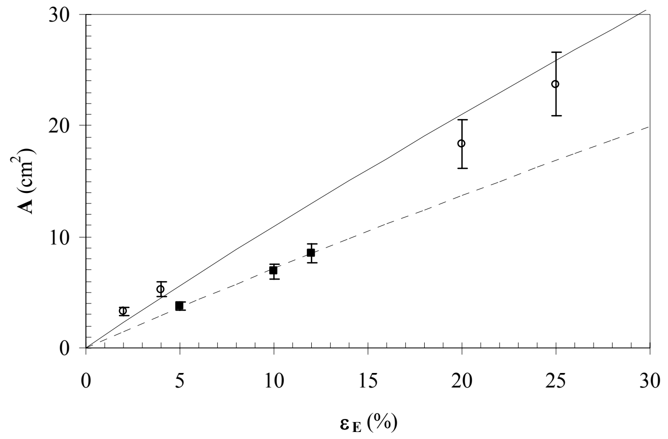

Figure 4.1 Effect of the engineering strain (ε_E) on the observed cross-sectional area (A) of citrus fruits of different radii (R_0) submitted to uniaxial compression testing at a crosshead speed of 15 mm s^{-1}: ■, - - -, R_0=34±2 mm;, O ——, R_0=43±1 mm. The continuous and broken lines were estimated as reported in the text.

4.1.1 Uniaxial Compression Testing

Figure 4.1 compares the observed cross-sectional area (A) as a function of the strain (ε_E) imposed for two classes of orange fruits having different original average radii (R_0) of 34±2 mm (closed symbols) and 43±1 mm (open symbols). The continuous and broken lines plotted in Fig. 4.1 were calculated using Eq.s (3.3-(3.9) and enabled the observed A values to be reconstructed with an average percentage error of 16%. By applying the conventional procedure (ASABE Standards, 2008), the predicted values of A were found to be underestimated by 67 to 26% as ε_E was increased from 2 to 25%. Thus, from such preliminary tests

Eq.s (3.3)-(3.9) appeared will be useful to estimate the construct the compressive stress (σ_E)-vs.-strain (ε_E)- curves of oranges fruits under squeezing.

4.1.2 Compression-Decompression Testing

To measure the permanent deformation of orange fruits with average initial radius (R_0) of 42±1 mm, several tests were performed using a constant cross-head speed of 15 mm s^{-1}. After applying an engineering strain in the range of 2-25%, the compression force was then released and each specimen was allowed to reassume its initial shape for as long as 60 s before determining newly its height (H_0') and mass (M_0'). As ε_E was increased up to 25%, the amount of oil and air squeezed out ($\Delta M = M_0 - M_0'$) was found to be negligible, being in average (0.002±0.001)% of the original fruit mass (M_0). On the contrary, the permanent deformation ($\Delta H = H_0 - H_0'$) tended to increase almost linearly up to (6.5±0.4)% of the initial fruit height, as shown in Fig. 4.2.

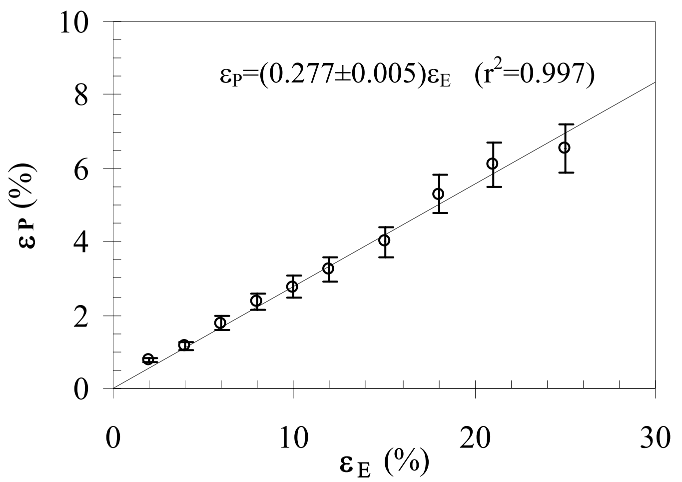

Figure 4.2 Effect of the engineering strain (ε_E) on the permanent deformation strain (ε_p) of orange fruits (R_0=42±1 mm) during compression-decompression tests performed at a crosshead speed (V_t) of 15 mm s^{-1}. The continuous line was calculated by using the least squares regression equation given in the figure.

4.1.3 Compression Testing

To study preliminarily the mechanical behaviour of the orange fruits examined, they were roughly assimilated to deformable membranes (*flavedo*) filled with an internal incompressible liquid. Thus, as suggested by Carin et al. (2003), the compression curves up to rupture, obtained for 5 orange fruits with approximately the same size (R_0=41.8±0.2 mm), variety and maturity, were compared by plotting the force per unit radius (F/R_0) against ε_E (Fig. 4.3). For all the specimens tested, fruit failure initiated at the equator and propagated towards the axis of symmetry with burst occurring for ε_{ER}=(33±4)%.

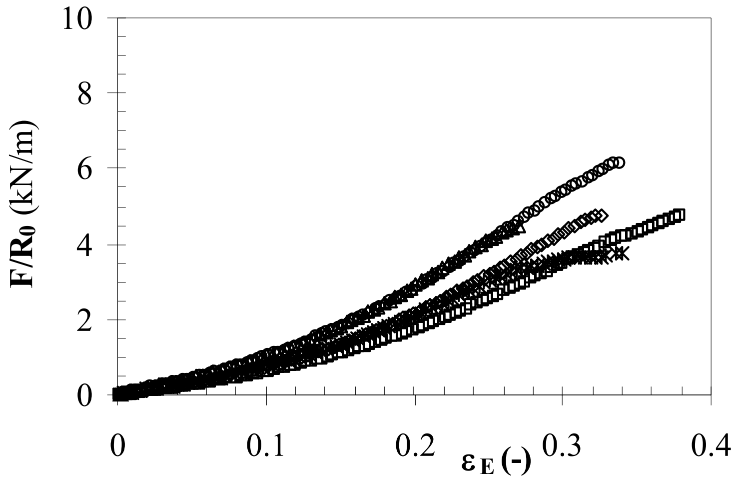

Figure 4.3 Specific compressive load (F/R_0) against engineering strain (ε_E) for 5 orange fruits (R_0=41.8±0.2 mm) submitted to uniaxial compression testing up to rupture using a crosshead speed of 15 mm s^{-1}.

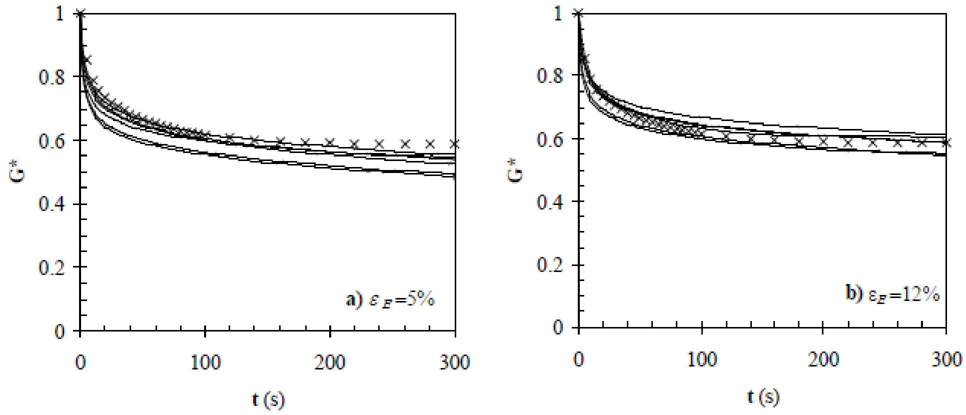

Figure 4.4 Dimensionless relaxation modulus $G^*(t, \varepsilon_E)$ versus time (t) referred to Tarocco orange fruits submitted to different engineering strains (ε_E: **a**, 5%; **b**, 12%) using a crosshead speed of 15 mm s^{-1}. Eq. (2.28) with the parameters A_i and τ_i reported in the text was used to plot the calculated G* data (×).

4.1.4 Stress-Relaxation Testing

To assess the range of validity of linear viscoelasticity, Tarocco orange fruits with average diameter of 69±3 mm were loaded at constant deformation rates of 5 or 15 mm s^{-1} to generate engineering strains in the range of 5-12%. The cross-head was stopped and the stress relaxation was monitored for as long as 300 s, this being much longer than the time required (0.2-1.6 s) to deform the samples (Pallottino et al., 2011b). During all tests the dimensionless relaxation modulus $G^*(t, \varepsilon_E)$ exhibited an asymptotically decaying trend with a residual value different from zero whatever the engineering strain and deformation rate tested (Fig. 4.4).

By applying the operating procedure described in §2.3.4, there was no statistically significant improvement in fitting the time course of any experimental dimensionless relaxation modulus by considering more than two Maxwell elements in parallel to an elastic spring element, these being characterized by the following relaxation times:

τ_1= 5.1 s ; τ_2= 51.3 s

Table 4.1 Dimensionless viscoelastic coefficients (A_i) of the generalised Maxwell model used to describe the main results of the 300-s stress relaxation tests performed on Tarocco orange fruit specimens with average diameter (D_{zo}) under different strains (ε_E) and cross-head speeds (V_T).

ε_E (%)	V_T (mm s^{-1})	D_0 (mm)	A_0 (-)	A_1 (-)	A_2 (-)
12	15	69±5	0.59±0.03	0.19±0.01	0.22±0.03
12	5	69±2	0.60±0.04	0.20±0.02	0.20±0.06
10	15	68±1	0.59±0.05	0.18±0.02	0.23±0.07
10	5	69±3	0.61±0.03	0.20±0.01	0.18±0.04
5	15	70±3	0.54±0.03	0.22±0.01	0.24±0.04
5	5	70±2	0.57±0.01	0.22±0.02	0.21±0.02

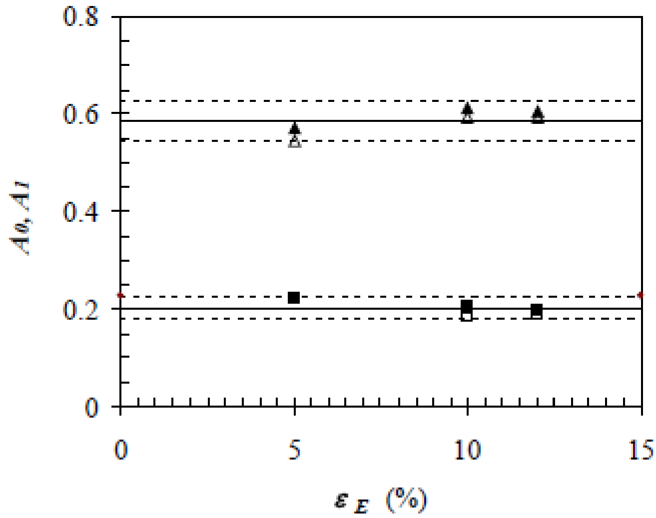

Figure 4.5 Dimensionless viscoelastic coefficients A_0 (△, ▲) and A_1(□, ■) versus applied initial engineering strain (ε_E) referred to Tarocco orange fruits with average diameter of 69±5 mm submitted to stress relaxation tests using a crosshead speed of 5 (closed symbols) or 15 (open symbols) mm s^{-1}. The continuous and broken lines show the mean values and standard deviations of the viscoelastic coefficients.

Thus, the smallest relaxation time (τ_1) was about 3 to 25 times the above loading times and this is approximately in line with the general rule that the relaxation curves are valid only for t greater than five to ten times the loading period (Rao, 1992b).

Table 4.1 shows the dimensionless coefficients (A_i) of a 5-element Maxwell body, which were estimated via the least-squares method. As ε_E or V_T was increased from 5 to 12% or from 5 to 15 mm s^{-1}, respectively, these viscoelastic constants (A_i) appeared to be approximately constant, as shown in Fig. 4.5:

$$A_0 = 0.59 \pm 0.04; A_1 = 0.20 \pm 0.02; A_2 = 0.21 \pm 0.05$$

In particular, the elastic component (A_0), responsible for the equilibrium residual stress, represented about 60% of the initial relaxation modulus $G^*(0,\varepsilon_E)$, this confirming that any orange fruit behaved as a linear viscoelastic solid, at least on the time-scale and deformation range examined. Moreover, the deformation strain up to 12% did not affect the relaxation time spectrum of the delayed elastic components. The cross diagonal symbols (×) plotted in Fig. 4.4 were calculated using eq. (2.28) and the average values of A_i reported above, this showing a limited range of variation among the experimental and calculated G*-vs.-t profiles whatever the engineering strain applied in the range of 5-12%.

4.1.5 Preliminary Conclusions

The real engineering stress-strain relationships for orange fruits submitted to uniaxial compression testing can be hardly extracted from typical force-deformation curves. To this end, it is necessary to assess accurately the real contact areas between the compression plates and the specimen during its compression by image analysis.

The preliminary stress-relaxation tests performed on Tarocco orange fruit allowed their rheological behaviour to be described as that of a linear viscoelastic solid for ε_E ranging from 5 to 12% of their initial height. In this linear viscoelasticity range, once the orange fruit structure had been quickly compressed and decompressed, it exhibited practically negligible permanent deformation, thus giving explanation for the operating procedure of the non-destructive on-line high-speed systems, currently available on the market to sort orange fruits on the basis of their individual firmness.

Further tests will be performed to substantiate such preliminary findings.

4.2 Contact area assessment via image analysis

By compressing any orange fruit along the z-axis, its original almost spherical shape resulted to be axisymmetrically squeezed in the upper and lower polar regions contacting the UTM plates.

The effective contact surface area (A_{EFA}) for any single sample, as detected by image EFA (Fig 3.2-A, -B, -C), was found to be quite irregular, especially at the smaller strains (Fig. 4). Nevertheless, when the average contours of A_{EFA} were calculated, it was possible to assimilate the shape of each contact area to quite a perfect ellipse (Fig. 4.6).

Despite an average variation of about 20%, the estimated A_{EFA} values appeared to vary linearly with ε_z (see continuous line in Fig. 4.7):

$$A_{EFA} = (71 \pm 3)\ \varepsilon_z \qquad (r^2 = 0.99) \qquad (4.1)$$

where A_{EFA} is expressed in cm^2 and ε_z is dimensionless.

The images acquired by the vertical (z) camera were also inscribed in a bounding box. Both measured sides were used to determine the semi-major (a_{BB}) and -minor (b_{BB}) axes of the *a priori* assumed elliptical contact area (A_{BB}). This was then calculated using Eq. (3.1), as listed in Table 4.2.

In Table 4.2 different letters were used to represent statistically significant differences according to the One-Way ANOVA and Student's t-test. In particular, there was a statistically significant difference in the F_z and E_S values between groups at the confidence level of 1%. On the contrary, whatever the compression strain applied the differences among the fruit diameters (D_{zo}, D_{xo}, D_{yo}, D_{eo},), as well as the fruit rind thicknesses (t_x, $t_{x'}$, $t_{y'}$, $t_{y'}$) and apparent Poisson's ratios (ν_x, ν_y), in the different regions tested resulted to be insignificant, thus confirming homogeneity and correct test randomization.

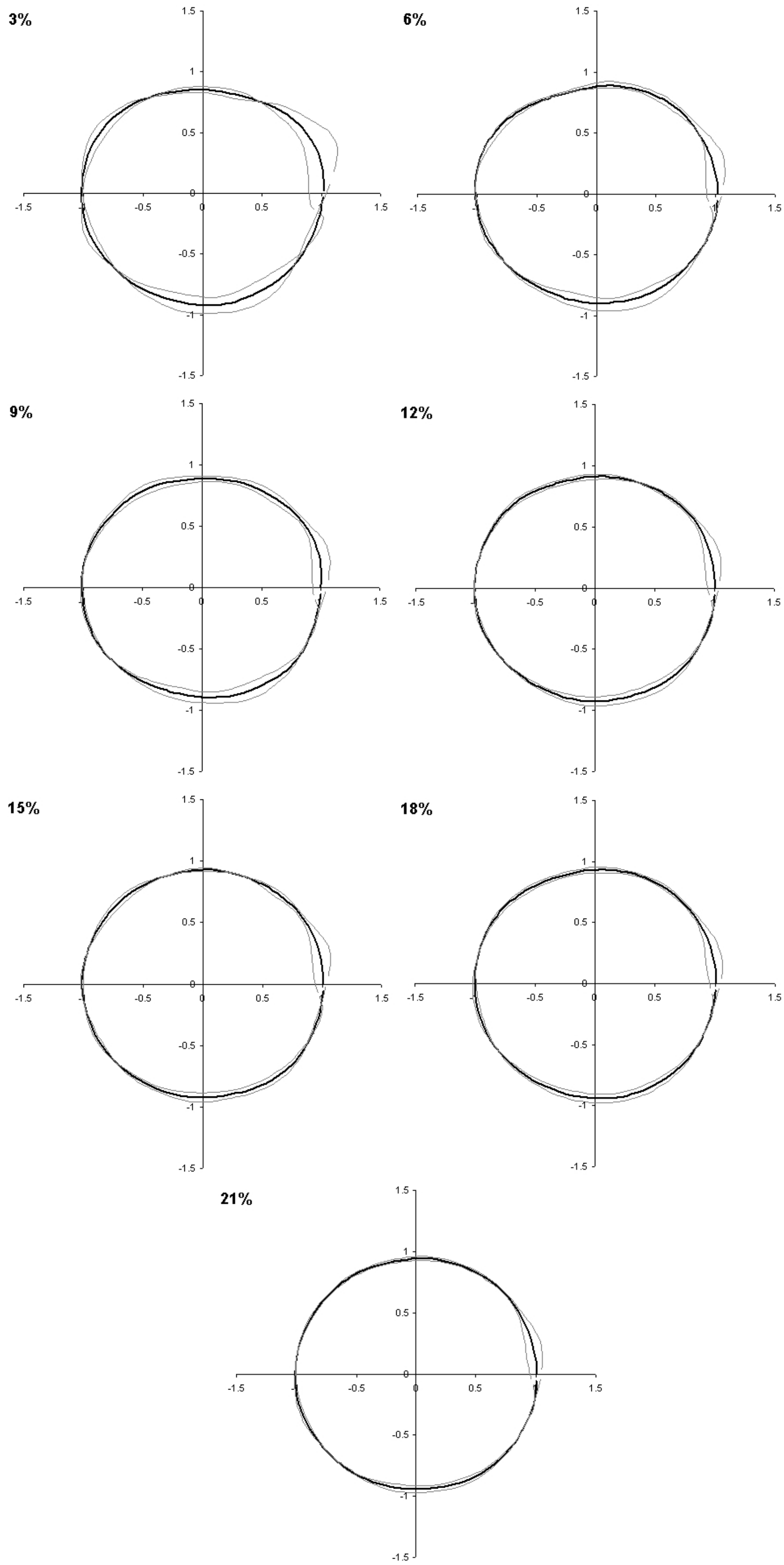

Figure 4.6 Effect of the engineering strain (εz) applied in the range 0-21% on the mean outline of the contact surface area (AEFA) (black line) with standard deviations (±, light grey and dark grey respectively), as estimated by the Elliptic Fourier Analysis.

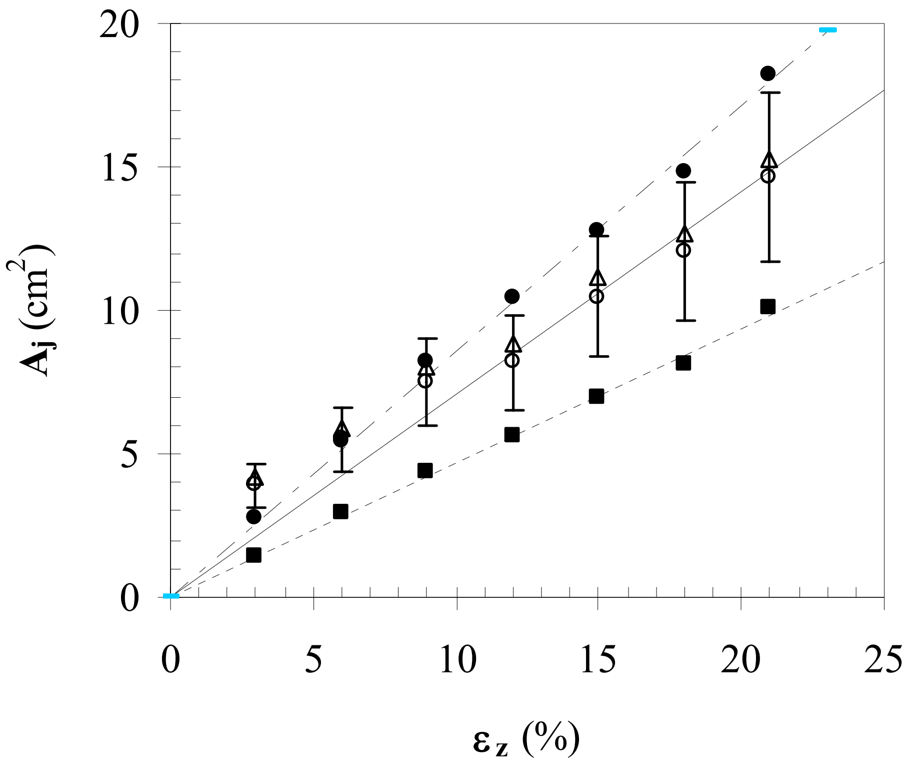

Figure 4.7 Effect of the engineering strain (ε_z) on the contact area (Aj), as acquired by image analyses using the EFA (A_{EFA}: ○) or bounding-box method (A_{BB}: △), or calculated via the Hertz equations shown in Table 2.1 (A_{ASM}: ■) or via Eq.s (3.8)-(4.5) (A_V: ◆). The continuous line was plotted using Eq. (4.1), while the broken and dotted lines coincided with their corresponding regression lines.

To test whether the experimental mean values of the contact areas A_{EFA} and A_{BB} were significantly different; their standardised normal difference (d) was compared with the classic inequality of the hypothesis test for means (Bennett & Franklin, 1954):

$$d = \frac{\left|A_{EFA} - A_{BB}\right|}{\sqrt{\frac{s_{EFA}^2}{n_{EFA}} + \frac{s_{BB}^2}{n_{BB}}}} \neq t_{\alpha,df} \qquad (4.2)$$

where A_j, s_j, and n_j are the mean value, standard deviation and overall number of samples for the two output variables tested at a given ε_z value, and df ($=n_{EFA} + n_{BB} - 2$) degrees of freedom.

Table 4.2 Main results of the image analyses acquired during uniaxial compression tests performed on groups of 20 orange fruits: effect of the engineering strain (ε_z) on the average values and standard deviations of the fruit resistance (F_z); initial diameters D_{xo}, D_{yo} and D_{zo} in the three orthogonal directions x, y, and z; diameter (D_{eo}) of the equivalent sphere; Poisson's ratios (ν_x and ν_y); apparent modulus of elasticity (E_S); rind thicknesses (t_j) along the 4 equatorial positions shown in Fig. 3.2; and contact surface area, as estimated by using the Elliptic Fourier Analysis (A_{EFA}) or bounding box method (A_{BB}). Different letters represent statistically significant differences according to One-Way ANOVA and Student's t-test for values of p≤0.01.

ε_z	F_z	D_{zo}	D_{xo}	D_{yo}	D_{eo}	ν_x	ν_y
%	N	mm	mm	Mm	mm		
3	8±2[a]	75±4[a]	75±4[a]	77±7[a]	75±4[a]	0.12±0.15[a]	0.17±0.15[a]
6	18±4[b]	75±4[a]	77±5[a]	76±4[a]	76±3[a]	0.14±0.10[a]	0.11±0.08[a]
9	27±4[c]	76±4[a]	77±6[a]	77±5[a]	76±4[a]	0.14±0.08[a]	0.13±0.08[a]
12	43±8[d]	75±4[a]	75±4[a]	74±4[a]	75±4[a]	0.12±0.04[a]	0.17±0.06[a]
15	57±7[e]	75±3[a]	73±4[a]	76±5[a]	74±3[a]	0.19±0.06[a]	0.16±0.06[a]
18	79±12[f]	73±4[a]	75±4[a]	74±4[a]	74±3[a]	0.18±0.07[a]	0.17±0.06[a]
21	106±20[g]	76±5[a]	75±5[a]	77±5[a]	76±5[a]	0.20±0.05[a]	0.20±0.07[a]
Overall		75±4	75±5	76±5	75±4	0.16±0.09	0.16±0.09
One-Way ANOVA p	0	0.296	0.228	0.192	0.347	0.007	0.003
Mean squares between groups	2471.4	20	29.52	36.19	16.19	0.02	0.02
Mean squares within groups	99	16.29	21.43	24.57	14.29	0.01	0.01

ε_z	E_S	t_x	$t_{x'}$	t_y	$t_{y'}$	A_{EFA}	A_{BB}
%		mm	mm	mm	mm	cm^2	cm^2
3	770±184[a]	2.2±0.4[a]	1.6±0.3[a]	1.8±0.4[a]	1.9±0.4[a]	3.9±1.1[a]	4.2±1.2[a]
6	616±127[b]	2.3±0.5[a]	1.7±0.4[a]	1.9±0.4[a]	1.9±0.4[a]	5.5±1.4[a]	5.9±1.6[a]
9	504± 69[c]	2.4±0.3[a]	1.6±0.3[a]	1.9±0.4[a]	1.9±0.5[a]	7.5±1.6[ab]	8.0±1.8[ab]
12	537±112[d]	2.2±0.5[a]	1.6±0.3[a]	1.8±0.4[a]	1.8±0.4[a]	8.4±1.6[ab]	8.8±1.4[ab]
15	520±69[e]	2.4±0.5[a]	1.7±0.2[a]	1.8±0.4[a]	1.8±0.3[a]	10.5±2.0[ab]	11.1±2.5[ab]
18	566±111[f]	2.1±0.5[a]	1.7±0.3[a]	1.9±0.6[a]	1.9±0.5[a]	12.1±2.4[ab]	12.6±2.5[ab]
21	557± 81[g]	2.1±0.3[a]	1.6±0.3[a]	1.8±0.4[a]	1.9±0.4[a]	14.7±2.6[b]	15.3±2.8[b]
Overall	**581± 91**	**2.2±0.4**	**1.6±0.3**	**1.8±0.4**	**1.9±0.4**		
One-Way ANOVA p	0	0.128	0.718	0.934	0.95	0	0
Mean squares between groups	164439	0.32	0.06	0.06	0.05	284	298.5
Mean squares within groups	12990	0.19	0.1	0.19	0.18	3.44	4.22

In this case, for $n_{EFA}=n_{BB}=20$ and $t_{0.01,38}\approx2.71$, for all data acquired it was possible to reject the hypothesis of inequality at a probability level of 0.01 ($d=0.73\text{-}0.91<2.71$).

By comparing the average values of A_{EFA} to those of A_{BB} against ε_z (Fig. 4.7), it was possible to note quite a good agreement, the mean percentage error between the two methods being of about 6.2%, even if the inscription of the contact area in a bounding box appeared to lead to a general overestimation of the effective contact areas (Table 4.2).

All common materials undergo a transverse expansion when compressed in one direction and vice versa. The magnitude of this transverse deformation is governed by a material property known as Poisson's ratio (ν). It is defined as minus the transverse strain divided by the axial strain in the direction of stretching force. The isotropic upper limit of 0.5 is also typical of rubbers and soft biological tissues (Rao, 1992a; Steffe, 1996). Tissue with a high level of cellular gas, such as apple flesh, would have values near to 0.2; whereas foods with high water content, such as fresh fruits and vegetables, would have a Poisson's ratio close to 0.5, such as potato or peach flesh (ASABE, 2008).

Table 4.2 lists the average values and standard deviations of the initial diameters D_{xo}, D_{yo} and D_{zo} in the three orthogonal directions x, y, and z for any orange fruit submitted to different vertical engineering strains (ε_z) together with the estimated values of the apparent Poisson's ratios ν_x and ν_y, defined as follows:

$$\nu_x = -\left(\frac{\Delta x/D_{xo}}{\Delta z/D_{zo}}\right) = -\frac{\varepsilon_x}{\varepsilon_z} \tag{4.3}$$

$$\nu_y = -\left(\frac{\Delta y/D_{yo}}{\Delta z/D_{zo}}\right) = -\frac{\varepsilon_y}{\varepsilon_z} \tag{4.4}$$

where Δx and Δy are the transverse deformations of each orange fruit under testing, as measured using cameras y and x, respectively.

Despite the wide variation in the deformations observed along the axis lines x and y as the result of the compression (Δz) applied, the average values of ν_x and ν_y practically coincided (0.16±0.09), this confirming the almost homogeneous behaviour of the fruit samples examined.

4.2.1 Contact area prediction using the ASABE standard method

The applicability of this model can be a priori validated by plotting the log of applied force (F_z) as a function of the log of deformation (ε_z). If the model is valid, the slope of the line should be 1.5 (Fridley et al., 1968; Arnold and Mohsenin, 1971). This was checked by plotting Fig. 4.8, the corresponding regression line being of the linear type:

$$\log(F_z)=(0.22\pm0.06)+(1.32\pm0.05)\log(\varepsilon_z) \qquad \text{for } \varepsilon_z\leq 21\% \qquad (4.5)$$

with a coefficient of determination r^2 equal to 0.99.

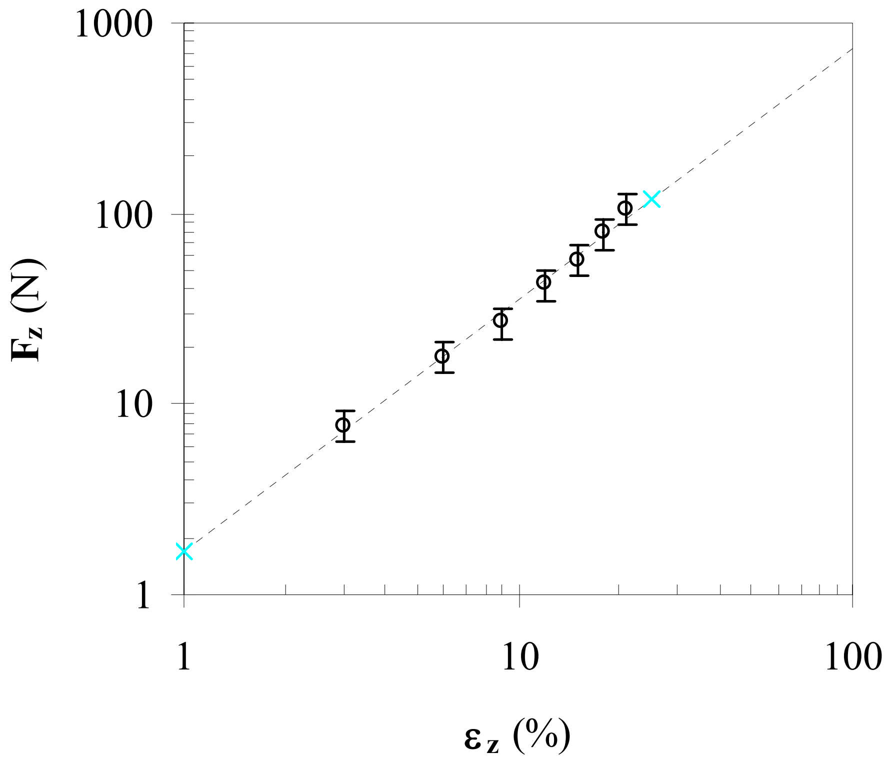

Figure 4.8 Bilogarithmic plot of the average values of the resulting compression force (Fz) against the compression strain (ε_z) referred to 20 replicated tests. The broken line represents the least squares regression line (4.5), while any vertical bar denotes an average coefficient of variation of ±18%.

By referring to the loading geometry shown in Fig. 2.8 and the equations listed in Table 2.1, in the case of almost spherical fruits undergoing testing via a CD with smooth, polished and flat surface ($R_{CD}=\infty$), such as that used to test Red Delicious apple fruits (ASABE 2008), the differences in the radii of curvature of the convex surface of the sample at the point of contact with the upper (R_U, R'_U) and lower (R_L, R'_L) plates can be neglected by resorting to a unique radius of curvature coinciding with the radius of the equivalent sphere having the same volume of the ellipsoid with diameters D_x, D_y and D_z, as viewed by the cams y, x, and z, respectively (Fig. 3.2). In the circumstances, the contact angle (θ) between the specimen and the compression device tends to 90°, this resulting in $c_1=c_2=1.0$, and $K_U=K_L\sim1.35$.

By referring to the aforementioned average value of the Poisson's ratio and initial diameter (D_{eo}) of the equivalent sphere (Table 4.1), the use of the equations listed in Table 2.1 allowed the cross-sectional area (A_{ASM}) to be estimated as a function of the vertical compressive strain (ε_z) for any orange fruit sample tested.

As shown in Fig. 4.7, use of the ASABE standard method (2008) resulted in a general underestimation of the effective contact area (A_{EFA}) values, the mean percentage error being of about 45%.

Finally, Table 4.2 lists the estimated values of the apparent modulus of elasticity (E_S) for the orange fruit samples tested. It can be noted that it reduced from 770±184 to 557±81 kPa as ε_z was increased from 3 to 21%, its average value being 581±91 kPa.

4.2.2 Contact area prediction assuming constant fruit volume

By referring to the loading geometry shown in Fig. 3.4 and to the initial diameter of the equivalent sphere for any orange fruit sample under testing (Table 4.2) and using Eq.s (3.3)-(3.9), it was possible to calculate the instantaneous cross-sectional area (A_V) of the deformed sample under constant volume as a function of the compressive engineering strain imposed (ε_z), as shown in Fig. 4.7.

Table 4.3 Main results of parallel plate compression tests up to rupture on 20 orange fruit samples: initial diameters D_{xo}, D_{yo} and D_{zo} in the three orthogonal directions x, y, and z; initial diameter (D_{eo}) of the equivalent sphere; the maximum strain ($\varepsilon_{z,max}$) and resistance ($F_{z,max}$) values; thickness of the orange rind in the 4 positions shown in Fig. 3.2; approximate circumference (C_F) and surface area (A_F) of the elliptic rind.

Sample n°	**D_{zo}**	**D_{xo}**	**D_{yo}**	**D_{eo}**	**$\varepsilon_{z,max}$**	**$F_{z,max}$**
	mm	mm	mm	Mm	%	N
1	80.6	80.8	86.9	83	31	212
2	79.5	79.2	84.4	81	23	193
3	78.9	89.4	88.1	85	28	250
4	78	75.3	83.2	79	26	199
5	78.4	87.1	83.6	83	33	229
6	75	78.5	77.1	77	40	185
7	75.7	84	78.7	79	25	267
8	79.2	77.3	83.2	80	30	235
9	74.6	77.7	78.7	77	30	224
10	80.1	88.3	83.2	84	31	217
11	82.6	92.2	87.7	87	31	276
12	79.6	82	84.8	82	30	250
13	77.7	78.9	83.2	80	26	179
14	77.3	80.4	83.2	80	35	198
15	78.8	80	84	81	34	242
16	72	86.3	75.5	78	35	189
17	82.3	82.4	85.7	83	28	232
18	78.9	82.4	86.1	82	28	234
19	73.9	77.7	82.4	78	27	199
20	74.9	74.1	79.5	76	28	187
Overall	78±3	82±5	83±3	81±3	30±4	220±28

Sample n°	t_x	$t_{x'}$	t_y	$t_{y'}$	C_F	A_F
	mm	mm	mm	mm	m	cm^2
1	4	2.39	1.58	1.99	0.264	4.2
2	2.35	1.23	1.19	0.77	0.257	2
3	1.71	1.8	1.59	1.66	0.279	4.4
4	2.13	1.42	1.47	1.61	0.249	3.5
5	3.33	1.44	1.83	1.87	0.268	3.9
6	1.83	1.58	1.45	1.75	0.244	3.5
7	2.11	1.33	1.6	1.31	0.256	3.3
8	1.83	1.58	1.51	1.45	0.252	3.7
9	1.98	1.77	1.77	1.38	0.246	3.4
10	2.13	2.04	2.84	1.74	0.269	4.7
11	2.61	1.84	1.85	1.75	0.283	4.9
12	2.5	1.99	1.94	1.95	0.262	5.1
13	1.85	1.45	1.82	1.14	0.255	2.9
14	1.82	1.63	1.45	1.13	0.257	2.9
15	2.2	1.75	1.78	1.64	0.258	4.2
16	1.99	1.49	1.68	1.52	0.255	3.8
17	2.58	1.07	1.59	1.29	0.264	2.8
18	1.59	1.39	1.71	1.32	0.265	3.5
19	1.7	1.55	1.24	1.48	0.252	3.1
20	1.9	1.12	1.55	1.43	0.242	2.7
Overall	2.2±0.6	1.6±0.3	1.7±0.3	1.5±0.3	0.26±0.01	3.6±0.8

In the circumstances, the estimated contact areas (A_V) differed from those derived from EFA (A_{EFA}) by about 19%. For $n_{EFA}=n_V=20$ and $t_{0.01,38}\approx 2.71$, it was possible to reject the hypothesis of equality at a confidence level of 0.01, their standardised normal difference (d) varying from 3.6 to 4.8 for the data acquired at $\varepsilon_z=3$, and 12 to 21%. Only at strains equal to 6 and 9%, the difference in the estimated A_j values resulted to be statistically negligible.

In conclusion, there is no rationale to further rely on the contact areas underestimated using the ASABE standard method (2008), especially if the real stress-strain relationships are to be extracted from the force-deformation curves monitored during parallel plate compression test.

4.3 Compression testing up to rupture

Another set of 20 samples was submitted to uniaxial compression tests up to rupture. Table 4.3 lists the original diameters along the 3 orthogonal directions x, y, and z and equivalent diameters (D_{eo}) for any sample group, the maximum values of strain ($\varepsilon_{z,max}$) and resistance ($F_{z,max}$), as well as the thickness of the orange rind in the 4 positions shown in Fig. 3.2, that were determined after fruit breakage.

In Fig. 4.9a the average values of fruit resistance are plotted against ε_z. Despite the mean coefficient of variation for all data collected was 18%, the data were well described by Eq. (3.10) for $\varepsilon_z \leq 21\%$ (see broken line in Fig. 4.9a). Thus, it can be noted a power-law relationship between F_z and ε_z.

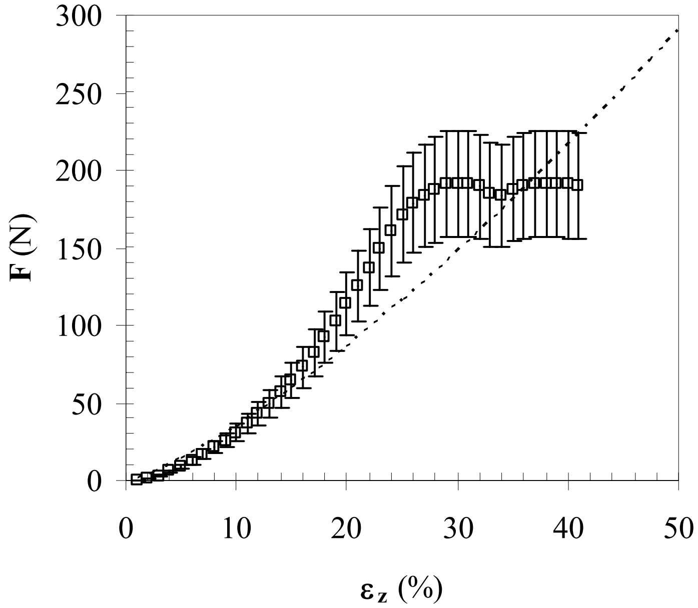

Figure 4.9 Main results of the parallel plate compression testing up to rupture performed on 20 orange fruit samples using a crosshead speed of 15 mm s^{-1}: **a)** Average fruit resistance (F_z) against engineering strain (ε_z);

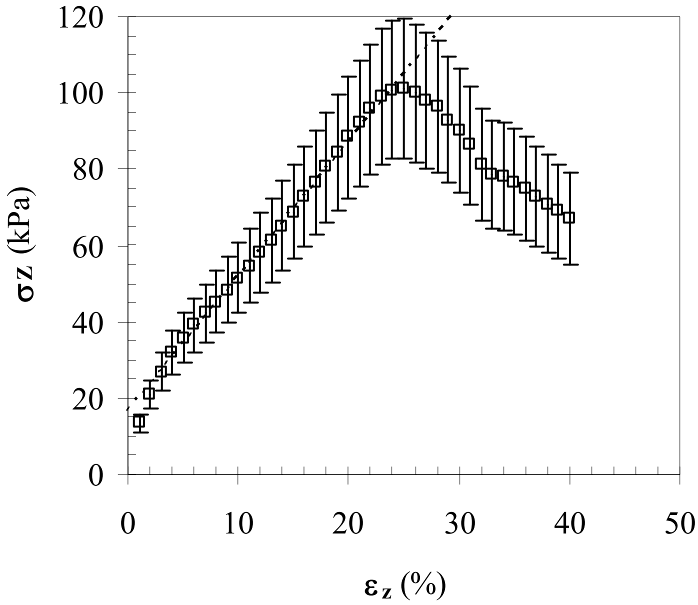

Figure 4.9 **b)** Average compressive engineering stress (σ_z) vs. ε_z.

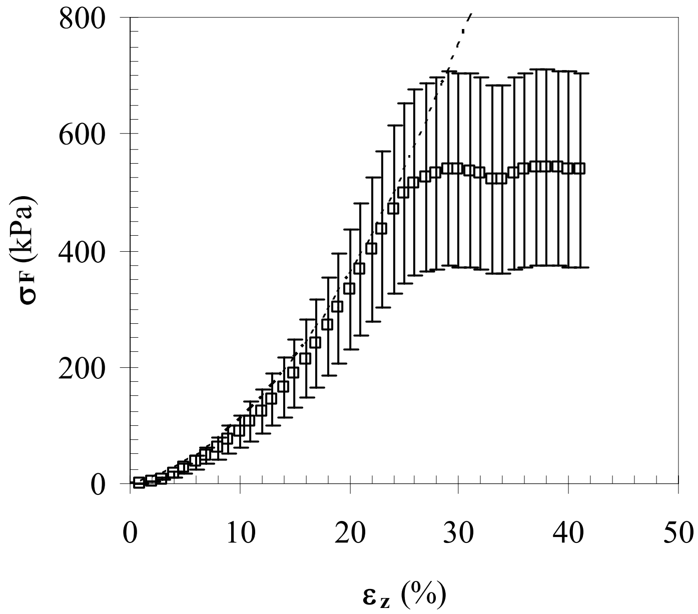

Figure 4.9 **c)** Average compressive stress for the orange rind only (σ_F) vs.ε_z.

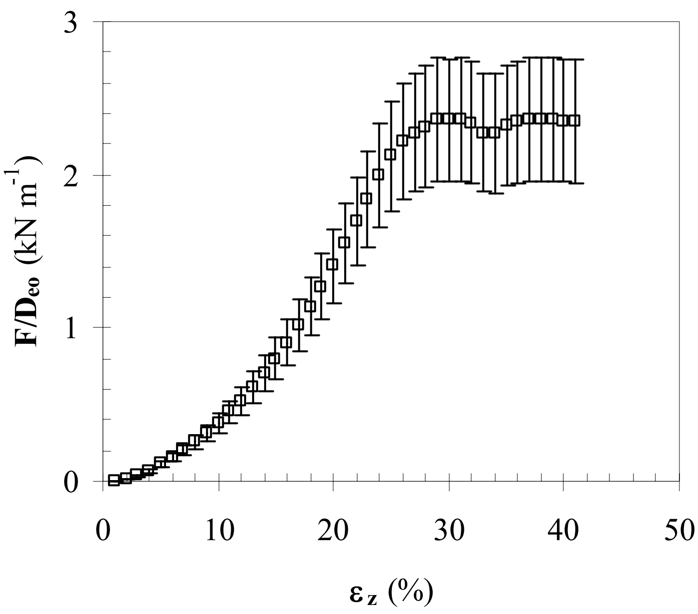

Figure 4.9 **d)** Average specific compressive load (F/D_{eo}) vs. ε_z.

By using Eq. (3.10), it was possible to convert the F_z-vs.-ε_z curve into the engineering stress(σ_z)-vs.-strain (ε_z) relationship (Fig. 4.9b).

Despite the uncertainty in the estimation of A, especially at strains smaller than 3%, the engineering stresses (σ_z) for any specimen assayed exhibited an initial trend of the power-law type that becomes practically of the linear type as ε_z was increased from 4% to 24%. Beyond such a strain, σ_z reached a maximum burst value (109±15 kPa) at ε_{zR}=(28±3)%, then tended to decline.

The linear region in the σ_z-vs.-ε_z curve enabled the apparent modulus of elasticity (E_O) of the whole orange fruit to be estimated (353±3 kPa, r^2=0.998).

To check for this behaviour, it was assumed that the compression force (F_z) impinged on the equatorial horizontal cross-section of the epicarp, this being estimated as follows:

$$A_F = C_F\, t_{min} \qquad (4.6)$$

with

$$C_F = 2\,\pi \sqrt{\frac{a^2 + b^2}{2}} \qquad (4.7)$$

where C_F is the circumference of the elliptic rind, and a and b are its semi-major and -minor axes along the axes x and y. The former was approximated via Euler's formula (Perry et al., 1963), while the others were estimated by halving the fruit diameters D_{xo} and D_{yo}. Finally, t_{min} is the minimum thickness of the rind with respect to the four values measured after fruit breakage in the positions shown in Fig. 3.2. All these data are reported in Table 4.3.

Thus, it was possible to obtain a rough measure of the compressive stress for the orange external rind only (σ_F=F/A_F), as shown in Fig. 4.9c.

The average concave upward relationship was described by the following polynomial model up to near the break point with coefficients of determination (r^2) greater than 0.999:

$$\sigma_F = E_F\, \varepsilon_Z + k\, (\varepsilon_Z)^2 \qquad (4.8)$$

where E_F is the apparent modulus of elasticity referred to the orange peel (=375±33 kPa), and k is an empirical constant (=7108±167 kPa), that represents a measure of the upward deviation from linearity or material densification capability. For k tending to zero, Eq. (4.7) reduces to Hooke's law.

The practical coincidence between the apparent moduli of elasticity of the orange fruit as a whole (E_O) and orange peel only (E_F) may be regarded as incidental, since they were related to different cross-sectional surface areas of the sample tested.

By assimilating the orange peel to an impermeable, elastic, homogeneous, and isotropic membrane, σ_F may be confused with the hydrostatic pressure exerted by the incompressible orange juice on the peel internal surface, responsible for the fruit lateral expansion. Burst occurred at σ_{FR}=533±103 kPa at ε_{zR}=0.30±0.03 for rind thicknesses ranging from 0.77 to 1.94 mm. However, the standard deviations are quite large (around 28% for σ_{FR}).

Since any fruit may be supposed to be initially spherical with an initial diameter D_{eo} and its rind initially constant in thickness (t_o), this being very small compared to the radius of curvature, the thin shell theory may be applied and bending effects ignored (Barthès-Biesel et al., 2002; Carin et al., 2003). In the circumstances, since the membrane is assumed very thin, the resulting stresses in the membrane may be replaced by elastic tensions (i.e., forces per unit length of a line element in the median plane). Thus, as suggested by Carin et al. (2003), the compression curves up to rupture, obtained for 20 orange fruit specimens with approximately the same size (D_{eo}=81±3 mm), variety and maturity, may be compared by plotting the force per unit diameter (F_z/D_{eo}) against ε_z (Fig. 4.9d). For all the specimens tested, fruit failure initiated at the equator and propagated towards the axis of symmetry with burst occurring for ε_{zR}=(30±4)%.

4.4 Viscoelastic Properties of Tarocco Orange

To represent statistically significant differences among the physical parameters characterizing each group of samples submitted to different engineering strains in the range of 5 to 20%, according to the One-Way ANOVA and Student's t-test, different letters were used, as shown in Table 4.4. In particular, whatever the compression strain applied, the differences among the initial fruit diameters (D_{zo}, D_{xo}, D_{yo}), mass (m_o) and volumes (V_o) of the four groups resulted to be insignificant at the confidence level of 99%, thus confirming homogeneity and correct test randomization. On the contrary, there was a statistically significant difference in the F_z and A values detected for ε_z ranging from 5 to 20%.

A typical image of a Tarocco orange fruit, as compressed at 20% of its initial height, is shown in Fig. 3.2. From the projection images X and Y it can be noted that the deformed fruit is axisymmetric.

4.4.1 Stress-Strain Relationship

To assess preliminarily the validity of the theory of contact between convex surfaces of elastic materials (ASABE, 2008), the observed values of F_z for all the groups of 20 specimens tested were plotted against ε_z on a double logarithmic plot (Fig. 4.10).

Table 4.4 Effect of the compressive engineering strain along the axis z (ε_z) on the mean initial fruit diameters along the x, y, and z axes (D_{zo}, D_{xo}, D_{yo}), mass (mo) and volume (V_o); permanent fruit deformations (δ_x, δ_y, δ_z); mass (δ_m) and volume (δ_V) losses after a stress relaxation testing of 15 min and a decompression of 5 min; fruit resistance (F_z) and contact area (A). Different letters represent statistically significant differences according to the One-Way ANOVA and Student's t-test for values of p≤0.01.

ε_z	D_{zo}	D_{xo}	D_{yo}	m_o	V_o	δ_x
[%]	[mm]	[mm]	[mm]	[g]	[cm^3]	[%]
5	76±3 ^{a}	83±6 ^{a}	80±4 ^{a}	227±22 ^{a}	262±33 ^{a}	0.4±0.8 ^{a}
10	74±3 ^{a}	79±6 ^{a}	78±3 ^{a}	212±23 ^{a}	238±30 ^{a}	0.4±0.7 ^{a}
15	75±4 ^{a}	81±4 ^{a}	79±5 ^{a}	221±28 ^{a}	251±39 ^{a}	0.9±0.6 ^{ab}
20	75±4 ^{a}	79±6 ^{a}	79±4 ^{a}	217±30 ^{a}	245±39 ^{a}	1.2±0.8 ^{b}
Overall	75±3	80±6	79±4	219±26	249±36	
p	0.487	0.135	0.342	0.318	0.186	0.001
MSBG (df=3)	9.78	57.52	16.98	805	2066.7	3.12
MSWG (df=76)	11.93	30.08	15.01	674.3	1257.8	0.53
ε_z	δ_y	δ_z	δ_m	δ_V	F_z	A
5	0.0±0.5 ^{a}	-2.1±0.2 ^{a}	-0.04±0.03 ^{a}	-1.7±1.0 ^{a}	15±3 ^{a}	5.5±0.9 ^{a}
10	0.3±0.5 ^{a}	-3.6±0.5 ^{b}	-0.03±0.02 ^{a}	-3.0±0.9 ^{b}	32±8 ^{b}	8.6±1.8 ^{b}
15	0.4±0.5 ^{a}	-5.6±0.7 ^{c}	-0.04±0.03 ^{a}	-4.3±1.0 ^{c}	55±9 ^{c}	11.2±2.2^c
20	0.6±0.7 ^{a}	-7.5±0.8 ^{d}	-0.04±0.03 ^{a}	-5.8±1.1^d	84±19 ^{d}	13.5±2.5 ^{d}
Overall	0.3±0.6		-0.04±0.3			
p	0.01	0	0.588	0	0	0
MSBG (df=3)	1.25	110.8	0.001	61.7	17973.5	236.9
MSWG (df=76)	0.31	0.36	0.001	1.01	128.8	3.79

MSBG Mean Squares between groups

MSWG Mean Squares within groups

It can be noted that not only such data substantially agreed with the regression line (4.5) previously established on the same type of Tarocco fruits for ε_z≤21% (Pallottino et al., 2011a), but also the slope of the line was statistically different from 1.5, this value being in agreement with the above theory (Arnold & Mohsenin, 1971; ASABE, 2008; Fridley et al., 1968). In the circumstances, it was impossible to estimate the apparent modulus of elasticity of Tarocco orange fruit, as well as the fruit-to-plate contact area (A) by means of Eq.s (2.15)-(2.28) in

ASABE standards (2008), thus justifying the assessment of the former via the so called bounding box method.

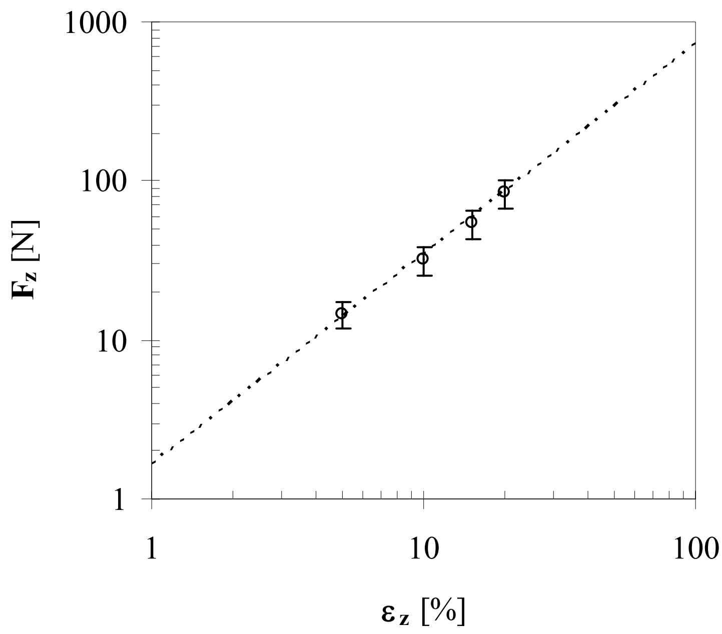

Figure 4.10 Bilogarithmic plot of the average values of the resulting compression force (F_z) against the compression strain applied (ε_z), each data being referred to 20 replicated tests. The broken line was plotted using Eq. (4.5).

The mean values of A, estimated in each group, under constant ε_z in the range of 5-20% were found to be statistically different at the significance level of 0.01, as shown in Table 4.4.

Thus, by using Eq.s (2.2) and (2.15) it was possible to convert the force-*vs.*-deformation curves into the engineering stress-*vs.*-strain relationships and via Eq. (2.15) to estimate the relaxation modulus $G(t,\varepsilon_z)$, respectively.

4.4.2 Stress Relaxation Testing

Some typical time courses of F_z during the stress relaxation tests for ε_z ranging from 5 to 20% were shown in Fig. 4.11.

By comparing the time course of the dimensionless relaxation modulus $G^*(t,\varepsilon_z)$ at different ε_z values, it was possible to reveal quite a similar asymptotically decaying trend with a residual value different from zero whatever the engineering strain applied (Fig. 4.12).

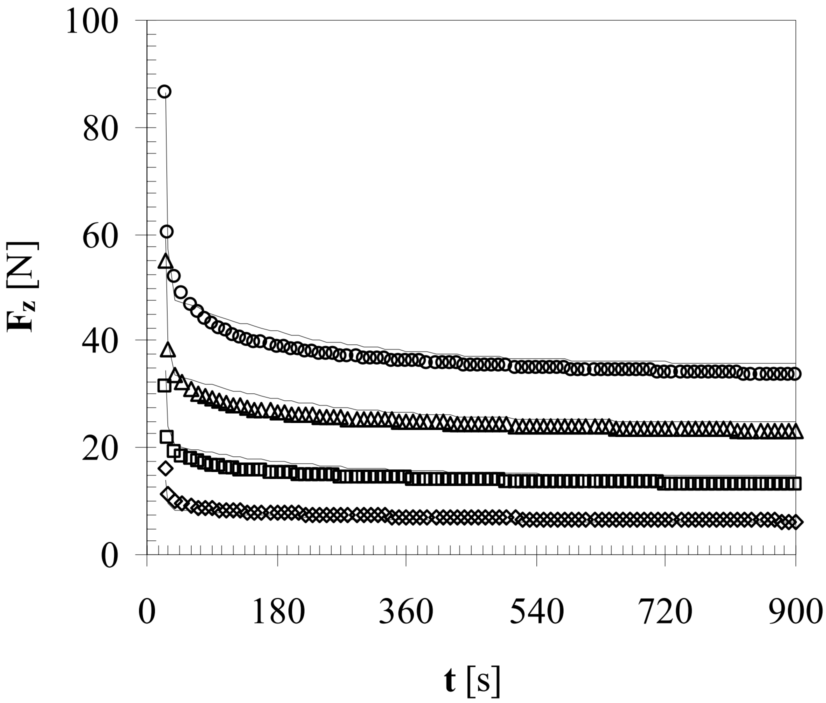

Figure 4.11 Typical relaxation of the compressive force (Fz) for Tarocco orange fruits submitted to several engineering strains (ε_z: ◊, 0.05; □, 0.10; △, 0.15; ○, 0.20): F_z versus time (t). The continuous lines were calculated using Eq.s (2.16), (2.28) and (4.5) as reported in the text.

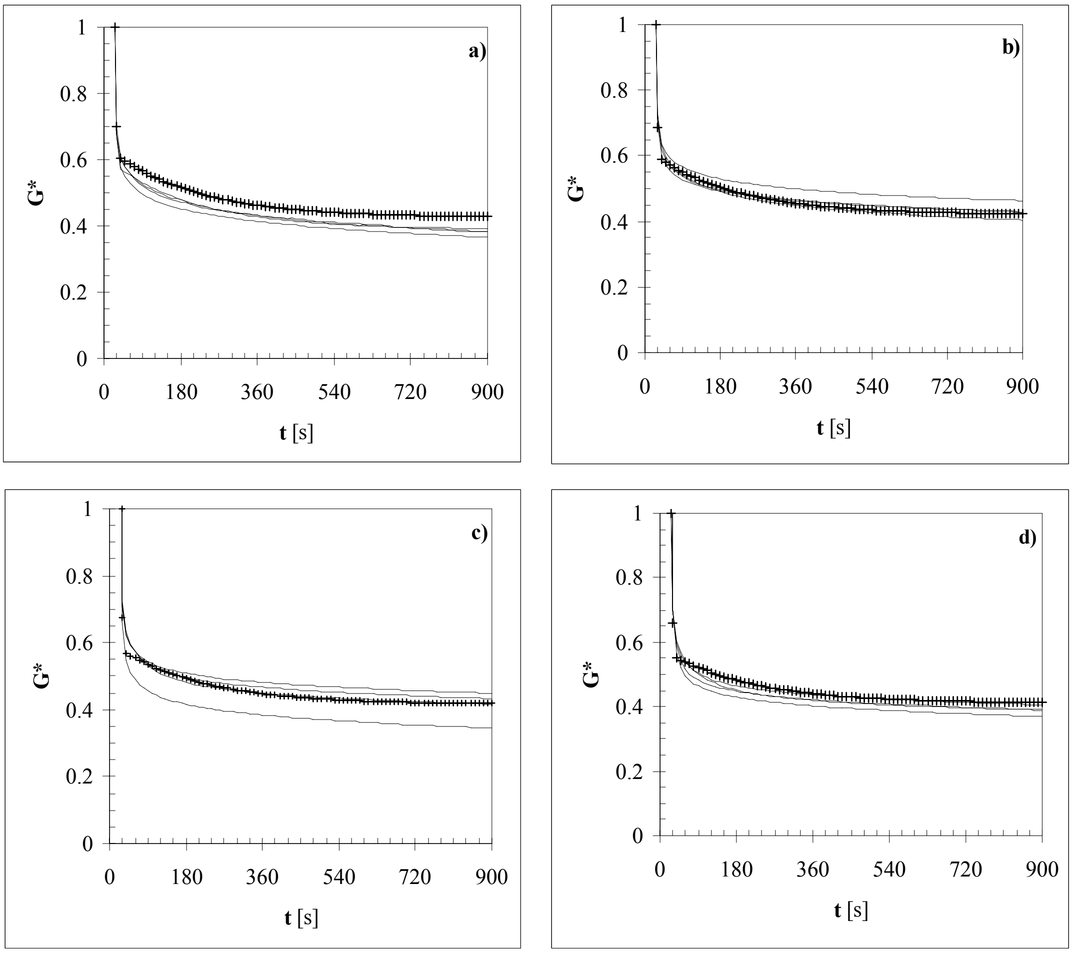

Figure 4.12 Experimental dimensionless relaxation modulus (G*: ——) versus time (t) referred to Tarocco orange fruits submitted to different engineering strains (ε_z: a, 5%; b, 10%; c, 15%; d, 20%) using a crosshead speed of 15 mm s-1. Eqs (2.16), (2.28) and (4.5) with the parameters Ai and τ_i reported in the text was used to plot the calculated G* data (+).

By applying the operating procedure described in Section 2.3.4 together with an initial steady spectrum of relaxation times (such as 0.1, 1, 10, 100, 1000, and 10,000 s) (Nussinovitch et al., 1989), there was no statistically significant improvement in fitting the time course of any experimental dimensionless relaxation modulus by considering more than two Maxwell elements in parallel to an elastic spring element, the former being characterized by the following relaxation times:

$\tau_1 = 2.04$ s ; $\tau_2 = 204$ s.

It is worth noting that the smallest relaxation time (τ_1) was about 2 to 10 times greater than the above loading times and this is approximately in line with the general rule that the relaxation curves are valid only for t greater than five to ten times the loading period (Rao, 1992a).

The experimental design used to assess the viscoelastic parameters was a Randomized Complete Block Design (RCBD) with four treatments and 20 samples (blocks). The response variables were the dimensionless coefficients (A_i) of a 5-element Maxwell body, which were estimated via Eq. (2.33) using the least squares method. Each set of responses from the RCBD was analyzed by ANOVA, where the interaction term was used as an estimate of the experimental error. Table 4.4 reports treatment means and standard deviations for any treatment together with Mean Squares and associated degrees of freedom (df) for any factor and response variable. No severe violations of basic ANOVA assumptions were revealed by residual analysis, because the block effects in the ANOVA F-tests were by far smaller than the corresponding critical F values at the significance level of 0.01. Moreover, there was strong evidence against the null hypothesis of equal treatment means for each response variable.

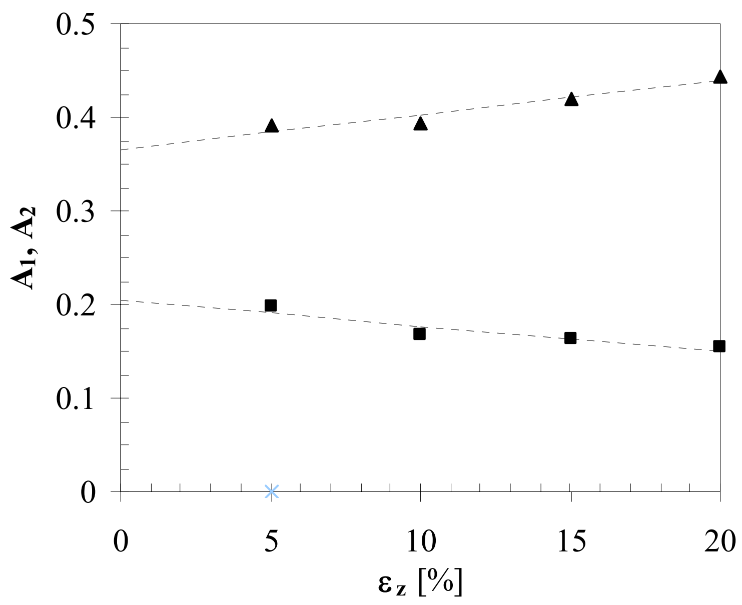

Figure 4.13 Dimensionless viscoelastic coefficients A1 (▲) and A2 (■) versus applied initial engineering strain ε_z) referred to Tarocco orange fruits submitted to stress relaxation tests using a crosshead speed of 15 mm s^{-1}. The broken lines were calculated using the regression equations listed in Table 4.5.

By correlating all responses A_i to ε_z via the least squares method (Table 4.5), it was possible to discover the A_0 was independent of the strain applied in the strain range examined, this parameter being responsible for the equilibrium residual stress corresponding to 42±2 % of the initial relaxation modulus.

On the contrary, the delayed elastic components A_1 and A_2 tended to increase or decrease with ε_z, respectively (Fig. 4.8), even if both of them might be regarded as constant in a more restricted range of compression strains (0-0.10).

Table 4.5 Effect of compressive engineering strain (ε_z) on the average values and corresponding standard deviations of the dimensionless viscoelastic coefficients (A_i) of the generalised Maxwell body used to describe stress relaxation tests together with the percentage error between the observed dimensionless relaxation modulus (G*) values and those calculated using Eq. (2.28) and analysis of variance for the linear model of A_i-vs.-ε_z.

ε_z	A_0	A_1	A_2	**Percentage Error**
(%)	(-)	(-)	(-)	(%)
5	0.41±0.04	0.39±0.05	0.20±0.03	1.4±0.2
10	0.44±0.03	0.39±0.03	0.17±0.02	1.3±0.2
15	0.42±0.03	0.42±0.03	0.16±0.02	1.4±0.2
20	0.40±0.03	0.44±0.03	0.15±0.02	1.6±0.2
	Mean Squares			
Strain (df=3)	0.005[ss1]	0.012[ss1]	0.0073[ss1]	
Block (df=19)	0.002[si2]	0.002[si2]	0.0004[si2]	
Sum of Squares of Errors (df=57)	0.001	0.001	0.001	
Regression Equation	(0.43±0.01)-(0.093±0.070) ε_z	(0.366±0.009)+ (0.365±0.069) ε_z	(0.204±0.006)-(0.273±0.046) ε_z	
r^2	0.15	0.51	0.56	
Regression (df=1)	0.002[si3]	0.033[ss3]	0.019[ss3]	
Residual (df=78)	0.001	0.001	0.001	

ss statistically significant at the confidence level p=0.01
si statistically insignificant at the confidence level p=0.01
1 $F_{0.01,3,57} = 4.15$; **2** $F_{0.01,19,57} = 2.24$; **3** $F_{0.01,1,78} = 6.97$

Also because the relaxation time spectrum of the delayed elastic components was unaffected whatever the compression strain up to 20%, any fruit was assimilated to a linear viscoelastic solid, at least on the time-scale examined and a 10% deformation range.

The cross symbols (+) plotted in Fig. 4.12a-d were calculated using Eq. (2.28) and the A_i values estimated via the regression equations listed in Table 4.5. These curves exhibited quite a good agreement with the experimental G*-vs.-t profiles whatever the engineering strain applied in the range of 5-20%.

Such a satisfactory agreement between the experimental and predicted instantaneous values of the compressive force F_z is also shown in Fig. 4.11, where the continuous lines were calculated by using Eq.s (2.16), (2.28) and (4.5).

Thus, as an orange fruit is compressed as shown in Fig. 3.2, its almost incompressible orange juice reacts by exerting an hydrostatic pressure on the peel internal surface, this causing firstly quite a rapid air release from albedo and then fruit lateral expansion.

In the circumstances, the mechanical response of the white spongy mesocarp or internal portion of the fruit as a whole may be associated to the first or second Maxwell element, respectively; whereas that of the outer mesocarp to the elastic component.

4.4.3 Permanent Deformation

To assess permanent fruit deformation after stress relaxation testing, the force applied to compress any specimen by 5 to 20% of its initial height was released and the fruit was let to reassume its initial shape for 5 min, this time being about 10 times longer than the longer relaxation time previously assessed on Tarocco fruits acquired in a local market (Pallottino et al., 2010). The fruit diameters along the axes x, y, and z were then newly determined by image analysis. Finally, fruit mass measurement accounted for likely oil or juice seepage.

The average values and standard deviations of the percentage permanent relative variations (δ_x, δ_y, δ_z) in the x, y, and z diameters, mass (δ_m) or volume

(δ_V) for each group of specimens submitted to different strains are shown in Table 4.4.

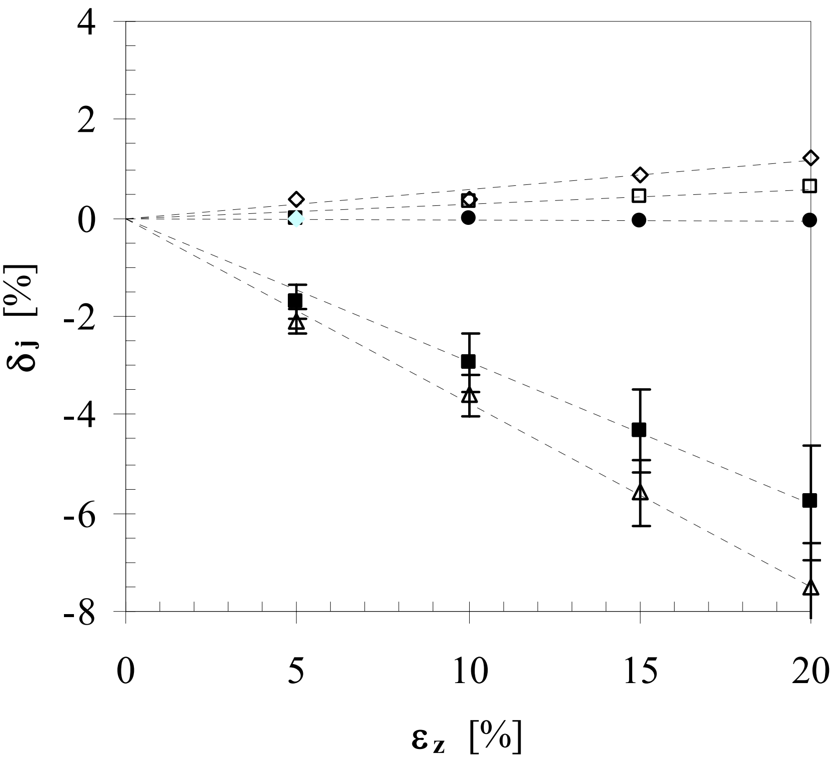

Figure 4.14 Effect of the initial engineering strain applied (ε_z) on the permanent deformation strains along the axis x (δ_x: ◊), y (δ_y: □) or z (δ_z: △), and on mass (δ_m: ●) or volume (δ_V: ■) variation of Tarocco specimens. The broken lines refer to the least squares regression lines, while the vertical bars to the average data percentage errors.

As shown in Fig. 4.14, the fruit compression along the axis z up to a strain of 20% resulted in a negligible percentage mass reduction (δ_m=-0.04± 0.03%) and in a percentage volume contraction increasing about linearly from -1.7 to -5.8%. This confirmed the aforementioned air release from albedo. It was also noted a permanent fruit contraction along the axis z increasing from -2.1 to -7.5% and a lateral expansion along the axis x or y increasing from 0.4 to 1.2% or from 0 to 0.6%, respectively. In particular, δ_y was about half of δ_x owing to the fact that the peel structure along the axis y was strengthened by the fruit-to-stalk attachment (Fig. 3.2).

4.5 Classification by Physico-Chemical and Sensory Testing

With reference to a marketable lot of 400 Tarocco orange fruits with an overall mass of about 150 kg and an average diameter D_{zo} of 75±4 mm, each fruit was preliminary numbered and then submitted to parallel plate compression testing so as to assess the fruit resistance for ε_z increasing from 0 to 5 % (step 0.5%) of the initial fruit height (D_{zo}).

Use of the principal components analysis (PCA) allowed the set of data collected to be univocally described by the only tension T_5 (=F_{z5}/D_{zo}), all the other collected $F_z(\varepsilon_z)$ values being auto-correlated. In particular, such a parameter varied from a minimum value of 179 N m^{-1} to a maximum value of 553 N m^{-1} with an average value (μ) of 310 N m^{-1}, a standard deviation (σ) of 67 N m^{-1}, and a practically normal distribution (Pallottino et al., 2011c).

Thus, by discarding approximately all the numbered fruits characterised by a T_5 value higher or smaller that the mean value plus or minus three standard deviations, it was possible to discriminate the remaining samples into three different classes, denoted as high (HF), medium (MF) or low (LF) firmness one, provided that T_5 approximately ranged from ($\mu+\sigma$) to ($\mu+2\ \sigma$), from ($\mu-½\ \sigma$) to ($\mu+ ½\ \sigma$) or from ($\mu-\sigma$) to ($\mu-2\ \sigma$), respectively.

4.5.1 Physico-chemical testing

Table 4.6 shows the average values and standard deviations for all the data collected for each of the three classes of 40 Tarocco orange fruits. Different letters were used to represent statistically significant differences according to the One-Way ANOVA and Fisher test.

In particular, there was a statistically significant difference in the values of the Magness-Taylor index (MT), tension T_5 and fruit rind thickness near the fruit peduncle (t_x) between groups at the confidence level of 99%. On the contrary, whatever the firmness class the differences among the fruit diameters (D_{zo}), as well as the other three fruit rind thicknesses ($t_{x'}$, $t_{y'}$, $t_{y'}$) and orange rind CIELAB coordinates (L_p^*; a_p^*; b_p^*) or colour differences (ΔE_p), resulted to be insignificant, thus confirming homogeneity and correct test randomization.

Table 4.6 One-way analysis of variance (ANOVA) to assess the statistically significance of the geometrical (initial diameter along the axis z - D_{zo}; orange rind thickness at the positions x, x', y and y' - t_x, $t_{x'}$, t_y, $t_{y'}$), physical (Magness-Taylor index - MT; tension at 5% deformation - T_5; CIELAB coordinates and colour difference of the orange rind of the whole fruit as such - L_p^*, a_p^*, b_p^*, ΔE_p, or halved - L_{ho}^*, a_{ho}^*, b_{ho}^*, ΔE_{ho}) and chemical (total soluble solid content – TTS; titratable acidity – TA; maturation index - MI) parameters used to characterise the Tarocco orange fruits used in this work, once randomly sorted in three high (HF), medium (MF) and low (LF) firmness classes.

Parameter Class	D_z	**MT**	T_5	L_p^*	a_p^*	b_p^*	ΔE_p	L_{ho}^*	a_{ho}^*
	(mm)	(N)	(N/m)	(-)	(-)	(-)	(-)		
HF	76 ± 5^{a}	73 ± 16^{a}	400 ± 17^{a}	62 ± 2^{a}	37 ± 2^{a}	58 ± 3^{a}	4 ± 2^{a}	37 ± 3^{a}	13 ± 2^{a}
MF	76 ± 4^{a}	60 ± 9^{b}	309 ± 10^{b}	62 ± 2^{a}	38 ± 1^{a}	58 ± 3^{a}	3 ± 2^{a}	42 ± 3^{a}	12 ± 1^{a}
LF	75 ± 4^{a}	49 ± 6^{c}	232 ± 6^{c}	62 ± 2^{a}	38 ± 2^{a}	59 ± 3^{a}	4 ± 2^{a}	43 ± 3^{b}	12 ± 2^{a}
Firmness Class Mean Squares	39.4^{si1}	11613^{ss1}	566195^{ss1}	14.5^{si1}	29.6^{si1}	26.6^{si1}	2.5^{si1}	801^{ss1}	33^{si1}
Sum of Squares of Errors	2319.6	14795	17501	523	338	1037	460	1044	343
F-ratio	0.995	45.9	1892.6	1.6	5.1	1.5	0.3	44.9	5.6
P	0.373	0	0	0.203	0.007	0.227	0.729	0	0.005

Parameter Class	b_{ho}^*	ΔE_{ho}	t_x	$t_{x'}$	t_y	$t_{y'}$	**TTS**	**TA**	**MI**
			(mm)	(mm)	(mm)	(mm)	(°Brix)	(% w/v)	(°Brix/%)
HF	10 ± 4^{a}	7 ± 3^{a}	2.1 ± 0.4^{a}	1.7 ± 0.4^{a}	1.8 ± 0.4^{a}	2.0 ± 1.0^{a}	12.2 ± 0.3^{a}	1.37 ± 0.03^{a}	8.9 ± 0.3^{a}
MF	11 ± 5^{a}	5 ± 3^{a}	1.8 ± 0.3^{a}	1.6 ± 0.3^{a}	1.7 ± 0.3^{a}	1.9 ± 0.3^{a}	11.7 ± 0.2^{b}	1.36 ± 0.06^{a}	8.7 ± 0.6^{a}
LF	17 ± 4^{b}	6 ± 3^{a}	1.7 ± 0.3^{ab}	1.5 ± 0.3^{a}	1.6 ± 0.3^{a}	1.8 ± 0.3^{a}	11.2 ± 0.1^{c}	1.42 ± 0.03^{a}	7.8 ± 0.3^{b}
Firmness Class Mean Squares	1294^{ss1}	59^{si1}	3.6^{ss1}	0.9^{si1}	0.9^{si1}	1.4^{si1}	2.0^{ss2}	0.01^{si2}	2.4^{si2}
Sum of Squares of Errors	2085	1095	13.1	12	13.2	45.4	0.5	0.02	1.5
F-ratio	36.3	3.1	15.9	4.3	3.9	1.8	20	2.5	7.3
P	0	0.047	0	0.015	0.023	0.168	0	0.137	0.013

The variations in the lightness coefficient (L_{ho}*) and yellow-blue hue component (b_{ho}^*) of the halved orange flesh, as well as the total soluble solid content (TSS), for the three classes were found to be statistically significant at the significance level of 0.01; while that in the halved orange flesh colour difference

(ΔE_{ho}) and maturation index (MI) was statistically significant at the confidence level of 95% (Table 4.6).

In other terms, the higher the MT index or T_5 value the greater the total soluble solid content and more noticeable the difference in the halved orange flesh colour, probably because of the smaller lightness coefficient (L_{ho}^*) and yellow-blue hue component (b_{ho}^*). Moreover, whatever the firmness class the resulting juices exhibited no statistically significant difference in titratable acidity (TA), whereas the maturation index for the oranges belonging to the high and medium firmness classes was practically constant and significantly different from that of those falling within the low firmness class.

By plotting the Magness-Taylor indexes (MT) against the tensions T_5 for any specimen tested (Fig. 4.15), it was possible to observe an average variation of the order of 20% for the MT data against an average one of less than 4% for the T_5 data, this resulting in quite a fair linear relationship (r=0.65).

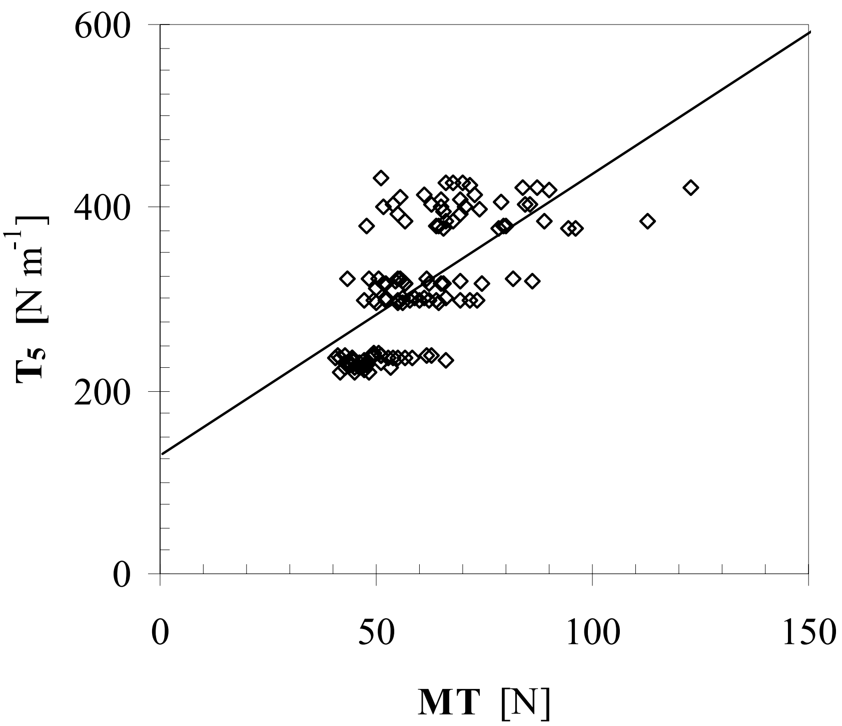

Figure 4.15 Relationship between the tension at a strain of 0.5 (T5) and Magness-Taylor index (MT) for all the Tarocco orange fruits classified in three firmness classes.

Nevertheless, the two measures appeared to be correlated, thus allowing the specific resistance per unit diameter at 5% deformation to be regarded as another non-destructive attribute of fruit firmness.

4.5.2 Sensory testing

Table 4.7 reports means and standard deviations for all the sensory attributes (Table 3.1) assessed by the panellists for the Tarocco orange fruits classified in the aforementioned firmness classes together with Sum of Squares (SS) and associated degrees of freedom (df) for all the main effects, and binary and ternary interactions. In particular, the three-term interaction (FC-P-R) was used as an estimate of the experimental error, that is the so called sum of squares of errors (SSE).

In the ANOVA F-tests the ratios between the mean sum of squares (SS) of any main effect or binary interaction and mean SSE were compared to the corresponding critical F values at the significance level of 0.01.

As shown by the probability levels listed in Table 4.7, there was strong evidence for the null hypothesis of equal firmness class means for the great majority of the sensory attributes perceived, that is fruit shape (FS), fruit shape defects (FSD), typical orange odour (TOO), off-odour (OO), juiciness (J), sweetness (SW), acidity (AC), bitterness (B), typical orange flavour (TOF), off-flavour (OF), and overall sensory evaluation (OSE). Only a few attributes, i.e., compactness (C), ease of peeling (EP), ease of segment separation (ESS), were able to discriminate the specimens belonging to the HF class from those of the LF one at the confidence level of 99%.

Table 4.7 Mean values and standard deviations of the sensory attributes (fruit shape - FS; fruit shape defects - FSD; compactness - C; ease of peeling - EP; ease of segment separation - ESS; typical orange odour - TOO; off-odour - OO; juiciness - J; acidity - AC; sweetness - SW; bitterness - B; typical orange flavour - TOF; off-flavour - OF; overall sensory evaluation – OSE) used to characterise the Tarocco orange fruits used in this work, once randomly sorted in three high (HF), medium (MF) and low (LF) firmness classes, and three-way analysis of variance (ANOVA) to assess their statistically significance by comparing the sum of squares (SS) of the main effects and binary interactions of three variables accounted for (firmness class – FC; panellist – P; replication - R) to that of errors (SSE), that was confused with the sum of squares of the ternary interaction (FC-P-R).

Attributes / **Parameter**	**FS**		**FSD**		**C**		**EP**		**ESS**		**TOO**		**OO**	
HF	7 ± 2^{a}		3 ± 2^{a}		7 ± 2^{a}		4 ± 2^{a}		4 ± 2^{a}		7 ± 2^{a}		2 ± 2^{a}	
MF	7 ± 2^{a}		3 ± 2^{a}		6 ± 2^{b}		5 ± 2^{b}		5 ± 2^{ab}		7 ± 1^{a}		2 ± 1^{a}	
LF	7 ± 2^{a}		4 ± 2^{a}		5 ± 2^{b}		6 ± 2^{b}		6 ± 3^{b}		7 ± 2^{a}		2 ± 1^{a}	
Main effects	**SS**	**F-ratio**	**SS**	**F-ratio**	**SS**	**F-ratio**	**SS**	**F-ratio**	**SS**	**F-ratio**	**SS**	**F-ratio**	**SS**	**F-ratio**
Firmness class (df= 2)	2.69	0.31^{si2}	13	1.41^{si2}	46.86	8.52^{ss2}	59.25	6.16^{ss2}	33.69	2.80^{si2}	1.19	0.37^{si2}	1.08	0.65^{si2}
Panellist (df=11)	77.94	1.61^{si3}	63.17	1.24^{si3}	109.61	3.63^{ss3}	116.67	2.21^{ss3}	112.82	1.71^{si3}	95.78	5.43^{ss3}	63.33	6.92^{ss3}
Replica (df= 1)	0	0.00^{si1}	9.39	2.03^{si1}	3.56	1.29^{si1}	2	0.42^{si1}	13.35	2.22^{si1}	1.39	0.87^{si1}	0.89	1.07^{si1}
Interactions														
FC-P (df=22)	41.64	0.43^{si4}	57.33	0.56^{si4}	85.14	1.41^{si4}	61.08	0.58^{si4}	78.97	0.60^{si4}	58.14	1.65^{si4}	11.58	0.63^{si4}
FC-R (df= 2)	0.75	0.09^{si2}	4.11	0.45^{si2}	4.86	0.88^{si2}	3.25	0.34^{si2}	41.03	3.41^{si2}	1.36	0.42^{si2}	0.36	0.22^{si2}
P-R (df=11)	33.33	0.69^{si3}	50.94	1.00^{si3}	34.11	1.13^{si3}	62	1.17^{si3}	14.82	0.22^{si3}	19.94	1.13^{si3}	50.44	5.51^{ss3}
SSE (df=22)	96.92		101.56		60.47		105.75		132.31		35.31		18.31	

Attributes / Parameter		J		SW		AC		B		TOF		OF		OSE	
HF		7±1 [a]		6±2 [a]		4±2 [a]		2±1 [a]		6±2 [a]		3±2 [a]		6±2 [a]	
MF		7±2 [a]		5±2 [a]		4±2 [a]		2±1 [a]		7±2 [a]		2±1 [a]		7±2 [a]	
LF		7±2 [a]		5±2 [a]		5±2 [a]		2±1 [a]		6±2 [a]		2±2 [a]		6±2 [a]	
Main effects		**SS**	**F-ratio**	**SS**	**F-ratio**	**SS**	**F-ratio**	**SS**	**F-ratio**	**SS**	**F-ratio**	**SS**	**F-ratio**	**SS**	**F-ratio**
Firmness class	(df= 2)	1.33	0.52[si2]	6.75	1.08[si2]	11.03	2.01[si2]	1.19	0.41[si2]	12.11	3.04[si2]	4.75	1.20[si2]	11.44	2.38[si2]
Panellist	(df=11)	109.38	7.75[ss3]	160	4.67[ss3]	251.61	8.33[ss3]	35.82	2.23[si3]	115.82	5.28[ss3]	46.04	2.12[si3]	72.61	2.75[si3]
Replica	(df= 1)	0.35	0.27[si1]	0.5	0.16[si1]	2	0.73[si1]	0.13	0.09[si1]	4.01	2.01[si1]	0.01	0.01[si1]	3.56	1.48[si1]
Interactions															
FC-P	(df=22)	27.67	0.98[si4]	25.25	0.37[si4]	40.64	0.67[si4]	18.14	0.57[si4]	45.22	1.03[si4]	71.58	1.65[si4]	45.56	0.86[si4]
FC-R	(df= 2)	2.11	0.82[si2]	4.75	0.76[si2]	0.58	0.11[si2]	2.58	0.89[si2]	4.78	1.20[si2]	0.86	0.22[si2]	1.44	0.30[si2]
P-R	(df=11)	4.82	0.34[si3]	26.17	0.76[si3]	23	0.76[si3]	10.71	0.67[si3]	36.82	1.68[si3]	20.15	0.93[si3]	31.11	1.18[si3]
SSE	(df=22)	28.22		68.58		60.42		32.08		43.89		43.47		52.89	

ss statistically significant at the significance level p=0.01.

si statistically insignificant at the significance level p=0.01.

1 $F_{0.01,1,22} = 7.95$

2 $F_{0.01,2,22} = 5.72$

3 $F_{0.01,11,22} = 3.18$

4 $F_{0.01,22,22} = 2.78$

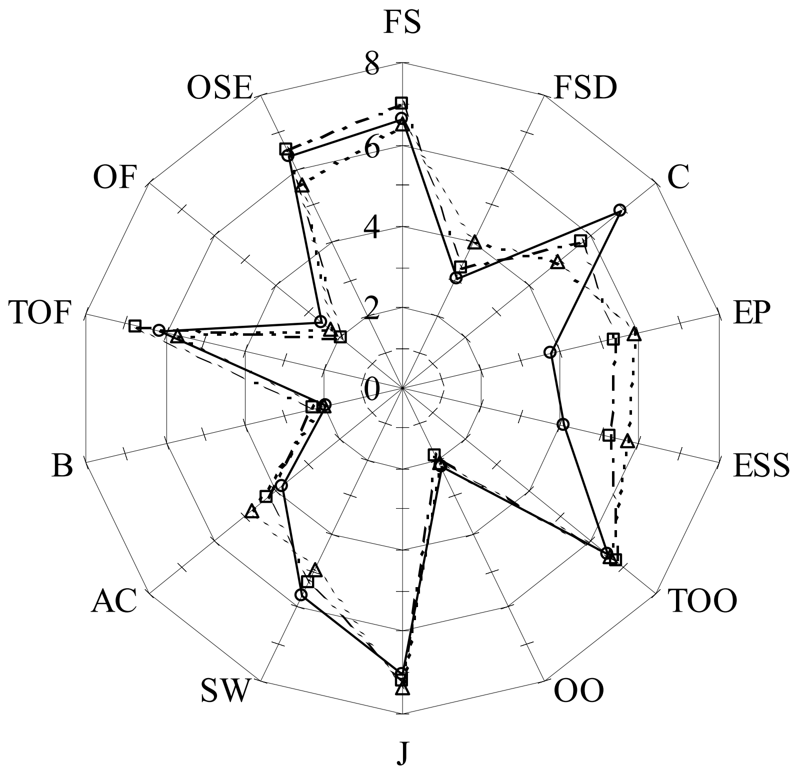

Figure 4.16 Sensory profiles of the Tarocco orange fruits belonging to different firmness classes (HF, ○, —; MF, □, — · —; LF, △, - -) evaluated by trained experts using 14 attributes: FS, fruit shape; FSD, fruit shape defects; C, compactness; EP, ease of peeling; ESS, ease of segment separation; TOO, typical orange odour; OO, off-odour; J, juiciness; AC, acidity; SW, sweetness; B, bitterness; TOF, typical orange flavour; OF, off-flavour; OSE, overall sensory evaluation.

From ANOVA, the following was derived:

i) the effect of the firmness class (FC) resulted to be statistically significant at $p \leq 0.01$ only on the basis of compactness (C), and ease of peeling (EP);

ii) the effect of panellists' response was statistically significant at $p \leq 0.01$ only for eight of the sensory attributes recognized, that is C, EP, TOO, OO, J, SW, AC, and TOF;

iii) the effect of replication was statistically negligible, thus confirming quite a good reproducibility whatever the attributes remarked;

iv) the interaction FC-P was statistically insignificant at $p=0.01$ whatever the sensory attributes assessed;

v) the interaction FC-R was statistically insignificant at $p=0.01$, this showing homogeneity in the specimens assayed during their re-evaluation by the professionals;

vi) the interactions P-R, being statistically insignificant at p=0.01, demonstrated that the panellists' responses were reliable.

Fig. 4.16 shows the corresponding sensory profiles for the Tarocco orange fruits belonging to the three firmness classes examined in this work. It can be noted that on the scale used all specimens of the high firmness class exhibited the highest or lowest intensity of the attributes denoted as compactness or ease of peeling (EP) or segment separation (ESS), respectively.

4.5.3 Multivariate analysis

The dataset of dimensions 54×14 (54 being the samples, subdivided into three firmness classes, and 14 being the independent variables, that is the sensory attributes assessed by skilled panellists) was autoscaled before PLS-DA.

The percentage of explained variance of the X block is reported in Table 4.8 for the 14 LVs calculated. The first 5 of them were retained as significant since they explained about 68% of the variance contained in the X block. In this way, by referring to the mean centre during the X-data preprocessing and to 5 latent variables, the model characterized by the best predictive ability entailed a classification percentage of the whole model of 64.8% for the training set and of 66.7% for the validation test, (Table 4.8).

From the results reported in Table 4.8, the performances of the best model appeared to be quite good, according to the values of RMSE calculated either in training (RMSEC= 0.53) or in validation (RMSECV=0.73).

The same conclusions can be drawn on the basis of the correct allocation of the samples within each firmness class produced by the model examined (Table 4.8). In fact, the allocation was equal to 83% for both the LF and HF classes, while it reduced to 33% for the samples in the medium firmness class (MF). More specifically, the confusion matrix (Table 4.9) confirmed a good allocation for the predicted samples in the LF and HF class (5 out 6 samples in testing).

On the contrary, the classification was poor for the predicted samples in the MF class (2 out 6 samples), the latter meaning that 4 out of 6 samples were misclassified, two per each of the other classes, LH and HF.

Table 4.8 Parameters utilised to build the model and results of the PLS-DA carried out on sensorial attributes and firmness classes regarding training and validation phases.

MODEL PARAMETERS	**VALUE**
Percentage variance explained on X-block by each LVs	(%)
LV1	19.74
LV2	18.5
LV3	15.44
LV4	6.65
LV5	7.39
LV6	4.64
LV7	5.26
LV8	4.29
LV9	3.02
LV10	4.65
LV11	3.27
LV12	2.49
LV13	2.86
LV14	0
X data preprocessing	mean centre
Z data preprocessing	none
m	5
Training	
RMSEC	0.53
Model Data classification (%)	
-Whole Data set	64.8
-LF class set	72.2
-MF class set	55.6
-HF class set	66.7
Validation	
RMSECV	0.73
Model Data classification (%)	
-Whole Data set	66.7
-LF class set	83.3
-MF class set	33.3
-HF class set	83.3

Table 4.9 Confusion matrix regarding the validation phase showing the samples correctly classified or misclassified by the performed PLS-DA.

Class	**Classified Samples**		
	LF	**MF**	**HF**
Observed			
LF	6	0	0
MF	0	6	0
HF	0	0	6
Predicted			
	LF	**MF**	**HF**
LF	5	1	0
MF	2	2	2
HF	0	1	5

Conclusions

The main results of this PhD thesis are the following:

1) Two image analysis-based methods (i.e., EFA and bounding box) were set up and allowed an accurate determination of the real contact area between the compression plates and specimen during parallel plate compression. The difference in both estimates was statistically insignificant at the 99% confidence level. Moreover, it was possible to demonstrate that the contact areas calculated using the ASABE standard method (2008), or assuming no variation in the volume of the fruit undergoing compression, were under- or over-estimated by 45% or 19%, respectively.

2) Knowledge of the real contact areas made an easy task to convert typical force-deformation curves into engineering stress-strain relationships for the orange fruit tested.

3) Alternatively, by assimilating any orange fruit to a deformable membrane filled with an internal incompressible juice and plotting the compression stress (σ_F) acting on the equatorial horizontal cross-section of the epicarp (A_{Fo}), it was possible to yield a classic concave upward σ_F-vs.-ε_z relationship provided that the orange peel thickness was immediately determined after fruit rupture. Unfortunately, such a procedure is a destructive one and cannot be applied to pilot on-line high-speed sorting systems.

4) By using the thin shell theory (Barthès-Biesel et al., 2002; Carin et al., 2003), it was possible to replace the stress exerted in the orange rind with the elastic tension (i.e., the fruit resistance per unit equivalent diameter, T), this appearing to be a useful parameter for grading orange fruit provided that the critical tension value and difference detectable by the average consumer is known.

5) The stress-relaxation tests performed here allowed the Tarocco orange fruit to be described as a linear viscoelastic solid for compressive strains up to 10% of its initial height. In this linear viscoelasticity range, not only the viscoelastic components A_i but also the relaxation time spectrum of the delayed elastic components were unaltered by the deformation strain applied. In particular, the elastic epicarp was responsible for the equilibrium residual stress, that represented about 42% of the initial relaxation modulus.

6) After any orange fruit had been submitted to stress relaxation testing for 15 min and decompressed for 5 min, it exhibited practically negligible mass loss (δ_m=-0.04± 0.03%), whereas the permanent volume contraction increased from 1.7±1.0 to 3.0±0.9% as ε_Z was increased from 5 to 10%.

7) Provided a 4-tray carton is used to pack the Tarocco orange fruits tested here, the load applied on each orange (with an average mass of about 0.22 kg - Table 4.4) in the lower tray would be F_z=3 m_o g ≈ 6.4 N. This would result in an apparent strain (ε_z) of 2.8%, as estimated via Eq. (4.5), and in a permanent reduction in the axis z (δ_z) of circa 1% (Fig. 4.14). Such a limited contraction is likely to enhance the market value of orange fruit through better presentation and explains why the maximum size for the corrugated board cartons of orange fruits is a bushel, this containing 48-64 orange fruit pieces displaced over 4 trays and weighing about 18 kg.

8) It was also possible to establish quite a linear relationship (r=0.65) between the tension at 5% strain (T5) and the Magness-Taylor (MT) index, this allowing T5 to be regarded as another non-destructive attribute of fruit firmness. Since the Magness-Taylor test has three main drawbacks (namely, it is destructive one and thus it cannot be used on-line, and its measurements are highly variable up to 30% - Barreiro, 1994), T5 assessment appears to be more repeatable and accurate.

9) By separating a marketable lot of Tarocco orange fruits into three different classes (i.e., high, HF; medium, MF; low, LF, firmness ones) on the basis of T5 as a discrimination parameter ranging from 376 to 432 N m-1, from 296 to 323 N m^{-1} or from 219 to 242 N m^{-1}, respectively, the specimens differed not only in the MT index, but also in fruit rind thickness near the fruit peduncle (t_x), lightness coefficient (L_{ho}*) and yellow-blue hue component (b_{ho}*) of the halved orange flesh, as well as total soluble solid content (TSS) of the resulting juice, at the significance level of 1%. All the other parameters assessed (i.e., fruit diameter - Dzo; fruit rind thicknesses - t_x', t_y', t_y'; orange rind CIELAB coordinates - L_p*; a_p*; bp* - or colour differences - ΔE_p; titratable acidity - TS; maturation index - MI) resulted to be insignificant.

10) These findings were also congruent with the panel assessment of the great majority of the sensory attributes, namely fruit shape (7±2), fruit shape defects (3±2), typical orange odour (7±2), off-odour (2±1), juiciness (7±2), acidity (4±2), sweetness (5±2), bitterness (2±1), typical orange flavour (6±2), off-flavour (2±2), and overall sensory evaluation (6±2). However, the sensory professionals recognized the greater compactness (7±2) and lower easiness of peeling (4±2) and segment separation (4±2) of the HF oranges with respect to the corresponding sensory attributes pertaining to the orange fruits grouped in the MF and LF classes (Table 4.7).

11) As shown by the multivariate analysis of results, the skilled panellists were enough sensible to discriminate between the Tarocco orange fruits owing to the LF and HF classes, but not so responsive to differentiate both of them from the samples classified in the middle firmness class (MF). This was in line with the analysis of variance detailed in Table 4.7, where the Tarocco orange fruits in the MF class were not statistically different from those in the LF class as concerning the attributes C, EP and ESS.

In conclusion, such results demonstrate the possibility of developing technological systems to select continuously orange fruits on the base of their tension, the main advantages of this parameter being quickness, repeatability, low cost and non-destructiveness. With specific reference to the Tarocco orange fruits examined here, it would be possible to recommend to sort on-line only the fruits with T_5 in the range of 375 to 445 N m^{-1} so as to limit or vanish Sicilian Tarocco orange fruit rejection after long shipping in foreign markets. In such a way, it would be possible to sort whole stocks by grading fruit per fruit and thus ensuring a longer shelf-life of a product with known textural characteristics. This is of paramount importance especially in abroad markets, where the consumers are up to pay a premium price for a niche product, such as blood orange fruit. Further work is needed to validate this operating procedure on a continuous pilot-scale sorting line.

Published Works and Congress Participations

Menesatti, P., Pallottino, F., Lanza, G., Paglia, G. (2009). Prediction of blood orange MT firmness by multivariate modelling of low alterative penetrometric data set: A preliminary study. *Postharvest Biol. Technol.*, 51: 434-436.

Pallottino, F. (2008). Rheometrical Characterization and Firmness Assessment of Citrus Cultivars by Non-Destructive Tests. In *Proceedings of the 13th Workshop on the Developments in the Italian PhD Research on Food Science and Biotechnology*, Alba (Italy), 10-12 September, 554-555.

Pallottino, F. (2009a). Use of image analysis to asses the effective surface area of orange fruit submitted to uniaxial compression tests. In Proc.s of the *14th Workshop on the Developments in the Italian PhD Research on Food Science and Biotechnology*, Oristano (Italy), 16-18 September, 337-339.

Pallottino, F., Costa, C., Menesatti, P., & Moresi, M. (2009b). Compression testing of orange fruit. In *Proc.s of the* 9th *International Conference on Chemical and Process Engineering*, Roma (Italy), 10-13 May, *Chemical Engineering Transactions 17*, 885-890.

Pallottino, F. (2010). Assessment of Tarocco Orange Fruit Firmness by Standard and Non-Destructive Tests. In Proc.s of the *15th Workshop on the Developments in the Italian PhD Research on Food Science and Biotechnology*, University of Naples – Federico II, Portici, 15-17 September.

Pallottino, F., Moresi, M., Giorgi, S., Menesatti, P. (2010) Orange fruit rheometrical characterization using stress-relaxation tests. In *Proc.s of the XVIIth World Congress of the International Commission of Agricultural and Biosystems Engineering* (CIGR), Québec City, Canada, June, 13-17, 2010, p. 256.

Pallottino, F., Costa, C., Menesatti, P., Moresi, M. (2011a) Assessment of the mechanical properties of Tarocco orange fruit under parallel plate compression, *Journal of Food Engineering* 103: 308-316.

Pallottino, F., Costa, C., Menesatti, P. & Moresi, M. (2011b). Tarocco Orange Fruit Viscoelastic Properties. Submitted to *Food and Bioprocess Technology.*

Pallottino, F., Antonucci, F., Lanza, M.C., Strano, M.C., Menesatti, P., Moresi, M. (2011c). Assessment of quality-assured Tarocco orange fruit sorting rules by combined phisico-chemical and sensory testings. Submitted to *Journal of Food Engineering.*

Acknowledgements

This research was supported by the Italian Ministry of Agriculture and Forestry Policy, special grant no. 9513 - *Ricerche e sperimentazioni nel settore dell'agrumicoltura italiana*.

Notation

A	contact area of the fruit submitted to parallel plate compression test (m^2)
a	empirical coefficient of Eq. (2.32) (s)
a_{BB}	semi-major axis of the contact area (m)
AC	acidity (dimensionless)
A_F	equatorial cross-section of the orange peel (m^2)
A_i	dimensionless viscoelastic coefficient of the generic i-th element of the generalised Maxwell body
a_j	generic semi-major axis of the contact area (m)
a_k*	bluish-green/red purple hue component for the generic k-th specimen (dimensionless)
a_V	radius of the upper equivalent spherical segment (m)
B	bitterness (dimensionless)
b_{BB}	semi-minor axis of the contact area (m)
b_k*	yellow-blue hue component for the generic k-th specimen (dimensionless)
C	compactness (dimensionless)
c_1, c_2	empiric constants defined in Table 2.1
C_F	circumference of the elliptic rind (m)
d	standardised normal difference, as defined by Eq. (4.2)
D_e	diameter of the equivalent sphere (m)
df	degrees of freedom
D_j	fruit diameter along the generic j-axis (m)
E_i	modulus of elasticity of the i-th spring (Pa)
E_O	modulus of deformability of whole orange fruit (Pa)
EP	ease of peeling (dimensionless)
ESS	ease of segment separation (dimensionless)
FC	firmness class variable
FS	fruit shape (dimensionless)
FSD	fruit shape defects (dimensionless)
F_z	Compression force applied along the z-axis (N)
G	relaxation modulus as defined by Eq. (2.15) (Pa)

G^*	dimensionless relaxation modulus as defined by Eq. (2.16)
H	sample height (m)
h	semi-deformation applied along the z-axis (m)
J	juiciness (dimensionless)
k	empirical constant, as defined by Eq. (4.8) (Pa)
K_U, K_L	empiric constants, as defined in Table 2.1 (dimensionless)
L_k^*	lightness coefficient for the generic k-th specimen (dimensionless)
m	minimum number of latent variables
MI	Maturation index (MI=TTS/TA, °Brix (% w/v)-1)
MT	Magness-Taylor index (N)
n	number of Maxwell elements
n_j	overall number of trials
OF	off-flavour (dimensionless)
OO	off-odour (dimensionless)
OSE	overall sensory evaluation (dimensionless)
P	panellist variable
p	significance level
p_V	parameter defined by Eq. (3.6) (m^2)
q	parameter defined by Eq. (3.7) (m^3)
R	replication variable
r	correlation coefficient
r^2	coefficient of determination
R_{CD}, R'_{CD}	Radii of curvature of the flat compression device (m)
R_L, R'_L	Radii of curvature of the convex surface of the sample at the point of contact with the lower plate (m)
R_U, R'_U	Radii of curvature of the convex surface of the sample at the point of contact with the upper plate (m)
R_V	radius of the lower equivalent spherical segment (m)
s^2	error's variance
s_j	standard deviation of the generic parameter or treatment j
SW	sweetness (dimensionless)

T	tension or specific fruit resistance per unit diameter at a generic strain (N m^{-1})
t	time (s)
T_5	tension or specific fruit resistance per unit diameter at a strain of 0.05 (N m^{-1})
TA	titratable acidity (% v/w of citric acid equivalent)
t_j	orange rind thickness in the generic j position (mm)
TOF	typical orange flavour (dimensionless)
TOO	typical orange odour (dimensionless)
TTS	total soluble solid content (°Brix)
$t_{\alpha,df}$	one-sided Student *t*-test
V	sample volume (m^3)
V_T	cross-head speeds (mm s^{-1})
x	generic coordinate along the x-axis (m)
X	matrix of the dependent variables
Y	dependent variable defined by Eq. (2.33)
y	generic coordinate along the y-axis (m)
Z	vector of the dependent variable
Z_i	generic dummy variable
z	generic coordinate along the z-axis (m)
z_V	parameter defined by Eq. (3.5) (m)

Greek Symbols

α	confidence level
Δ	parameter defined by Eq. (3.8) (m^3)
ΔE	colour difference as defined by eq. (3.26)
Δx	sample deformation along the x-axis (m)
Δy	sample deformation along the y-axis (m)
Δz	sample deformation along the z-axis (m)
δ_j	permanent deformation along the generic j-th axis as defined by Eq. (12) (dimensionless)

δ_m	relative variation in fruit mass as defined by Eq. (3.12) (dimensionless)
δ_V	relative variation in fruit volume as defined by Eq. (3.13) (dimensionless)
ε_j	engineering strain along the generic j-axis (dimensionless)
ε_z	engineering strain along the axis z as defined by Eq. (2.15) (dimensionless)
η_i	viscosity of the fluid filling the i-th dashpot (Pa s)
μ	average value of compression tension at a strain of 0.05 (N m^{-1})
ν	apparent Poisson's ratio (dimensionless)
ν_M	overall number of statistically significant Maxwell elements (dimensionless)
σ	standard deviation of compression tension at a strain of 0.05 (N m^{-1})
σ_F	compression stress acting on the equatorial horizontal cross-section of the epicarp (=F_z/A_F, Pa)
σ_z	engineering stress along the z-axis as defined by Eq. (2.1) (Pa)
τ_i	relaxation time of the i-th Maxwell element (s)

Subscripts

ASM	referred to the ASABE Standard Method
BB	referred to the bounding box
C	calculated
CD	referred to the compression device
d	referred to the degrees of freedom of the mean sum of squares on the bottom of the F-ratio
e	experimental
EFA	referred to the Elliptic Fourier Analysis
F	referred to flavedo
ho	referred to the halved orange
max	maximum

min	minimum
n	referred to the degrees of freedom of the mean sum of squares on the top of the F-ratio
o	initial
O	referred to the whole orange fruit
p	referred to the orange peel
R	referred to fruit rupture
S	referred to the fruit sample
V	referred to the hypothesis of constant sample volume
x	referred to axis x
y	referred to axis y
z	referred to axis z

References

Abbott, J.A., Massie, D.R. (1998). Nondestructive sonic measurement of kiwifruit firmness. *J. Ame.r Soc. Hort. Sci.*, 123(2), 317-322.

Anonymous. (1975). Glossary of terms relating to the sensory analysis of food. British Standard 5098. British Standards Institution, London.

Arnold, P.C. & Mohsenin, N.N. (1971) Proposed techniques for axial compression tests on intact agricultural products of convex shape. *Transactions of the ASAE*, 14, 78-83.

Arnold, P.C., & Mohsenin N.N. (1971). Proposed techniques for axial compression tests on intact agricultural products of convex shape. *Transactions of the ASAE*, 14, 78-83.

ASABE Standards. (2008). Standards Engineering Practices Data. Compression test of food materials of convex shape. *America Society of Agricultural and Biological Engineers*, 55th edn., ASABE, St. Joseph, MI, USA, pp. 671-678.

Barcaccia, G. & Falcinelli, M. (2007). Genomica e Biotecnologie genetiche. In: *Genetica e Genomica,* Vol. 3, Liguori Ed., Milano,. (ISBN: 978-88-207-3743-6) p. 334

Barreiro, P., Ruiz-Altisent, M., Valero, C., García-Ramos, J. (2004). Fruit Post-harvest Technology: Instrumental Measurement of Ripeness and Quality. In: R. Dris, S.M. Jain (Eds). *Production practices and quality assessment of food crops.* Vol. 3. Quality handling and evaluation, Kluwer Academic Publishers, New York, pp. 321-340.

Barthès-Biesel, D., Diaz, A., Dhenin, E. (2002). Effect of constitutive laws for two-dimensional membranes on flow-induced capsule deformation. *J Fluid Mech*, 460, 211-222.

Bennett, C.A., & Franklin, N.L. (1954). *Statistical Analysis in Chemistry and the Chemical Industry*. Wiley, New York, 176–185.

Bertola, N.C., Bevilacqua, A.E., Zaritzky, N.E. (1991). Changes in rheological and viscoelastic properties and protein breakdown during the ripening of “Port Salut Argentino” cheese. *International Journal of Food Science and Technology*, 26, 467-478.

Blahovec, J. (1996). Stress relaxation in cherry fruit. *Biorheology*, 33(6), 451-462.

Bonina, F., Saija, A., Tomaino, A., Lo Cascio, R., Rapisarda, P., Dederen, J.C.

(1998). In vitro antioxidant activity and in vivo photoprotective effect of a red orange extract. *Int. J. Cosmet. Sci.*, 20, 331-342.

Bourne, M.C. (1974). Comparison of results from the use of the Magness-Taylor pressure tip in hand- and machine-operation. *Journal of Texture Studies*, 5, 105-108.

Bourne, M.C. (2002). Food texture and viscosity: Concept and measurement. 2nd edn. Academic Press, London.

Brennan, J.G., 1984. Sensory analysis of foods (J.R. Piggott). Elsevier Applied Science.

Burgos, J.A., Gutiérrez, A., Moltó, E. (2002). A firmness sensor for assessing texture in fruit. Proc Intnl Conf Agricultural Engineering. Budapest, June 30-July 4, Pa-per 02-PH-025.

CAC/GL 21. (1997). Available at: www.codexalimentarius.net/download/standards/394/CXG_021e.pdf. Accessed 12/11/2010.

CAC/RCP 44. (1995). Available at: www.codexalimentarius.net/download/standards/322/CXP_044e.pdf. Accessed 12/11/2010.

CAC/RPC 53. (2003). Available at: http://www.justice.gov.md/upload/Baza%20de%20date/Materiale%202009/Legislatie/Codex%20Stan%2053-2003.pdf. Accessed 12/11/2010.

Carin, M., Barthès-Biesel, D., Edwards-Levy, F., Postel, C., & Andrei, D.C. (2003). Compression of biocompatible liquid-filled HAS-Alginate capsules: determination of the membrane mechanical properties. *Biotechnol. Bioeng. 82*, 207-212.

Chen, P. (2001). Application of elastic theory to high-speed impact sensing of fruits. 3rd IFAC/CIGR, Workshop on Control Applications in Post-Harvest and Processing Technology. Tokyo, Japan, Oct 3-5.

Chen, P., Tang, S., Chen, S. (1985). Instrument for testing the response of fruits to impact. Proc ASAE Winter Me-eting, Chicago, Ill, USA. Paper 85-3537.

Chen, P., Ruiz-Altisent, M. (1996). A low-mass impact sensor for high-speed firmness sensing of fruits. Proc Intnl Conf Agricultural Engineering.

Madrid. September 23-26, Paper 96F-003.

Chen P., Tjan, Y. (1998). A real-time impact sensing system for on-line firmness sensing. Proc Intnl Conf Agricultural Engineering. Oslo. August 24-27, Paper 98-F-006.

Chen, P., Thompson, J. (2000). Development of a firmness tester for pears. The California Pears Advisory Board, Post Harvest Research Report.

Chen, P., Sarig, Y., Thompson, J.F. (2000). A hand-held impact sensor for firmness sensing of fruits. Proc Postharvest Congress, Jerusalem, March 26-31.

Choi, C.H., Abbott, J.A., Park, B., Chen, Y.R. (1997). Prediction of soluble solid and firmness in apple by visible/near infrared spectroscopy. Proc 5th Intnl Symposium on fruit, nut and vegetable production engineering, Davis, California, USA, September 3-10.

Clayton M., Biasi, B., Mitcham, B. (1998). New devices for measuring firmness of cherries. *Perishables Handling Quarterly*, 95, 2-4.

CODEX STAN 1. (1985). General Standard for the Labelling of Prepackaged Food. Available at: www.codexalimentarius.net/download/standards/32/CXS_001e.pdf. Accessed 12/11/2010.

CODEX STAN 193. (1995). Available at: www.codexalimentarius.net/download/standards/17/CXS_193e.pdf. Accessed 12/11/2010.

Coggins, C.W., Henning, G.L. (1988). A comprehensive California field study of the influence of preharvest applications of gibberellic acid on the rind quality of Valencia oranges. *Israel J. Bot.*, 37, 145-154.

Costa, C., Menesatti, P., Paglia, G., Pallottino, F., Aguzzi, J., Rimatori, V., Russo, G., Recupero, S., Reforgiato Recupero, G. (2009). Quantitative evaluation of Tarocco sweet orange fruit shape using opto-electronic elliptic Fourier based analysis. *Postharvest Biology and Technology 54*, 38-47.

Costa, C., Menesatti, P., Aguzzi, J., D'Andrea, S., Antonucci, F., Rimatori, V., Pallottino, P., Mattoccia, M. (2010). External shape differences between sympatric populations of commercial clams *Tapes decussatus* and T.

philippinarum. *Food and Bioprocess Technology 3*, 43-48.

Crampton, J.S. (1995). Elliptic Fourier shape analysis of fossil bivalves: some practical considerations. *Lethai, 28*, 179–186.

D'Aquino, S. Palma, A., Schirra, M., Di Martino Aleppo, E., Fronteddu, F., A-gabbio, M. (2006). Preharvest calcium and gibberellic acid application to delay ageing and physiological alterations of the peel in clementines (*Citrus reticulata Blanco*; Sardinia). *Italus Hortus*, 13(5), 132-136.

De Belie, N., Schotte, S., Lammertyn, J., Nicolai, B., De Baerdemaeker, J. (2000). Firmness changes of pear fruit before and after harvest with acoustic im-pulse response technique. *J. Agr. Eng. Res.*, 77(2), 183-191.

Del Nobile, M.A., Chillo, S., Mentana, A., Baiano, A. (2007). Use of the generalized Maxwell model for describing the stress relaxation behaviour of solid-like foods. *Journal of Food Engineering*, 78, 978-983

DeLong, J.M., Prange, R.K., Harrison, P.A., McRae, K.B. (2000). Comparison of a new firmness penetrometer with three standard instruments. *Postharvest Biology and Technology*, 19, 201-209.

Desmet, M., Lammertyn, J., Scheerlinck, N., Ver-Linden, B.E. (2002). A pendulum for testing puncture injury susceptibility of tomatoes. Proc Intnl Conf Agricul-tural Engineering. Budapest, June 30-July 4. Paper 02-PH-038.

Di Martino Aleppo, E., Lanza, G., Strano, M.C. (2002). Effects of GA3 sprays on the quality of Tarocco nucellare orange fruit [*Citrus sinensis* (L.) Osbeck]. Proceedings, Scientific meeting of Italian Horticultural Society, Spoleto, Perugia (Italy), 23-25 Apr., pp. 207-208.

Diezma, B., Ruiz-Altisent, M., Orihuel, B. (2002). Acoustic impulse response for detecting hollow heart in seedless watermelon. Postharvest Unlimited. Leuven, Belgium, paper P-034.

Fekete, A., Felföldi, J. (2000). System for fruit firmness evaluation. Proc Intnl Conf Agricultural Engineering. Warwick, UK, July 2-7. Paper 00-PH-034.

Ferguson, L., Ismail, M.A., Davies, F.S., Wheaton, T.A. (1982). Pre- and postharvest gibberellic acid and 2,4-dichlorophenoxyacetic acid applications for increasing storage life of grapefruit. *Prac. Fla. state Hort. Soc.*, 95, 242-

245.

Fidelibus, M.W., Davies, F., Cambell, C.A. (2002). Gibberellic acid application timing affects fruit quality of processing oranges. *HortScience*, 37(2), 353-357.

Fridley, R.B, Bradley, R.A., Rumsey, J.W., Adrian, P.A. (1968). Some aspects of elastic behavior of selected fruits. *Transactions of the ASAE*, 11, 46-49.

García-Ramos, F,J, Ortiz-Cañavate, J., Ruiz-Altisent, M., Díez, J., Flores, L., Homer, I., Chávez, J.M. (2003). Development and implementation of an on-line impact sensor for firmness sensing of fruit. *J. Food. Eng.*,58(1), 53-57.

García-Ramos, F,J,, Valero, C., Homer, I., Ortiz-Cañavate, J., Ruiz-Altisent, M. (2005). Non-destructive fruit firmness sensors: a review. *Spanish Journal of Agricultural Research*, 3(1), 61-73.

Gómez, H.A., Pereira, G.A., He, Y. (2006). Non-destructive measurement of acidity, soluble solids and firmness of Satsuma mandarin using Vis/Nir-spectroscopy techniques. *Journal of food engineering*, 77, 313-319.

GREEFA (2008). Available at: http://www.greefa.nl/it/i_nostri_moduli_ifd.htm. Accessed 11/12/2010.

Gutiérrez, A., Burgos, J.A., Moltó, E. (2003). Estimación de la firmeza de los melocotones en una línea de con-fección precomercial. Proc III Congreso de Agroingenie-ría, Cordoba. Spain, September 24-27, pp. 1158-1163.

Harker, F.R., Maindonald, J.H., Jackson, P.J. (1996). Penetrometer measurement of apple and kiwifruit firmness: operator and instruments differences. *J. Am. Soc. Hort. Sci.*, 121, 927-936.

Harker, R., Hallett, I. (2004). Fruit texture studies at HortResearch. *The Orchadist*, New Zealand (Dec.), pp. 48-51.

Harrison, I. (2003). Non-destructive testing for fruit quality assurance. Innovations in Food Technology. Available at http://www.sinclair-intl.com/images/info_page/sinclair_iq_articles/Innovations_In_Food_Tech.pdf. Accessed 02/23/2010.

Hassan, B.H., Alhamdan, A.M. Elansari, A.M. (2005). Stress relaxation of dates at khalal and rutab stages of maturity. *Journal of Food Engineering*, 66, 439-445.

Hodgson, R.W. (1967). Horticultural varieties of citrus. In: W. Reuther, L.D. Batchelor, H.J. Webber (Eds.). Citrus Industry: Crop Protection. Vol. I: History, World Distribution, Botany, and Varieties. Univ. Calif., Berkeley.

Homer, I., Ortiz-Cañavate, J., Moreda, G., Morabito, S., Ruiz-Altisent, M. (2002). Evaluation of a non-destructive impact sensor on-line for determination of firmness of peaches and apples. Proc Intnl Conference on Agricultural Engineering. Budapest. June 30-July 4. Paper 02-PH-026.

Hou, D.X. (2003). Potential mechanisms of cancer chemoprevention by anthocyanins. *Current Molecular Medicine*, 3(2), 149-59.

Howarth, M.S., Shmulevich, I., Raithatha, C. Ioannides, Y. (2003). Online non-destructive avocado firmness assessment based on low-mass impact technique. In: Proceedings of the 5th World Avocado Congress (Actas V Congreso Mundial del Aguacate), pp. 679-685.

Hung, Y.C., McWatters K.H., Prussia, S.E. (1998). Sorting performance of a nondestructive laser air-puff firmness detector. *Appl. Eng. Agr.*, 14, 513-516.

Jarén, C., 1994. Detección de la textura de frutos por medio de impactos no destructivos: Desarrollo y aplicaciones del procedimiento de clasificación. Doctoral Thesis. Universidad Politécnica de Madrid.

Jarén, C., Garcia-Pardo, E. (2002). Using non-destructive impact testing for sorting fruits. *J. Food Eng.*, 53(1), 89-95.

Jay, M., Lancelin, N., Llichou, J., Chapon, J.F., Guinot, E., Brunninck, M. (2000). Qualité des abricots: analyse sur les varietés Goldrich et Hargrand. *Infos Ctifl*, 161, 34-38.

Kader, A.A. (2002). Quality and safety factors: definition and evaluation for fresh horticultural crops. Postharvest Technology of Horticultural Crops, University of California ANR Publication, 3311, 279-85.

Kennard, R.W., & Stone, L.A. (1969). Computer aided design of experiments. *Technometrics* 11: 137-148.

Kim, M.H., Okos, M.R. (1999). Some physical, mechanical, and transport properties of crackers related to the checking phenomenon. *Journal of Food Engineering*, 40, 189-198.

Kozma, A. & Cunningham H. (1962). Tables for calculating the compressive surface stresses and deflections in the contact of two solid elastic bodies where principal planes of curvature do not coincide. *Journal of Industrial Mathematics* (Detroit, MI, USA) 12, 31-40.

Kuhl, F.P., & Giardina, C.R. (1982). Elliptic Fourier features of a closed contour. *Comp. Graph. Image Process 18*, 236-258.

Ladaniya, M.S. (2008) Citrus fruit: biology, technology and evaluation, p 198. *Academic Press*, San Diego, CA, USA.

Lammertyn, J., Nicolai, B., Ooms, K., De Smedt, V., Baerdeamaeker, J. (1998). Non-destructive measurement of acidity, soluble solids, and firmness of Jonagold apples using NIR-spectroscopy. *T. ASAE*, 41(4), 1089-1094.

Landahl, S., Jancsók, P.T., De Baerdemaeker, J. (2002). Dependence of the acoustic impulse technique on the development of apple on and off the tree. Proc Intnl Conf Agricultural Engineering. Budapest. June 30-July 4. Paper 02-PH-029.

Lanza G., Barbagallo, S., Calandra, M.R., Calvitti, M., D'Anna, R., Pedrotti, C. Porto, M.E. (2005). Evaluation of cold treatment against mediterranean fruit fly in "Tarocco" oranges. Proceedings 5th International Postharvest Symposium. *Acta Hort.*, 682, 2141-2145.

Lehman-Salada, L. (1996). Instruments and operator effects on apple firmness readings. *HortScience*, 31, 994-997.

Limanond, B., Castell-Perez, M.E., Moreira, R.G. (2002). Modeling the kinetics of corn tortilla staling using stress relaxation data. *Journal of Food Engineering*, 53, 237-247.

Lu, R. (2001). Predicting firmness and sugar content of sweet cherries using near-infrared diffuse reflectance spectroscopy. *T. ASAE*, 44(5), 1265-1271.

Maccarone, E., Rapisarda, P., Fanella, F., Arena, E., Mondello, L. (1998). Cyanidin-3-(6"-malonyl)-glucoside. An important anthocyanin of blood orange juice. *Ital. J. Food Sci.*, 10, 367-372.

Macfie, H.J.H., Bratchell, N., Greenhoff, K.G., Vallis, L.V. (1989). Designs to balance the effect of order of presentation and first-order carry-over effects in hall tests. *Journal of SensoryStudies* 4: 129-148.

Macnish, A.J., Joyce, D.C., Shorter, A.J. (1997). A simple non-destructive method for laboratory evaluation of fruit firmness. *Aust. J. Exp. Agr.*, 37, 709-13.

Magness, J.R. Taylor, G.F. (1925). An improved type of pressure tester for the determination of fruit maturity.USDA Circular 350.

Mancini M, Moresi M & Rancini R (1999a) Uniaxial compression and stress relaxation tests on alginate gels. Journal of Texture Studies, 30, 639-657.

Mancini, M., Moresi, M. & Rancini, R. (1999b). Mechanical properties of alginate gels: Empirical characterisation. *Journal of Food Engineering*, 39, 369-378.

Masi, P. (1989) Characterization of history-dependent stress-relaxation behaviour of cheeses. *Journal of Texture Studies*, 19, 373-88.

Massart, D.L., Vandeginste, B.G.M., Deming, S.M., Michotte, Y., Kaufman, L. (1988). *Chemometrics: a textbook*. Elsevier, Amsterdam.

McGlone, V.A., Abe, H., Kawano, S. (1997). Kiwifruit firmness by near infrared light scattering. *J. Near Infrared Spec.*, 5, 83-89.

McGlone, V.A., Ko, S.M.W., Jordan, R.B. (1999). Non-contact fruit firmness measurement by the laser air-puff method. *T. ASAE*, 42(5), 1391-1397.

McGuire, R.G. (1992). Reporting of objective color measurements. *HortScienc*e 27 (12): 1254-1255.

Menesatti, P., Pallottino, F., Lanza, G., Paglia, G. (2009). Prediction of blood orange MT firmness by multivariate modelling of low alterative penetrometric data set: A preliminary study. *Postharvest Biol. Technol.*, 51: 434-436.

Mohsenin, N. (1970). Physical properties of plant and animal materials. Gordon and Breach Science Publishers. USA. 734 pp.

Mohsenin, N.N., Mittal, J.P. (1977). Use of rheological terms and correlation of compatible measurements in food texture research. *Journal of Texture Studies*, 8, 395-408.

Moltò, E., Selfa, E., Pons, R., Fornes, I. (1996). Non-destructive measuring firmness using impact sensors. Proc Intnl Conf on Agricultural Engineering. Madrid. September 23-26. Paper 96F-014.

Montgomery, D. C. (2005) *Design and Analysis of Experiments*, 6th Edition, John

Wiley & Sons, Inc., USA.

Moskowitz, H.R. (1987). Food Texture. Instrumental and sensory measurement. Marcel Dekker, Inc., New York.

Muramatsu, N., Sakurai, N., Yamamoto, R., Nevins, D.J., Takahara, T., Ogata, T. (1997). Comparison of non-destructive acoustic method with an intrusive method for firmness measurement of kiwifruit. *Postharvest Biol. Tec.*, 12, 221-228.

Nussinovitch, A., Peleg, M., Normand, M.D. (1989). A modified Maxwell and a nonexponential model for characterization of the stress relaxation of agar and alginate gels. *Journal of Food Science*, 54, 1013-1016.

Oberbacher, M.F. (1965). A method to predict the post-harvest incidence of oleocellosis on lemons. *Proc. Fla. state Hort. Soc.*, 78, 237-240.

Oranfrizer Srl (2008). Giorgio Buda, Scordia (CT). Personal comunication.

Ortiz, C. (1999). Sistemas instrumentales de detección y cuantificación de la lanosidad en melocotón. Doctoral Thesis. Universidad Politécnica de Madrid.

Ortiz, C., Barreiro, P., Correra, E., Riquelme, F., Ruiz-Altisent, M. (2001). Non-destructive identification of woolly peaches using impact response and near-infrared spectroscopy. *J. Agr. Eng. Res.*, 78(3), 281-289.

Pagliarini, E. (2002) *Valutazione sensoriale: aspetti teorici, pratici e metodologici*. Ulrico Hoepli Editore, Milano.

Pallottino, F. (2008). Rheometrical Characterization and Firmness Assessment of Citrus Cultivars by Non-Destructive Tests. In *Proceedings of the 13th Workshop on the Developments in the Italian PhD Research on Food Science and Biotechnology*, Alba (Italy), 10-12 September, 554-555.

Pallottino, F. (2009a). Use of image analysis to asses the effective surface area of orange fruit submitted to uniaxial compression tests. In Proc.s of the *14th Workshop on the Developments in the Italian PhD Research on Food Science and Biotechnology*, Oristano (Italy), 16-18 September, 337-339.

Pallottino, F., Costa, C., Menesatti, P., & Moresi, M. (2009b). Compression testing of orange fruit. In *Proc.s of the* 9th *International Conference on Chemical and Process Engineering*, Roma (Italy), 10-13 May, *Chemical*

Engineering Transactions 17, 885-890.

Pallottino, F., Moresi, M., Giorgi, S., Menesatti, P. (2010) Orange fruit rheometrical characterization using stress-relaxation tests. In *Proc.s of the XVIIth World Congress of the International Commission of Agricultural and Biosystems Engineering* (CIGR), Québec City, Canada, June, 13-17, 2010, p. 256.

Pallottino, F., Costa, C., Menesatti, P., Moresi, M. (2011a) Assessment of the mechanical properties of Tarocco orange fruit under parallel plate compression, *Journal of Food Engineering* 103: 308-316.

Pallottino, F., Costa, C., Menesatti, P. & Moresi, M. (2011b). Tarocco Orange Fruit Viscoelastic Properties. Submitted to *Food and Bioprocess Technology.*

Pallottino, F., Antonucci, F., Lanza, M.C., Strano, M.C., Menesatti, P., Moresi, M. (2011c). Assessment of quality-assured Tarocco orange fruit sorting rules by combined phisico-chemical and sensory testings. Submitted to *Journal of Food Engineering.*

Peano, C., Reita, G., Chiabrando, V. (2006). Firmness and soluble solids assessment of nectarines by NIRS spectroscopy. *Acta Hort. (ISHS)*, 713, 465-469.

Peleg, M. (1987) The basic of solid foods rheology. In: HR Moskowitz (ed.) Food Texture. *Instrumental and sensory measurement*, Marcel Dekker, Inc., New York, 3-33.

Perry, R.H., Chilton, C.H., Kirkpatrick, S.D. (1963). *Chemical Engineers' Handbook*, 4th Ed., McGraw-Hill Book Co., New York, p. 2-6.

Planton, G. (1991). Tomate-Mesure de la fermeté au Durofel 25. *Infos Ctifl*, 74, 17-20.

Porat, R., Feng, X., Huberman, M., Galili, D., Goren, R., Goldschmidt, E.E. (2001). Gibberellic acid slows postharvest degreening of “Oroblanco” citrus fruits. *HortScience,* 36(5), 937-940.

Ragni, L., Berardinelli, A., Guarnirei, A. (2010). Impact device for measuring the flesh firmness of kiwifruits. *Journal of Food Engineering*, 96, 591-597.

Rao, M.A. (1992a). Measurement of viscoelastic properties of fluid and semisolid foods. In: M.A. Rao & J.F. Steffe (eds) *Viscoelastic properties of foods*, Elsevier Applied Science, London, pp.207-231.

Rao, V.N.M. (1992b). Classification, description and measurement of viscoelastic properties of solid foods. In: MA Rao & JF Steffe (eds) *Viscoelastic properties of foods*, Elsevier Applied Science, London, pp. 3-47.

Rao, M.A., Steffe, J.F. (1992). Viscoelastic properties of foods. Elsevier Applied Science, London.

Rapisarda, P., Fanella, F. Maccarone, E. (2000). Reliability of analytical methods for determining anthocyanins in blood orange juices. *Journal of Agricultural and Food Chemistry*, 48(6), 2249-2252.

Rapisarda, P., Russo, G. (2000). Fruit quality of five Tarocco selections grown in Italy. *Proc. Int. Soc. Citricult*, 2, 1149-1153.

Rapisarda, P., Bellomo, S.E., Intrigliolo, F. (2001). Anthocyanins in blood oranges: Composition and biological activity. In: S.G. Pandalai, (Ed.). Recent Res. Devel. Agric. Food Chem. Research Signpost 5, 217-230.

Reid, M.S. (1985). Product maturation and maturity indices. Postharvest Technology of Horticultural Crops. Univ. of Calif. Ext. Special Pub. n. 3311.

Rivero, L.G., Grierson, W., Soule, J. (1979). Resistance of “Marsh” grapefruit to deformation as affected by picking and handling methods. *J. Amer. Soc. Hort. Sci.*, 104, 551-554.

Rodríguez-Sandoval, E., Fernández-Quintero, A. Cuvelier, G. (2009). Stress relaxation of reconstituted cassava dough. *LWT Food Science and Technology*, 42, 202-206.

Rohlf, F.J. (2006). *TpsDig Ver. 2.10, digitalized landmarks and outlines*. Dept. of Ecology and Evolution, State Univ. of New York at Stony Brook.

Rohlf, F.J., & Slice, D. (1990). Extensions of the Procrustes method for the optimal superimposition of landmarks. *Syst Zool 39*, 40–59.

Ruiz-Altisent M., Ortiz-Canavate, J. (2005). Instrumentation and procedures for commercial non-destructive determination of firmness of various fruits. In: Proceedings of the 2005 ASAE Annual Meeting, ASAE Paper n° 056176.

Sabatier, R., Vivein, M., & Amenta, P. (2003). Two approaches for Discriminant

Partial Least Square. In: Schader M., Gaul W. & Vichi, M. (Eds.) *Between Data Science and Applied Data Analysis*. Springer-Verlag, Berlin.

Salvadores, M.C., Jarén, C., Iarana, I., Marañón, M. (2000). Apple mealiness detection by mechanical impacts. Proc Intnl Conf on Agricultural Engineering. Warwick. July 2-7. Paper 00-PH-026.

Sarig, Y., Nahir, D. (1973). Deformation characteristics of "Valencia" oranges as an indicator of firmness. *HortScience*, 8(5), 391-392.

Shmulevich, I., Galili, N., Rosenfeld, D. (1996). Detection of fruit firmness by frequency analysis. *T. ASAE*, 39(3), 1047-1055.

Shmulevich, I., Galili, N., Howarth, M.S. (2003). Non destructive dynamic testing of apple for firmness evaluation. *Postharvest Biology and Technology*, 29, 287-299.

Sinclair International. (2008). Available at: http://www.sinclair-intl.com/pages/iq_main.html. Accessed 11/12/2010.

Sjöström, M., Wold, S., Söderström, B. (1986). PLS Discrimination plots. In: Gelsema E.S & Kanals L.N. (Eds.) *Pattern Recognition in Practice II*. Elsevier, Amsterdam.

Skinner, G.E., Rao, V.N.M. (1986). Linear viscoelastic behavior of frankfurters. *J. Texture Studies*, 17, 421-432.

Sozer, N., Dalgic, A.C. (2007). Modelling of rheological characteristics of various spaghetti types. *European Food Research and Technology*, 225, 183-190.

Stan 245 (2004). Codex Standard for Orange. Available at: http://www.codexalimentarius.net/web/more_info.jsp?id_sta=10372. Accessed 12/11/2010.

Steenkamp, J.B. (1997). Dynamics in consumer behaviour with respect to agricultural and food products. In: B. Wierenga, A. van Tilburg, K. Grunert, J.B. Steenkamp, M. Wedel (Eds.). *Agricultural Marketing and Consumer Behavior in a Changing World*. Kluwer Academic Publishers, Dordrecht, pp. 143-188.

Steffe, J.F. (1996). Rheological methods in food process engineering, 2nd edn. Freeman Press, East Lausing, MI, USA.

Steinmetz, V., Chrocon, M., Bellon, V., Garcia, J.L., Barreiro, P., Verstreken, L.

(1996). Sensors for fruit firmness assessment: comparison and fusion. *J. Agr. Eng. Res.*, 64(1), 15-27.

Studman, C.J. (1999). Fruit and vegetables: fruit and vegetable quality. CIGR Handbook of Agriculture Engineering, 4, 243-272.

Studman, C.J. (2001). Computers and electronic in postharvest technology. A review. *Computers and Electronics in Agriculture*, 30, 109-24.

Timoshenko, S.P., Goodier, J.N. (1951). Theory of Elasticity. McGraw-Hill, New York.

Tjan, Y. (1997). High speed fruit-firmness grading system using low-mass impact technique. Thesis of Master of Science, University of California. USA.

Tressler, D.K., Joslyn, M.A. (1961). Fruit and Vegetable Juice-Processing Technology. AVI Publ. Co., Westport, USA.

Tumminelli, R., Conti, F., Maltese, U., Pedrotti, C., Bordonaro, E. (2005). Effect of 2,4-D, 2,4-DP, Triclopir and GA_3 on the pre-harvest fruit drop and senescence of “Tarocco commune” blood oranges in Sicilian orchards. *Acta Hort.*, 682, 801-806.

Turrell, F.M., Monselise, S.P., Austin, S.W. (1964). Effect of climatic district and of location in tree tenderness and other physical characteristics of citrus fruit. *Bot. Gaz.*, 125, 158-170.

UNI ISO 8589 (1990) Analisi sensoriale – Criteri generali per la progettazione di locali destinati all’analisi. *Ente Nazionale Italiano di Unificazione*, Milano.

USDA. (2003). United States Standards for Grades of Oranges (Texas and States other than Florida, California and Arizona). Agricultural Marketing Service, Washington DC, USA. Available at: www.ams.usda.gov/AMSv1.0/getfile?dDocName=STELPRDC5050384. Accessed 12/11/2010.

Valero, C., Bowerman, E., Crisosto, C.H., Garner, D., Slaughter, D. (2003). Introducing non-destructive flesh color and firmness sensors to the tree fruit industry. Int. Conference on Quality in Chains, Wageningen, Holland, 6-9 July, 2003. *Acta Horticulturae*, 604, 597-600.

Wang, J., Gòmez, A.H., Pereira, A.G. (2006). Acoustic impulse response for measuring the firmness of mandarin during storage. *Journal of Food*

Quality, 29(4), 392-404.

Wrolstad, R.E. (2001). The possible health benefits of anthocyanin pigments and polyphenolics. Available at: http://lpi.oregonstate.edu/ss01/anthocyanin.html. Accessed 2010-09-01.

Zude, M., Herold, B., Roger, J.M., Bellon-Maurel, V., Landahl, S. (2006). Non-destructive tests on the prediction of apple fruit flesh firmness and soluble solids content on tree and in shelf life. *Journal of Food Engineering*, 77, 254-260.